AGE DEPENDENT CHANGES IN NEURONAL VULNERABILITY AND ITS METABOLIC SUBSTRATES

by

MARK STEPHEN CHITOLIE

A thesis submitted to

The University of Birmingham

for the degree of

MASTER OF PHILOSOPHY

College of Medical and Dental Sciences

School of Clinical and Experimental Medicine

The University of Birmingham

November 2012

Abstract

Ageing is an important biological issue affecting all organs in the body. Following from earlier suggestions that the primary neuronal cultures could be aged *in vitro*, the first aim of this project was to define the survival and vulnerability of cultured cerebellar granule neurones maintained in culture for < 60 days. Although there was an age-dependent decrease in neuronal number, the remaining neurons were viable. Using this 'ageing in a dish model' as a possible *in vitro* model, the project then assessed the age-dependent changes in neuronal vulnerability, particularly in response to glutamatergic stimulation. Overall, with age in culture, there was an increased sensitivity to glutamate that was associated with a larger Ca^{2+} influx and a greater level of Ca^{2+} sequestration by the mitochondria. The size of the mitochondrial Ca^{2+} load was dependent not only upon the amplitude of the Ca^{2+} signal but also on the length of time that the cytosolic Ca^{2+} ($[Ca^{2+}]_i$) remained elevated. Providing that sufficient time was allowed, the mitochondria retained, even in the older neurones, their ability to recover from the elevated Ca^{2+}. This work provides more insight into the underlying mechanisms which contribute to the increase in neuronal vulnerability during the ageing process.

I dedicate this thesis to my mother and my late father (R.I.P),

for supporting me, for encouraging me

and most of all

for always believing in me

Acknowledgment

I would like to thank the University of Birmingham for the privilege of studying at the university's medical school, with a studentship and full funding for this project. I would like to acknowledge my supervisor Dr Emil Toescu for all his help, guidance and support. He has been an excellent supervisor, friend and mentor. I would also like to thank Dr Margaret Eggo, Dr Sunny Ramasamy and Dr Malcolm Buchanan for their encouragement throughout my project. Finally I would like to say a special thank you to all of my loved ones, friends and family who have supported me along this journey, without you this would not be possible.

Contents

Table of Figures

1 The theories of ageing

Ageing is an inevitable consequence of life which has an impact on every living organism. The severity of the effect due to the ageing process shows enormous variability between individuals. These can be very mild symptoms, such as a slight degree of memory loss, to others which are far more severe, which can often be an early sign that the individual may be developing a neurodegenerative disease. The high association between the process of ageing and neurodegenerative disease (Cleveland and Rothstein 2001; Mattson 2004; Cookson 2005) is a strong argument for investigating the underlying mechanisms that give rise to the more severe implications associated with ageing of the brain. Even though there is a clear association between normal ageing and neurodegenerative diseases such as Alzheimer's disease (AD), there are differences which show that the two are separate processes. One important difference is that there is a high degree of neuronal loss associated with AD in the hippocampus CA1, which is not seen during normal ageing (West, Coleman et al. 1994). It is suggested that during normal ageing, alterations in the synaptic network and not neuronal loss, is the important factor behind the process of ageing (Morrison and Hof 1997). A greater understanding of the causes of these physiological changes in neuronal networks could hopefully lead to a mechanism that could slow the impaired functioning of the neurones and allow improved methods for the early diagnosis of individuals who may be developing neurodegenerative disease.

The start point of this investigation into the age-dependent changes in neuronal vulnerability begins with the various theories relating to the ageing process. These include the Ca^{2+} hypothesis, the free radical theory and the role of the mitochondria in the ageing process.

1.1 *The Ca^{2+} hypothesis of ageing*

1.1.1 The theory and evidence behind the hypothesis

The Ca^{2+} hypothesis of ageing was first described during the 1980's and regarded Ca^{2+} as a key factor in the neuronal ageing process (Khachaturian 1987; Khachaturian 1991; Khachaturian 1994). The theory suggested that deregulation of intracellular Ca^{2+} ($[Ca^{2+}]_i$) resulted in neuronal death which is associated with a decline in the numbers of neurones (however it is now generally accepted that the numbers of neurones do not decrease with age and that it is the synaptic connectivity and functioning of the neurones which is impaired) (West, Coleman et al. 1994; Morrison and Hof 1997). Support for this Ca^{2+}-based theory of ageing came from research in neurodegenerative diseases such as Alzheimer's disease (AD). Ageing and neurodegenerative diseases are highly associated, with the risk of developing one of these diseases strongly correlated with age (Increased risk: AD ≥85-years of age (Mattson 2004), Parkinson's disease ≥70-years of age (Cookson 2005) and

amyotrophic lateral sclerosis ≥40-years of age (Cleveland and Rothstein 2001)). The symptoms of AD include the loss of memory and cognitive decline (Mattson 2004) which are displayed during normal ageing in milder forms known as age-associated memory impairment (Crook, Bahar et al. 1987; Coria, Gomez de Caso et al. 1993; Larrabee and Crook 1994; Barker, Jones et al. 1995; Koivisto, Reinikainen et al. 1995; Larrabee and McEntee 1995) and age-associated cognitive decline (Levy 1994; Hanninen, Koivisto et al. 1996; Rosenzweig and Barnes 2003). Another connection between ageing and neurodegenerative disease, is that the β-amyloid protein associated with AD has been shown to affect homeostasis of $[Ca^{2+}]_i$ (Mattson, Cheng et al. 1992; Camandola and Mattson 2010).

More evidence for the Ca^{2+} hypothesis of ageing has come from studies showing age-dependent changes in crucial parts of the cell involved in the homeostasis of $[Ca^{2+}]_I$ (See *chapter 5.1* for a review on Ca^{2+} homeostasis). This is illustrated in the age-dependent increase in the density of L-type voltage-gated Ca^{2+} channels (L-VGCC) which result in larger Ca^{2+} influx into the cytosol in older neurones (Thibault and Landfield 1996; Thibault, Porter et al. 1998). Another difference associated with age, is the developmental change in the subunit composition of the ionotropic (in particular the NMDA which has the largest permeability for Ca^{2+}) (Xia, Ragan et al. 1995; Wong, Liu et al. 2002; Arundine and Tymianski 2003; Fu, Logan et al. 2005; Zhou and Baudry 2006) and metabotropic glutamate receptors (Attucci, Clodfelter et al. 2002), which are mechanisms for the release of Ca^{2+} into the cytosol and are also important initiators of glutamate excitotoxicity (Olney, Collins et al. 1986; Rothman and Olney 1986; Dirnagl, Iadecola et al. 1999; Lee, Zipfel et al. 1999). In addition,

the release of Ca^{2+} from the endoplasmic reticulum by the inositol (1,4,5) triphosphate (IP_3) receptor and the ryanodine receptor (Bodhinathan, Kumar et al. 2010; Bruno, Huang et al. 2011) have also been shown to be affected by age (Puzianowska-Kuznicka and Kuznicki 2009).

Age-dependent changes in mechanisms which lower the $[Ca^{2+}]_i$ have also been demonstrated, with regional down regulation of the Ca^{2+}-binding protein calbindin-28 (Verkhratsky and Toescu 1998), a decrease in the activity of the plasma-membrane Ca^{2+}-ATPase (PMCA) including a lower affinity for calmodulin binding to the PMCA in brain synaptic plasma membranes (Michaelis, Bigelow et al. 1996; Zaidi, Gao et al. 1998; Mata and Sepulveda 2010) and decreases in both the forward movement and reversal of the Na^+/Ca^{2+}-exchanger (NCE) in rat cerebro-cortex nerve endings (Michaelis, Johe et al. 1984; Canzoniero, Rossi et al. 1992). Studies have suggested that the decline in the efficiency of these extrusion mechanisms represent the delayed recovery observed in aged neurones following glutamate stimulation (Khodorov, Fayuk et al. 1996) however, this delay may also be due to the slow unloading of the mitochondria's Ca^{2+} (Brocard, Tassetto et al. 2001).

1.1.2 Calcium as a signal for neuronal death

Alterations in Ca^{2+} homeostasis can lead to excessive levels of $[Ca^{2+}]_I$, which if not restored back to resting $[Ca^{2+}]_i$ concentrations can induce neuronal death (Toescu 1998). Even though it is established that there is no neuronal loss associated with

the ageing process (West, Coleman et al. 1994; Morrison and Hof 1997), it is important to have a general understanding of the mechanisms of death in neurones, since part of this project will involve identifying age-dependent vulnerabilities. The two processes of death that will be described in this section are apoptosis and necrosis. There are two main pathways for the induction of apoptosis, the intrinsic and extrinsic. Only the intrinsic pathway will be discussed in this introduction, since this pathway is related directly to the mitochondria and is affected by Ca^{2+} concentration and oxidative stress which form part of the theory of ageing explored within this project (See *figure 1.1*).

Apoptosis can be thought of as cellular 'suicide', since it is a well organised mode of programmed cell death initiated internally by the cell (Kerr, Wyllie et al. 1972). During the early stages of apoptosis, the genomic DNA within the nucleus becomes fragmented (karyorrhexis) and the appearance of convoluted folds in the plasma membrane know as 'blebbing' emerges (Kerr, Wyllie et al. 1972). This blebbing continues to expand until it eventually detaches forming 'apoptotic bodies', which are recognised by macrophages and destroyed by the process of phagocytosis. The neuronal network linking neighbouring neurones degrades, the nuclear chromatin condenses (pyknosis) and the cell shrinks in size. In conditions where macrophages are at low levels or even non-existent (e.g. *in vitro* conditions), the apoptotic bodies undergo lysis, releasing their cytosolic contents, a process known as 'secondary necrosis'. Apoptosis accounts for the mechanism of death from numerous diseases including HIV (Basanez and Zimmerberg 2001), Alzheimer's disease (Cotman and

Anderson 1995), Huntington's disease (Hickey and Chesselet 2003) and has been linked to neuronal death following stroke (Barinaga 1998).

The Bcl-2 is part of a family of proteins which have both pro-apoptotic members (Bax, Bac, Bad, Bik, Bid, Bim and Bclx(s)) and inhibitory members (Bcl-2, Bclx, and Mcl-1) (Nicholls and Budd 2000). Studies have shown that high levels of Bcl-2 expression is associated with a reduction in the movement of Ca^{2+} from the endoplasmic reticulum (Baffy, Miyashita et al. 1993) to the cytosol and mitochondria resulting in higher levels of resistance when exposed to apoptotic stress (Pinton, Ferrari et al. 2000). During intrinsic apoptosis, the apoptotic inducing signal initiates the migration of the apoptotic activator protein Bax, to the Bcl-2 protein located on the outer mitochondrial membrane (Krajewski, Tanaka et al. 1993; Ali, Coggins et al. 1997; Nicholls and Budd 2000) and triggers the release of cytochrome c into the cytosol.

The movement of cytochrome c into the cytosol was originally believed to be a result of the opening of the mitochondrial permeability transition pore (MPTP) (See *chapter 1.2.2*) (Green and Reed 1998; Kowaltowski, Naia-da-Silva et al. 1998; Marzo, Brenner et al. 1998; Kroemer and Reed 2000) however various studies have associated opening of the MPTP with necrosis since apoptosis can occur without the presence of cyclophilin-D (Nakagawa, Shimizu et al. 2005; Dejean, Martinez-Caballero et al. 2006). More recently, a channel known as the mitochondrial apoptotic channel (MAP), which is regulated by the Bcl-2 gene family has been described as the route of entry for the cytochrome c into the cytosol (Pavlov, Priault

et al. 2001; Guo, Pietkiewicz et al. 2004; Dejean, Martinez-Caballero et al. 2005; Dejean, Martinez-Caballero et al. 2006).

Cytochrome c is an important protein located on the outside of the inner mitochondrial membrane (inter-membrane space) and is involved in the electron transport chain of aerobic respiration (See *chapter 1.2.1*). It is capable of binding to both cytochrome c1 (Complex III) and cytochrome c oxidase (Complex IV) transporting electrons between the two complexes (Nicholls and Budd 2000). Movement of cytochrome c to the cytosol allows it to interact with the apoptotic protease factor APAF-1 (Li, Nijhawan et al. 1997; Zou, Henzel et al. 1997). The APAF-1 then starts the caspase cascade by binding to procaspase-9. Caspases are a family of cysteine proteases, which are found at low concentrations in cells as 'procaspase' which is the inactive form of 'caspase' (Nicholls and Budd 2000). Binding of the APAF-1 to the procaspase-9 activates the caspase converting it to caspase-9. The caspase-9 then cleaves procaspase-3 converting it to the active caspase-3 (Li, Nijhawan et al. 1997). The caspase 3 then goes on to cleave and activate other caspases inducing apoptosis, (e.g. caspase-6, which then activates caspase-7) (Yonish-Rouach, Resnitzky et al. 1991) which degrades the cytoskeleton, leading to cell shrinkage.

Necrosis is characterised by swelling of the matrix, eventually leading to the rupture of the plasma membrane and leakage of the cytosolic contents. Another key difference between necrosis and apoptosis is that apoptosis requires ATP in order to complete the numerous steps of the pathway whereas necrosis occurs when ATP

levels are depleted. This makes necrosis a key trigger of death when the mitochondrial membrane potential is dissipated resulting in the loss of the proton motive force (See *chapter 1.2.1*) leading to depletion of ATP. Studies have shown that the level of ATP found in the cell is a major factor in whether a cell dies via the necrotic or apoptotic pathway (Eguchi, Shimizu et al. 1997). Inhibition of the ATP-synthase (in the absence of glucose) in order to deplete ATP levels, showed a shift in the mechanism of death from an apoptotic pathway to a necrotic pathway (Eguchi, Shimizu et al. 1997). Stimulating the production of ATP then shifted the balance of neuronal death back towards apoptosis. Moreover as the ATP levels diminish, so to do all the mechanisms involving energy, including the ATPase ion pumps. This results in disruption of homeostasis in the cell leading to the characteristic swelling of the mitochondria and eventual death.

Necrosis has always been defined as a slow process of death triggered by pathological events which may suddenly occur, unlike apoptosis which is a much more organised and calculated mode of death, however more recently it has been shown to be a more highly controlled and ordered mechanism of death (Edinger and Thompson 2004).

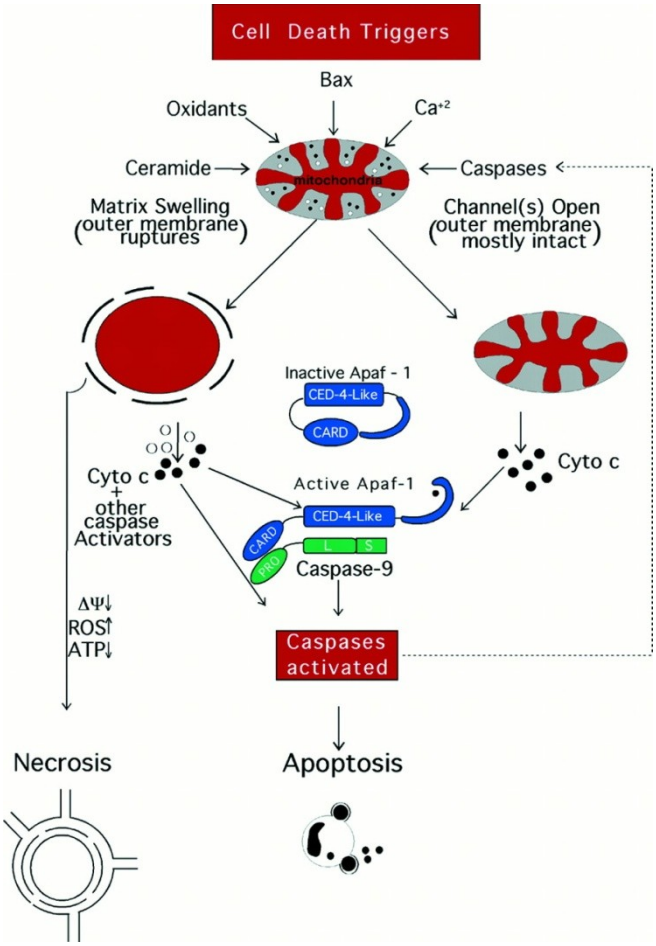

Figure 1.1 **Model for caspase activation by mitochondria (Figure taken from Green and Reed's review on mitochondria and apoptosis (Green and Reed 1998)).**

Multiple stimuli such as Bax, oxidants, Ca^{2+} overload, active caspases, and perhaps ceramide can trigger mitochondria to release caspase-activating proteins, among which are cyto c (solid circles) and possibly other proteins such as AIF and intramitochondrial caspases (open circles). Two general mechanisms for release of caspase-activating proteins from mitochondria have been proposed: one involves osmotic disequilibrium leading to an expansion of the matrix space, organellar swelling, and subsequent rupture of the outer membrane (left); the other envisions opening of channels in the outer membrane (without concomitant organellar swelling), thus releasing cyto c from the intermembrane space of mitochondria into the cytosol. Cyto c activates caspases by binding to Apaf-1, inducing it to associate with procaspase-9, thereby triggering caspase-9 activation and initiating the proteolytic cascade that culminates in apoptosis. Cells in which mitochondria have ruptured are at risk for death through a slower nonapoptotic mechanism resembling necrosis because of loss of the electrochemical gradient across the inner membrane ($\Delta\Psi$m), production of ROS, and declining ATP production.

1.2 *The mitochondria, ROS and ageing*

1.2.1 Glycolysis and oxidative phosphorylation

Before describing the role of the mitochondria and the production of reactive oxygen species (ROS) in the ageing process, it is important to have an outline of the metabolic activity carried out by this key organelle, in particular focussing on the electron transport chain in oxidative phosphorylation.

All living organisms undergo the process of respiration in order to provide ATP which is essential for normal cellular functioning. The energy harvested from ATP is required for numerous processes, including the plasma-membrane Ca^{2+}-ATPase, the endoplasmic reticulum Ca^{2+}-ATPase and the Na^{+}-glucose transporter. The two biochemical mechanisms used for generating ATP are glycolysis and oxidative phosphorylation (which includes the Krebs cycle (Krebs 1970), the link reaction and the electron transport chain). Glycolysis is an anaerobic process (does not require oxygen) taking place in the cytosol of the cell, which generates a net production of two ATP and four reduced NAD (NAD_{RED} - $NADH+H^{+}$). The Krebs cycle is an aerobic process (requires oxygen) taking place in the matrix of the mitochondria (Krebs 1970), generating a total of three NAD_{RED}, one reduced FAD (FAD_{RED} - $FADH_2$) and two ATP per cycle (i.e. six NAD_{RED} and two FAD_{RED} per molecule of glucose). This gives rise to a total of forty ATP with a net total of thirty-eight ATP generated from glycolysis and oxidative phosphorylation. The NAD and FAD are

coenzymes that function as electron- or proton-carriers, transporting protons and electrons from the matrix to the electron transport chain. They can exist in both oxidised (NAD^+, FAD) or reduced forms ($NADH+H^+$, $FADH_2$).

In normal resting state, the proton concentration inside the matrix of the mitochondria is low in comparison to the intermembrane space and the cytosol. This is because the outer mitochondrial membrane is permeable to H^+, allowing the H^+ to pass freely between the intermembrane space and the cytosol. The inner mitochondrial membrane however, is impermeable to H^+, preventing the movement of H^+ from the intermembrane space to the matrix. Consequently, an electrochemical potential is formed between the mitochondrial matrix and the intermembrane space. Coupled to this is the formation of a concentration gradient. These two factors combined create the proton motive force (Mitchell and Moyle 1969).

The proton motive force is defined by the following equation:

$$\Delta p \text{ (mV)} = \Delta\psi_m - (2.3\ RT/F)\Delta pH$$

(At 37ºC, $\Delta p = \Delta\psi_m - 60\Delta pH$) (Abdel-Hamid and Tymianski 1997)

Where Δp is the proton motive force, $\Delta\psi_m$ is the mitochondrial membrane potential, R is the gas constant, T is the absolute temperature, F is Faradays constant and ΔpH is the pH across the inner mitochondrial membrane.

During the oxidation of NAD, two electrons and two H^+ are released into solution. The two electrons are able to enter the respiratory chain at complex I and reduce UbH_2/UQ. The two electrons released from the oxidation of FAD cannot enter the respiratory chain at complex I since their redox potential are too negative, so they reduce the UbH_2/UQ via complex II instead (Papa 1996; Lesnefsky and Hoppel 2006). The electrons are then transferred to complex III where they reduce cytochrome c (Complex III), finally ending up at complex IV (also known as cytochrome c oxidase) (Papa 1996). It is at this complex where four electrons are passed on to molecular O_2 where it is converted to H_2O.

Complexes I, II and IV act as proton pumps (Schultz and Chan 2001), using energy released from electrons moving down the redox potential gradient (Mitchell's chemiosmotic theory (Mitchell and Moyle 1967; Mitchell 1976)) to pump H^+ out of the matrix. This removal of the H^+ from the matrix to the intermembrane space creates an electrochemical potential gradient across the inner mitochondrial membrane. The main way in which protons can enter back into the matrix is via complex V (known as ATP synthase). Three H^+ enter through this complex and uses the energy from the proton motive force to phosphorylate ADP to ATP. This phosphorylation of ATP is coupled to the oxidation of cytochrome c oxidase resulting in the transfer of the electrons to the final electron acceptor O_2, which combines with the two H^+ to form H_2O (Lesnefsky and Hoppel 2006).

The major driving force behind the production of ATP is the proton motive force which is determined by the $\Delta\psi_m$ and is tightly coupled to ATP demand (Dimroth, Kaim

et al. 2000). Disruption of the $\Delta\psi_m$ with protonophores, such as CCCP or FCCP, causes reversal of the ATP synthase (Dimroth, Kaim et al. 2000; Schultz and Chan 2001), resulting in rapid depletion of extra-mitochondrial ATP as the mitochondria desperately tries to re-establish its $\Delta\psi_m$.

1.2.2 Mitochondria, free radicals and ageing

When the levels of $[Ca^{2+}]_i$ increase, the mitochondria has the capacity to buffer some of this Ca^{2+} helping to reduce the $[Ca^{2+}]_i$ (Duchen 1999). Movement of the Ca^{2+} into the mitochondria is facilitated through the mitochondrial Ca^{2+}-uniporter (Duzenli, Bakuridze et al. 2005). Lower levels of mitochondrial Ca^{2+} uptake induce a small depolarisation in the mitochondria which has been shown to increase the rate of oxidative phosphorylation (Nicholls and Budd 2000; Toescu 2000). Driving of the electron transport chain is associated with a greater production of reactive oxygen species (ROS), since the probability of the electrons leaking out of the complexes becomes more significant (Turrens and Boveris 1980; Turrens, Alexandre et al. 1985; Turrens 1997; Kudin, Bimpong-Buta et al. 2004). Studies have shown electron leakage resulting in the formation of ROS, occurring at both Complex I (Turrens and Boveris 1980) and Complex III (Turrens, Alexandre et al. 1985) of the electron transport chain, with mixed opinions as to which of the two complexes produces the most ROS (Complex I (Kudin, Bimpong-Buta et al. 2004) and Complex III (Turrens 1997)).

One of the consequences of generating high levels of ROS, is that the ROS are able to mutate mtDNA (Barja 2004) leading to alterations in the amino acid sequence of the polypeptide chains expressed by that mutated version of the gene. This ultimately affects the folding of the polypeptide chain during formation of the protein. Changing of the three-dimensional structure of a protein could render it dysfunctional and could have fatal implications to the cell, for example when affecting the active site of an enzyme this can result in the inability of the enzyme-substrate complex from being formed, preventing the reaction from being catalyzed. Comparisons of the effects of ROS on DNA have shown that the mitochondrial DNA (mtDNA) has a higher mutation rate in comparison to nuclear DNA (Barnard, Robertson et al. 1997). Since mtDNA is situated in the matrix, which is also the home of the electron transport chain and is responsible for the transcription of a number of enzymes involved in the electron transport chain, it is in a prime target for ROS damage. The mtDNA codes for polypeptides involved in the electron transport chain, for rRNA and also for tRNA (Beal 2005). Evidence for the importance of the role of damaged mtDNA in ageing comes from a study showing an increase in the number of mtDNA point mutations in brains autopsied from older subjects who had suffered from AD, in comparison to brains obtained from younger subjects (Ito, Ohta et al. 1999). Added support also comes from studies using knock-out mice that lack the genes for the expression of the mtDNA polymerase PolgA, which is involved in the copying and proof-reading of mtDNA. These mice lacking the PolgA appeared to have accelerated ageing, such as greying of hair, hair-loss, reductions in bone density, muscle weakness, hearing loss and a reduction of up to 50% in life span (Trifunovic, Wredenberg et al. 2004; Kujoth, Hiona et al. 2005).

Mutations in the mtDNA can directly affect the proteins involved in aerobic respiration which could result in a lowering in the rate (or complete halt) of ATP synthesis, meaning the cell would have to rely more heavily upon glycolysis (anaerobic respiration) for its energy supply. If the energy produced in the cytosol by glycolysis were insufficient to meet the energy demands of the cell, then this would lead to neuronal death since the cell would be unable to drive important metabolic pathways. Also, these dysfunctional respiratory proteins may increase the susceptibility for electron leakage from the electron transport chain resulting in further oxidative damage.

Additional evidence for the role of ROS in the ageing process comes from studies showing that elevated levels of anti-oxidants increases life-span in various organisms (Finkel and Holbrook 2000). The over-expression of superoxide dismutase (SOD) (Tyler, Brar et al. 1993; Tower 2000) and methionone sulfoxide reductase A (Ruan, Tang et al. 2002), have both been shown to increase lifespan in transgenic *Drosophila melanogaster*. Over-expression of catalase in the mitochondria of mice increased their life-span (Schriner, Linford et al. 2005), so did the administration of substances which act as antioxidants in *C. elegans*, (Melov, Ravenscroft et al. 2000).

Reducing respiratory chain activity by a calorie-restricted diet has been explored to see if it is associated with a lower production of ROS, which would result in an increase in life-span. A calorie-restricted diet consists of a nutrient-vitamin rich diet with a 30-70% decrease in calorie intake. It has been demonstrated that restriction of an organism's calorie intake, results in prolongation of their life span (Merry 2002;

Barja 2004), which may arise from a decrease in metabolism leading to a decrease in ROS production. This metabolic rate theory of ageing would mean that more metabolically active organisms would suffer the effects of age faster since they would accumulate more ROS from the electron transport chain. However studies have shown that it is not the metabolic rate which is of importance but the rate at which ROS is produced since these two factors are not always directly correlated. This is demonstrated in birds which have a high metabolic activity but low rates of ROS production (Ku, Brunk et al. 1993; Finkel and Holbrook 2000). Another factor to consider when assessing calorie-restricted diets, is that a recent study has shown that the calorie-restricted diet may only be beneficial to specific strains of mice and may have an adverse effect on other strains (Liao, Rikke et al. 2012), which suggests that genetics has a key underlying role in ageing.

Apart from causing damage to DNA and proteins, ROS can also trigger the opening of the mitochondrial permeability transition pore (MPTP) (Kowaltowski, Castilho et al. 1996). This pore is a Ca^{2+}-dependent voltage-gated channel, permeable to solutes <1500 kD (Bernardi 1999; Stavrovskaya and Kristal 2005). It is located in the inner mitochondrial membrane and allows the movement of cations from the matrix to the intermembrane space. Transition of the pore is induced by many factors including depolarisation of the inner mitochondrial membrane by Ca^{2+} and by exposure to ROS (Kroemer and Reed 2000; Friberg and Wieloch 2002; Beal 2005). It is thought that transition of the pore involves the protein cyclophilin-D, which is activated by large concentrations of Ca^{2+} in the mitochondria and by oxidative stress (Tanveer, Virji et al. 1996). The MPTP can be blocked using cyclosporine A which interferes with

binding of the cyclophilin-D to the MPTP (Baines, Kaiser et al. 2005). Formation of the MPTP during very high Ca^{2+} concentrations in the absence of cyclophilin-D has been shown (Brustovetsky and Dubinsky 2000), suggesting that there may be two mechanisms for forming the MPTP based on the size of the Ca^{2+} load in the mitochondria (Li, Brustovetsky et al. 2009). Once the MPTP has been established, there is a complete disruption of the mitochondrial membrane potential, leading to irreversible mitochondrial dysfunction (Kowaltowski, Naia-da-Silva et al. 1998) and the release of cytochrome c which can then trigger apoptosis (See *Chapter 1.1.2*) (Green and Reed 1998).

Other evidence for the role of mitochondria in neuronal ageing comes from the structural and functional changes in mitochondria associated with age (Toescu, Myronova et al. 2000). This includes a decrease in the rate of oxidative phosphorylation (Papa 1996; Lesnefsky and Hoppel 2006), with reduced activity of Complex I (Haripriya, Devi et al. 2004; Cocco, Sgobbo et al. 2005), Complex IV (Tian, Cai et al. 1998; Ojaimi, Masters et al. 1999; Haripriya, Devi et al. 2004) and ATP-synthase (Guerrieri, Capozza et al. 1992). This reduction in the activity of oxidative phosphorylation may result from age-dependent changes in the fluidity of the mitochondrial membrane (Toescu, Myronova et al. 2000), or by the accumulated damage to the electron transport chain by ROS over time. Decreasing of the movement of electrons along the electron transport chain, coupled with the age-dependent changes in the composition of the complexes can increase the chance of electron leakage from the electron transport chain, causing more ROS production,

leading to more oxidative damage in the cell (Chen and Lesnefsky 2006; Lesnefsky and Hoppel 2006).

The central concept evolved from this free radical theory of ageing (Harman 1956) is that the harmful effects of ageing arise from the accumulated damage from ROS over time. The assumption is made that older individuals would have generated more ROS damage during the course of their lifetime since they have been metabolically active for a longer length of time, so the chance of electron leakage leading to ROS production is significantly increased.

1.3 *Aims of the project*

- The first aim of this project was to fully define and characterise the 'ageing in a dish' model. This involved assessing viability and stability of the cerebellar granule neurones as they were maintained in culture conditions. The objective was to determine whether this can be used as a viable *in vitro* model for studying the effects of ageing.

- The second aim was to identify differences in vulnerability between young and aged neurones towards glutamate excitotoxicity. To then fully explore the

dynamics of the glutamate-induced neuronal death and to see if this was correlated with age.

- The third aim was to investigate the functional parameters of glutamate excitotoxicity, in particular the effect of glutamate on $[Ca^{2+}]_i$ and its relationship with the mitochondria. The focus was on how the $[Ca^{2+}]_i$ affects the sequestration of Ca^{2+} by the mitochondria and the dynamics underlying this relationship. In addition how this relationship was affected by the ageing process.

- The final aim was to correlate the age-dependent vulnerability of neurones with the age-dependent changes in cellular physiology. This was important to help understand some of the factors that may be involved in the neuronal impairment associated with the ageing process and relate this to the various theories of ageing.

2 Methods

Since several experimental procedures were used throughout this project, each chapter has its own specific 'methods' section. The methods described in this chapter are used throughout the entire project and are applicable to all of the following chapters.

2.1 *Primary culture of cerebellar granule neurones*

2.1.1 Dissection procedure

For the preparation of primary neuronal cultures, 4-5 post-natal *Wistar* rat pups aged between 5 and 8 days old (postnatal (P) 5-8) were sacrificed according to Schedule 1 of the Animals (Scientific Procedures) Act 1986. After decapitation, the head was sterilised with 70% ethanol and a mid-sagital incision was made through the skin. Using scissors, two cuts were made from the foramen magnum towards the ear on both sides of the head. A transverse incision was then made through the skull, starting from the midline extending horizontally towards the left. Using forceps, the skull was peeled away exposing the brain. The entire cerebellum was isolated and transferred into ice-cold dissection medium (referred to as 'complete medium') containing 137mM NaCl, 5.4mM KCl, 4.2mM $NaHCO_3$, 15mM Glucose, 1.26mM $CaCl_2$, 0.5mM, $MgCl_2$ and 0.4mM $MgSO_4$, at pH 7.4 (Sigma, UK). With the aide of a

dissecting microscope, forceps and fine scissors, the meninges were carefully removed and the cerebellum separated from the colliculi ventrally and the cerebral peduncles dorsally. Following this, the cerebellum was placed into a 'Ca^{2+}-Mg^{2+} free' medium (CMF) which has the same basic composition of the 'complete' medium with the exclusion of $CaCl_2$, $MgCl_2$, and $MgSO_4$. This procedure was then repeated in each of the rat pups in order to obtain 4-5 cerebella.

2.1.2 Isolation of cerebellar granule cells

The cerebella were finely chopped using a scalpel and transferred into a 15ml centrifuge tube (Falcon, UK) containing 2ml CMF medium. To initiate the enzymatic dispersion process, 0.5ml of a mixed preparation containing the cysteine protease papain (Worthington, UK) and EDTA (Sigma, UK), was added to the 2ml CMF medium containing the cerebella, giving a final papain concentration of 7-10U/ml. The overall mixture containing the CMF medium, cerebella, papain and EDTA was then incubated at 35ºC for 15 minutes.

At the end of the 15 minute incubation period, the centrifuge tube was removed from the incubator and 9.5ml of CMF medium was added to the cerebella/protease mixture, giving a final volume of 12ml. The preparation was then centrifuged at 1000rpm for 5 minutes. Once completed, the supernatant containing the papain, cysteine and EDTA was gently removed, taking care not to dislodge the pellet (containing the cerebellar granule cells) from the bottom of the centrifuge tube. The next enzymatic step was to digest any released DNA by adding 0.5ml DNase

(500U/ml) (Sigma) and 4mM $MgCl_2$ (which is an essential cofactor of DNase) to 2ml CMF medium. In the presence of DNase, the pellet was triturated with three glass pipettes each with a decreasing bore hole ranging from 2mm to 0.5mm (15 times with each pipette) and then the cells were passed through a 40µm cell strainer (Falcon, UK) to separate the cells. To start re-adjusting the cells to the normal extracellular concentration of divalent cations, 6ml of complete medium (containing Ca^{2+} and Mg^{2+}) with 6ml CMF medium was added to the cells and centrifuged for 5 minutes at 2500rpm. The supernatant containing the DNase and $MgCl_2$ was then discarded and replaced with a combination of 6ml 'complete' medium with 6ml 'Eagle's Basal Medium (BME) start' medium (which contains the same composition as the 'complete' medium however it has 25mM KCl instead of 5.4mM KCl which is in agreement with all literature referring to the growth of rat cerebellar granule neurones cultures (Toescu and Verkhratsky 2000). The pellet was again triturated using the pipette with the smallest bore size and centrifuged at 2500rpm for another 5 minutes. Finally the supernatant was replaced with 12ml 'BME start' medium and the pellet separated using the pipette with the smallest bore size.

2.1.3 Preparation of the culture slips.

For many experiments, especially those involving imaging or handling of individual cultures, the granule cell cultures were grown on glass cover-slips (Nunc, UK) spanning 13mm in diameter and with a thickness of 1.5mm. Since the experiments in this project required the neuronal cultures to be maintained long-term, it was vital that the cover-slips were thoroughly cleaned and sterilised in order to reduce the amount of cross-contamination with other cells or micro-organisms. To achieve this, a two stage cleaning and sterilising process was adopted. Each of the two stages was carried out in a laminar flow cabinet which helped reduce the risk of contamination from particles and microbes found in the air. During the first stage of the process, approximately 300 glass cover-slips were placed into a glass beaker containing the detergent Hellmanex (Hellma GMBH and Co., UK) (1.5%v/v). The cover-slips were left submerged in the Hellmanex for between 45-60 minutes and kept in an incubator at 35ºC in order to breakdown any grease or dirt attached to the surface of the glass. The Hellmanex was then discarded and the cover-slips were washed three times with sterilised deionised water (autoclaved) to ensure that all of the detergent was completely removed from the surface of the glass, before being placed in 100% ethanol. Once this first stage had been completed, the cover-slips could be stored for at least one week provided that they have been kept submerged in the ethanol in a sealed container.

The second stage of the cleaning procedure involved the hand-cleaning of each individual cover-slip using lens paper (Whatman, UK) in order to remove any smears

or debris on the glass. Each cover-slip was then rinsed in 100% ethanol before being flame dried using a Bunsen burner. Each sterilised cover-slip was then placed into one of the wells of a sterile 24-well microplate (Falcon, UK).and stored with the microplate lid on in the laminar flow cabinet.

On the day prior to culturing, the cover-slips were coated with 25µM/ml poly-D-lysine hydrobromide (PDL (Product number: P6407) – diluted in autoclaved de-ionised dH_2O) (Sigma, UK), which enhances binding of the neuronal cells to the glass surface. Using a glass pipette, 2-3 drops of the PDL solution was placed in the centre of each cover-slip and the microplate lid returned back to the plate. Once all of the cover-slips were coated with the PDL solution, the microplates were covered in aluminium foil to reduce any evaporation of the PDL and left in the laminar flow cabinet for 24 hours (minimum of 3 hours prior to plating). The PDL was then removed and the cover-slips were washed three times with sterilised deionised dH_2O. Finally the cover-slips and microplates were allowed to dry inside the laminar flow cabinet ready for use.

2.1.4 Plating the cerebellar granule cells directly on glass cover-slips.

At the end of the various enzymatic/mechanical stages of the neuronal isolation and separation process, the cerebellar granule cells were plated onto the glass cover-slips at a cell density of 7.0 million cells/ml. A cell counter was used to estimate the number of cells/ml in the cell suspension obtained at the end of the isolation procedure and the required dilutions were done with 'BME start' medium. From the final cell suspension, 40µL of the medium containing 7-million cells/ml was plated onto each cover-slip, so that each cover-slip contained 280,000 cells.

The plated cells were incubated (35ºC, 5%CO_2) for 2.5 hours to adhere to the glass cover-slips, after which 0.5ml 'BME start' medium was added to each well completely immersing the cover-slips. In order to prevent further proliferation of non-neuronal glial cells, 10µM cytosine-arabinoside (Sigma, UK) was added to each well 36-48 hours post plating. Plating of the neurones directly to the bottom of the microplate involved exactly the same procedure as describe for plating on cover-slips.

2.1.5 Feeding the cells

In order to maintain the well-being of the cultures, the neurones required as with any other cells in culture, a scheduled protocol of feeding. This was done to ensure that the amounts of nutrients (e.g. glucose) and the ionic concentration of the medium were kept constant.

Cerebellar granule cells are particularly sensitive to a complete replacement of the medium, and thus for almost all neuronal culture protocols, only partial replacement of the culture medium is recommended. Therefore every 5-7 days, 100µl of the culture medium from each individual well was removed and replaced with 150µl of fresh 'feeding' medium. The only difference between this feeding medium and the 'BME start' medium is that the feeding medium contains a higher concentration of 32mM glucose (Sigma, UK). The importance of this increased glucose concentration was to replenish the glucose levels in the culture medium which may have been depleted through the glycolytic pathways for ATP synthesis. The extra 50µl of medium was added to compensate for any loss of culture medium through evaporation, although the incubator contained humidified air. To ensure that the pH of the feeding medium was equilibrated and had reached the correct temperature, it was maintained in an incubator (35ºC, 5% CO_2) for at least 30 minutes prior to feeding.

2.2 *Statistical Analysis*

In order to assess any statistical significance in the data, the following techniques were used: mean values, standard error of the mean, one-way ANOVA and linear regression.

One-way ANOVA analysis determines significant differences between groups of data when changing one variable at any one time. This statistical technique was used to identify significant differences between the responses of the young and old *in vitro* age groups. It was also used to show significant differences in the responses of neurones from the same *in vitro* age group when exposed to different glutamate concentrations or experimental protocols (For example varying the length of glutamate stimulation).

One-way ANOVA analysis was combined with linear regression, which is a useful statistical tool for evaluating correlation between two different parameters. This was used throughout the thesis to assess the correlation between the various parameters investigated, for example the glutamate $[Ca^{2+}]_i$ load and the CCCP-induced mitochondrial Ca^{2+} unload.

All of the statistical tests were performed using Microsoft Excel 2007 and the software was also used to draw the graphs representing the data.

3 The “ageing in a dish” model

3.1 *Models of ageing*

The ageing process affects all living organisms, and various tissues respond in a different manner to this process. Taking into account the fact that the neurones are post-mitotic cells, the brain is surprisingly resilient to the effect of ageing, with little neuronal loss during the course of life (Terry, DeTeresa et al. 1987; Freeman, Kandel et al. 2008). However, one of the features of the ageing process, that affects also the brain, is an increase in cellular vulnerability to a host of cytotoxic effects (Toescu 2005). One possibility to study this process of increased vulnerability is to investigate neuronal behaviour and responsiveness to metabolic stressors in experimental material (brain, brain slices, and acutely dissociated neurones) obtained from aged animals. Such extensively used approaches, have nevertheless some limitations, as in long lead-up time (a rodent is considered aged when over 18-20 months) and significant costs. Such limitations lead scientists to attempt to develop and refine models which mimic at least some of the features and characteristics of the normal ageing process. The use of such *in vitro* models of ageing have become valuable tools when investigating the mechanisms both underlying and affected by the ageing process, since they allow numerous factors to be manipulated over various lengths of time.

One issue that must be addressed when working with *in vitro* neuronal models is that of regional heterogeneity. Different regions of the brain have different functions, resulting from different patterns of connectivity, and imposing different levels of activity on neurones. It is possible that some of these functional characteristics could result in different patterns of ageing and of increased vulnerability. A classical example of such regional heterogeneity is represented by the dopaminergic neuronal population of the substantia nigra, a population which has an increased susceptibility to the effects of ageing (Bannon and Whitty 1997; Cragg, Rice et al. 1997) and which result, in humans, in the significant increase in the symptomatology of Parkinson's disease with age. Generally, because of the diversity of neuronal phenotypes, it is possible that various different populations of neurones might respond in different ways dependent upon the stimuli or protocols applied. Using a mixture of neuronal types in one model may give misleading results when, for example, studying cellular mechanisms such as Ca^{2+} homeostasis, that might show a high degree of region-specificity (Hartmann, Eckert et al. 1996; Satrustegui, Villalba et al. 1996; Verkhratsky and Toescu 1998). Hartman *et al*. (Hartmann, Eckert et al. 1996) showed that both the initial resting level of intracellular Ca^{2+} ($[Ca^{2+}]_i$) and the amplitude of the intracellular Ca^{2+} increase induced by KCl depolarisation were lower in aged mice in the hippocampus and cortex; however, this observation was not applicable in the cerebellum or striatum, indicating region specificity. This illustrates the importance of studying specific cell types independently in order to avoid any such issues related to region specificity, which is why using a primary cell culture of cerebellar granule cells is a very attractive method since it contains very few other cell types.

The closest *in vitro* models for brain ageing are the organotypic slices. The slices contain a preserved neuronal network, which provides for the study of more specific and natural means of neuronal stimulation (e.g., transynaptic stimulation) and also allows the study at both the global and local levels (Newell, Barth et al. 1995; Rytter, Cronberg et al. 2003; Birgbauer, Rao et al. 2004; Katsuki and Akaike 2004; Cho, Wood et al. 2007; Michinaga, Hisatsune et al. 2010; Gerace, Scartabelli et al. 2012). The major downside to using this preparation is that the slices obtained from aged animals cannot be maintained in culture for any period of time longer than 6 hours, unlike the slices obtained from animals up to 2 weeks old that can be maintained for days to weeks.

Successful primary neuronal cultures are generated by harvesting cells from very young animals (for cerebellar granule neurone cultures, pups must be between 3 and 7 days old). A number of earlier studies have shown that neurones 'aged in the dish' show similar responses to stimuli as those studied in aged brain slices, such as the responses induced by simple depolarisation with KCl in primary cultured cerebellar granule neurones (Toescu and Verkhratsky 2000; Xiong, Camello et al. 2004) in comparison to acute cerebellar brain slices (Kirischuk and Verkhratsky 1996). These studies used the fluorescent Ca^{2+} dye Fura-2 to monitor changes in $[Ca^{2+}]_i$ in conjunction with the mitochondrial membrane potential dye rhodamine 123, which identifies changes in the polarisation status of the mitochondria. Both the primary culture (Toescu and Verkhratsky 2000; Xiong, Camello et al. 2004) and the acute slices (Kirischuk and Verkhratsky 1996) showed similarities in the age-related responses to the simple KCl depolarisation, in particular to the time taken to restore

$[Ca^{2+}]_i$ back to normal cellular levels after the depolarisation induced Ca^{2+} influx. Both models showed that aged neurones took longer to recover to the elevation in $[Ca^{2+}]_i$ as opposed to the younger neurones.

Further evidence supporting the ageing in a dish model comes from work investigating the effect of ageing on Ca^{2+} channel currents and the density of voltage-gated Ca^{2+} channels in the hippocampus. Similar findings were observed in both hippocampal slices (Campbell, Hao et al. 1996; Herman, Chen et al. 1998) and primary cultures of hippocampal neurones (Blalock, Porter et al. 1999) whereby the overall Ca^{2+} channel currents increased with age in the hippocampus. Moreover the density of voltage-gated Ca^{2+} channels was also shown to be age-dependent which would explain why there are larger Ca^{2+} channel currents in aged neurones since there are more voltage-gated Ca^{2+} channels.

3.2 *Aim*

This stage of the project is focussed on further characterisation of the 'ageing in a dish model' and not just reconfirming the validity of using primary cultured cerebellar granule neurones to study ageing. In particular it will provide dynamic information assessing neuronal numbers, neuronal viability and the overall stability of the cells as their time maintained in culture increases.

3.3 *Methods*

3.3.1 Method for counting the number of neurones in a fixed field over time

In a laminar flow cabinet, a needle (Sterilin, UK) sterilised with ethanol and heat was used to etch a grid onto the bottom surface of each of the four wells in a 4-well micro-plate (Iwaki, Japan) (See figure 3.1). This grid acted as a unique positional map for each of the wells, allowing specific locations on the grid to be revisited and monitored over time. The cerebellar granule neurones were plated directly onto the base of the microplate containing the etched grid using the same cell plating density and procedure for plating directly onto a microplate described in *chapter 2.1.4*.

A total of two separate fields were defined in each of the microplate's 4-wells. Phase contrast images of the designated regions (identified by their specific grid location, noted at the first image acquisition) were captured at regular time intervals using a x20 objective and a CCD camera with frame grabber (Matrix Vision).

Overall, this simple procedure provided an accurate, time-dependent method of sampling which could be used to assess the survival of the neurones in culture.

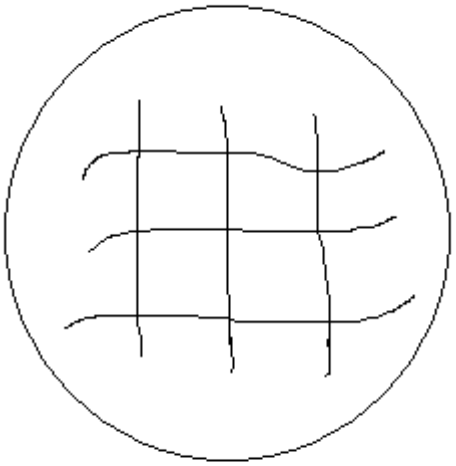

Figure 3.1. **Schematic drawing of the grid.**

This shows an example of a grid marked out on the bottom of one of the microplate's 4 wells. The cerebellar granule neurones were plated directly onto this grid which enabled positional information to be collected for the assessment of neuronal survival.

3.3.2 Method for assessing neuronal viability by using a dual load with Calcein-AM / Propidium iodide or Hoechst / Propidium iodide

The membrane impermeable DNA-binding dye Propidium iodide (Pi) (Sigma, UK) (Tanke, van der Linden et al. 1982; Sattler, Charlton et al. 1997) was used at a concentration of 5µg/ml to identify any non-viable neurones. The Pi was used in combination with either the fluorescent DNA-labelling dye Hoechst 33342 (H33) (Molecular Probes, UK) used at a concentration of 4µg/ml or the membrane permeable fluorescent dye Calcein-AM (Molecular Probes, UK) (Wang, Terasaki et al. 1993) used at a concentration of 5µM. All dilutions, incubations and measurements were performed using 'experimental' medium (containing 145mM NaCl, 5mM KCl, 10mM HEPES, 1mM $MgCl_2$x6, 1.5mM $CaCl_2$, 12mM Glucose (Sigma, UK).

A fluorescent microscope (Olympus BXW150) was connected to an intensified GenIV camera (Roper Instruments, UK) to capture the fluorescent images, a monochromator (Cairn Research Ltd., UK) to provide the excitation light and the computer software MetaFluor / MetaMorph (Universal Imaging, USA) to control the wavelength settings. All measurements were recorded with either a x20 or x60 water immersion lens and a DIC filter which excluded 75% of the fluorescent light to reduce photobleaching of the fluorescent dyes. Digital images of the fields of interest were obtained by substituting the intensified GenIV camera with a Nikon digital camera.

The Pi can be excited by both UV light and a wavelength of 540nm to give a bright red fluorescent signal (emission wavelength 617nm). The excitation wavelength for H33 is 352nm with an emission spectrum of 461nm and the excitation wavelength for calcein is 490nm with an emission wavelength of 520nm. When dual-loading cells with calcein and Pi two excitation wavelengths were used (475nm for calcein and 360nm for Pi) with an emission wavelength of 510nm. Loading cells with the combination of H33/Pi was more straightforward only requiring a single excitation wavelength of 360nm and an emission wavelength of 510nm.

In total, one bright-field image and one fluorescent image was taken from 3-5 different fields within each cover-slip. The data obtained from these 3-5 fields were then averaged together to give one value. In order to quantify the amount of viable (blue fluorescent) cells versus non-viable (red or bright blue fluorescent) cells, images of the fields taken with the Nikon camera were uploaded to the program CorelDraw (Coral). Non-viable neurones, viable neurones and background regions were highlighted using selection tools within the program and the intensity of each region was determined by the software. These intensity readings were used to calculate the percentage of viable cells to non-viable cells.

3.3.3 Immunocytochemistry

Granule neurones were plated onto culture slips at the usual plating density of 300,000 cells/culture slip and cultured in their normal way (See *Chapter 2.1.4*). Two representative culture slips at DIV 7 were selected for the immunocytochemistry. Cells were fixed using 4% paraformaldehyde (Sigma, UK) for 30 minutes. The paraformaldehyde was then removed and disposed of according to health and safety guidelines. The culture slips were washed three times with phosphate buffered saline (PBS) (Gibco, UK) with an interval of 5 minutes between each wash to completely remove any remaining paraformaldehyde. The culture-slips were then incubated for 30 minutes in a PBS buffer containing 5% fetal calf serum (Sigma,UK) to block any unspecific antibody binding and 0.1% Triton X100 (Sigma, UK) in order to permeabilise the membranes, thereby allowing the primary antibody to enter into the neurones. After completion of the blocking and permeabilisation stage, the PBS solution (containing the 5% fetal calf serum and 0.1% Triton X100 was removed and the primary antibodies were added.

A monoclonal antibody for Microtubule-associated protein 2 (MAP2) (Invitrogen, UK) was used to identify all neurones at a dilution of 1:500 which was sufficient for labelling of the neurone's dendrites. A monoclonal antibody for glial fibrillary acidic protein (GFAP) was used to identify any astrocytes in the culture. The GFAP monoclonal antibody (Invitrogen, UK) was used at a dilution of 1:1000 to label the astrocytes. Both primary antibodies were diluted together in one solution of PBS+0.1% Triton X100 (referred to as "PBS+Tri"). The culture slips coated with the

neurones were then incubated in the primary antibodies for 1 hour at room temperature (21°C).

At the end of the primary antibody load, the "PBS+Tri" solution containing the primary antibodies was removed and the culture slips were washed three times in "PBS+Tri" (with a 5 minute interval between each wash). The fluorescent label Fluorescein Isothiocyanate (FITC) anti-mouse (Molecular Probes, UK) was used to detect the GFAP and the fluorescent label Texas Red anti-rabbit IgG (Molecular Probes, UK) was used to detect the MAP2. They were diluted at a concentration of 1:50 in "PBS+Tri" and incubated at room temperature for 30 minutes. The secondary labelled antibodies were then removed and the culture slips were washed three times in "PBS+Tri" with the usual 5 minute interval between each wash. The nuclear dye Hoescht H33342 (H33) was diluted to a concentration of 5μM in "PBS+Tri" and the culture slips were incubated with the dye for 30 minutes at room temperature. The H33 was then removed and the culture slips were washed three times with "PBS+Tri" in the usual way. A final wash with distilled H_2O (three times with 5 minute interval between each wash) was performed to prevent the accumulation of any salt deposits from the "PBS+Tri" in the culture, which may crystallise and become labelled.

The culture slips were then mounted onto a glass microscope slide using one drop of Vectashield (Vector Laboratories Ltd., UK). Excess Vectashield was removed by applying a tissue at the edges of the culture slip, taking great care not to remove any of the cells. The microscope slide was left overnight to dry (in the fridge at 3ºC and covered in foil to protect from exposure to light). Once dry, the cover-slips were

sealed to the microscope slide by applying nail varnish to its edges. The cover-slips were then viewed using a fluorescent microscope. The optimal wavelengths used for viewing FITC were an excitation wavelength of 488nm with an emission wavelength of 530nm. For viewing Texas Red, the excitation wavelength was 595-605nm with an emission wavelength of 620nm.

3.4 *Results*

3.4.1 Establishing a start point for normalising the data

Although it is well known in the practice of neuronal primary cultures that with time there is a gradual decrease in the number of neurones, there is relatively little quantitative data on this process. To allow comparisons between different cultures at different ages, from different fields, there is the need to establish data normalisation. Here this normalisation was achieved by assessing the changes in the number of neurones present in a field of view in reference to an initial time point. However, deciding the initial time point is complicated by the fact that culture dynamics might be affected in the first few hours or days by at least two factors: a) the possible demise of some cells following the trauma of the isolation procedure and b) the fact that at least some of the neurones in the cultures could still be in the last mitotic phase.

To help establish the population dynamics in these early stages of cultures, the number of neurones were counted in two designated fields per culture slip and averaged together to give one single value (per culture slip). These counts were performed in the same specified fields for 5 consecutive days, starting with the first day post-plating (i.e. Days *in vitro* (DIV) 1) and repeated on two different culture slips.

As expected, the appearance at DIV 1 and the changes from DIV 1 to DIV 2 were too variable to allow that point to be taken as a reference point, and the detailed analysis was started at DIV2. Examples of a typical set of phase-contrast images are shown in *figure 3.2.a* and *figure 3.2.b*, while *figure 3.3* shows the neuronal numbers observed at different time-points (DIV 2-5).

Analysis of the number of neurones counted in each specified window (see *figure 3.3 Panel A*) using one-way ANOVA showed no significant difference between DIV 2 and the following 3 DIV (*F*-statistic=0.56, P-value>0.05, n=2). The numbers of neurones were then expressed as a percentage of DIV 2 (see *figure 3.3 Panel B*), which also showed no significant difference between the number of days in culture and the number of neurones counted in that specified field (*F*-statistic=5.39, P-value>0.05, n=2).

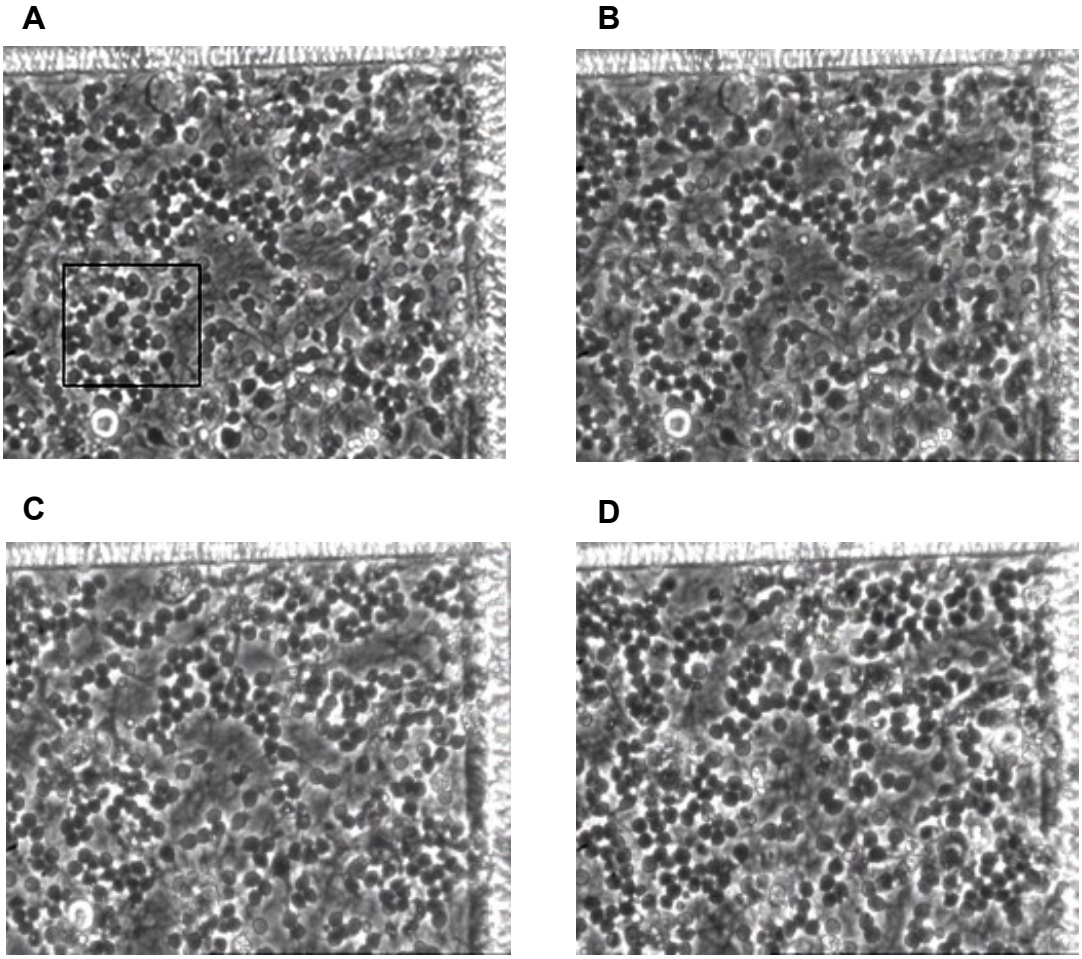

Figure 3.2.a **The first five days after plating.**

Bright-field phase contrast images taken from the same field at different 'days *in vitro*' (DIV). (*A*) DIV 2, (*B*) DIV 3, (*C*) DIV 4, (*D*) DIV 5.

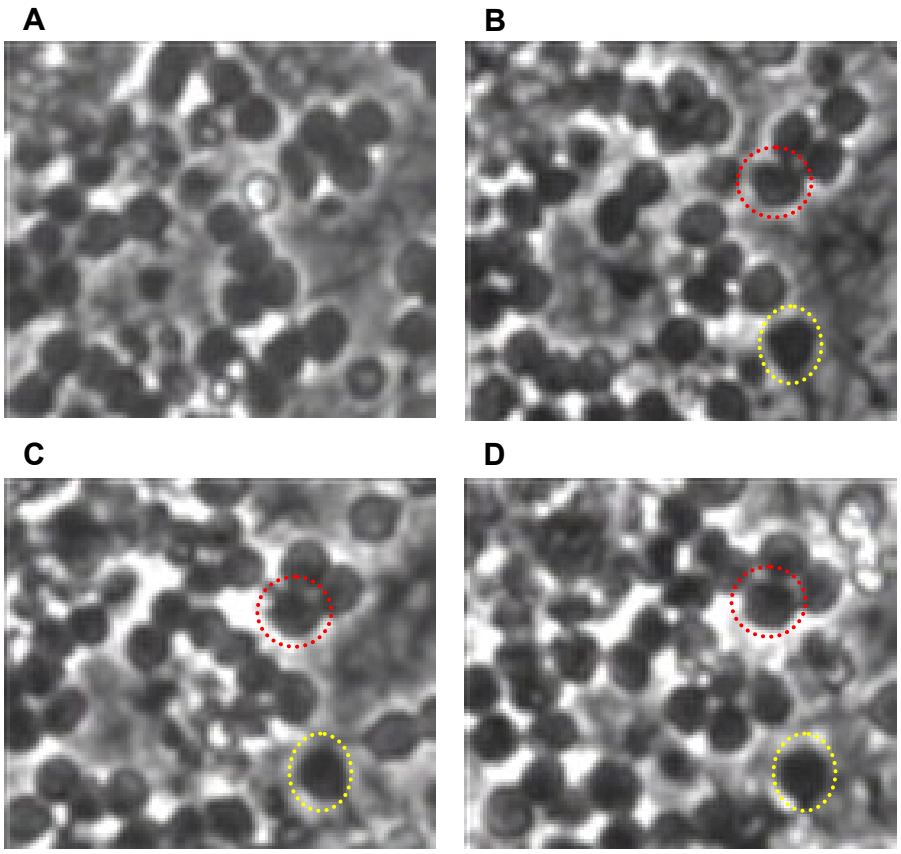

Figure 3.2.b. **Magnified details of the region marked in Fig. 3.2.1 a.**

(*A*) DIV 2, (*B*) DIV 3, (*C*) DIV 4 (*D*) DIV 5. Images (*A*)-(*D*) are magnified regions from the square highlighted in the previous image. The red and yellow circles show two neurones at 3, 4 and 5 days *in vitro*.

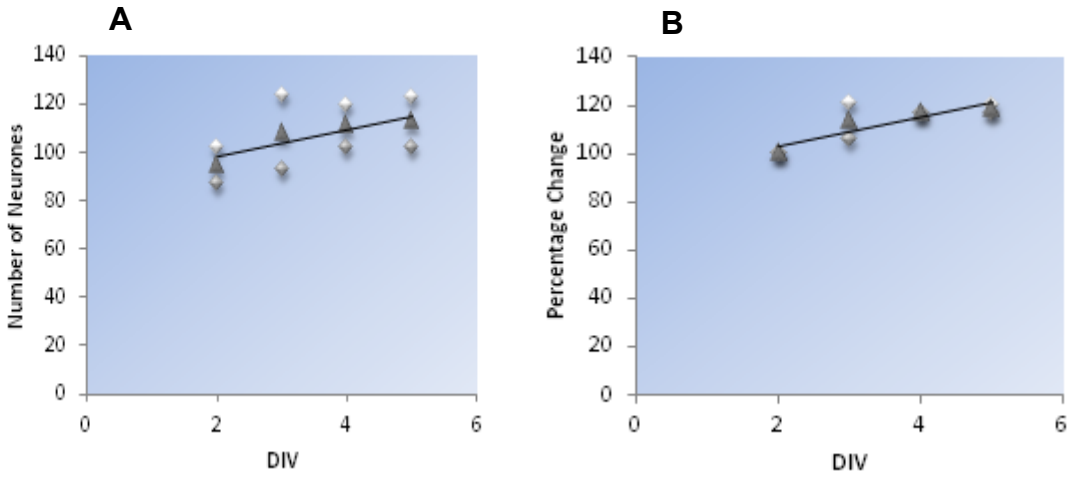

Figure 3.3. **Count of neuronal numbers for the first 5 days in culture**

Panel A shows the actual number of neurones counted at DIV 2-5. The data comes from 2 different culture slips plated with neurones from the same culture. Two fields were marked out on each culture slip and the numbers of neurones in each field was counted and averaged together to give one single value for that culture slip. This was repeated for five consecutive days (See *Chapter 3.1.1* for method used to count the numbers of neurones). *Panel B* shows the percentage change in neuronal numbers. The numbers were expressed as a percentage change against the DIV 2 count for that specific culture slip. The regression line is drawn on the graph and the predicted y values for the examined DIV were calculated. For both *Panel A* and *B*, the black triangle represents the mean of the two neuronal counts. Linear regression analysis on the fields, resulted in the equation: for neuronal numbers [Surviving neurones]=87.2+5.6xDIV, and the ANOVA analysis showed no significant difference from DIV 2 to DIV 5 from zero ($p>0.05$); Percentage of neurones [Surviving neurones]=91.5+5.9xDIV, and the ANOVA analysis showed no significant difference from DIV 2 to DIV 5 from zero ($p>0.05$).

3.4.2 Neuronal survival – Neuronal numbers decrease with age

The next step was to assess the changes in neuronal numbers as a function of the time in culture. Overall, neuronal cell numbers vary over time, gradually decreasing in number with the age in culture. In panel A of *figure 3.4* each data point represents the average number of neurones counted in two different fields of view from one culture well per culture; as explained in *Materials and Methods* section, the manual tracking system allowed a return to the same field of view at later times and counting of the remaining neurones. To allow a direct comparison (between different cultures) of the changes in the number of neurones remaining in the culture with time, for each culture, the DIV 2-5 values were taken as reference (100%) and the subsequent values, for each individual culture, were expressed as a percentage of these values; the resulting data are plotted in *figure 3.4* Panel B. One-way ANOVA analysis of this set of data shows that survival of the neurones and therefore the numbers of neurones in culture changed significantly with increasing maintenance age *in vitro* (*F*-statistic=4.00, P-value<0.01). Using linear regression, the equation of the line was y= -1.44xDIV+106.3 with R^2=0.97, indicating a linear decrease of 1.44% neurones per DIV. Therefore after 4 weeks of *in vitro* maintenance, 60% of neurones were still present in the culture.

The changes in neuronal morphological appearance are illustrated in *figure 3.5.* Both bright-field images were taken from the same primary culture in the same field using a x20 objective. *Panel A* shows the DIV 10 neurones, whereas *panel B* was taken at DIV 28. The two boxes (yellow and red) show cells which have 'survived' the ageing

process and remained in their original fixed position on the culture slip. The neurones highlighted in yellow appeared unaffected with age and looked similar in size at DIV 28 as they did at DIV 10. The neurones highlighted in red however did show a change in their morphology by appearing shrunken and visually smaller at DIV 28 in comparison to DIV 10. This heterogeneity in age-induced changes in morphological appearance is very important since it shows that not all of the neurones were affected by the ageing process to a similar degree. The significance of these changes in the neurones morphology or mobility was not investigated further.

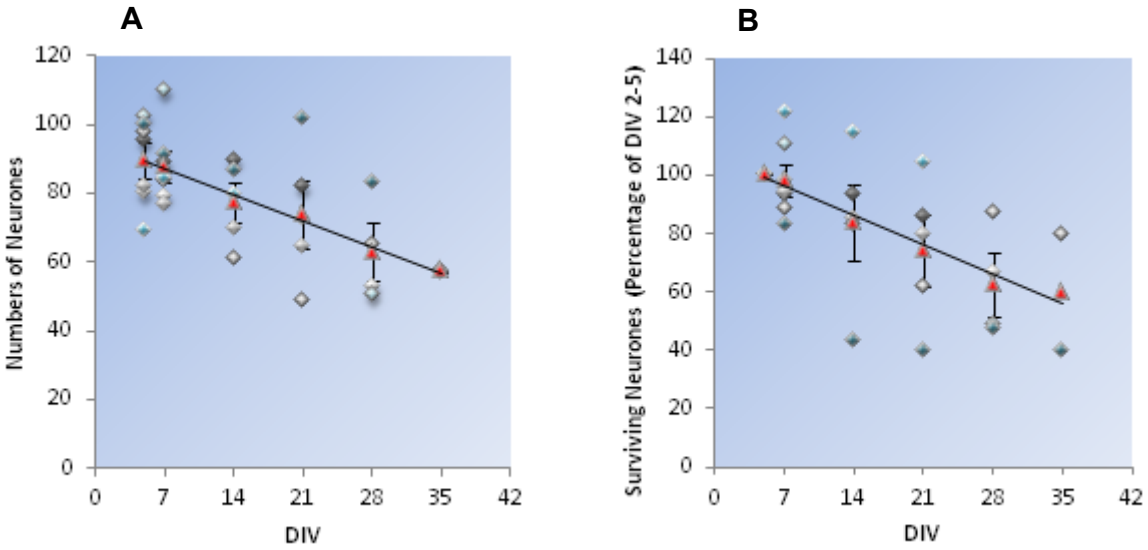

Figure 3.4. **Effect of the age of culture on neuronal numbers.**

Panel A shows the actual number of neurones counted on individual fields of view from several cultures (each culture labelled with a different coloured marker), at various time points, starting with DIV 2. From each culture a well was selected for these measurements, and 2 individual fields of view were chosen per well; each data point on the graph represents the average of these 2 fields (See *Chapter 3.1.1* for method used to count the numbers of neurones). For the data in *Panel B*, for each individual culture the number of neurones counted at DIV 2-5, was taken as reference (100%) and all the remaining readings in that particular culture were calculated as a percentage of that value, and displayed on the graph. A linear regression analysis on the fields, resulted in the equation [Surviving neurones]=106–1.44xDIV, and the ANOVA analysis showed a significant difference in the numbers of neurones counted as the days *in vitro* increases (*F*-statistic=4.00, P-value<0.01). The regression line is drawn on the graph for the examined DIV.

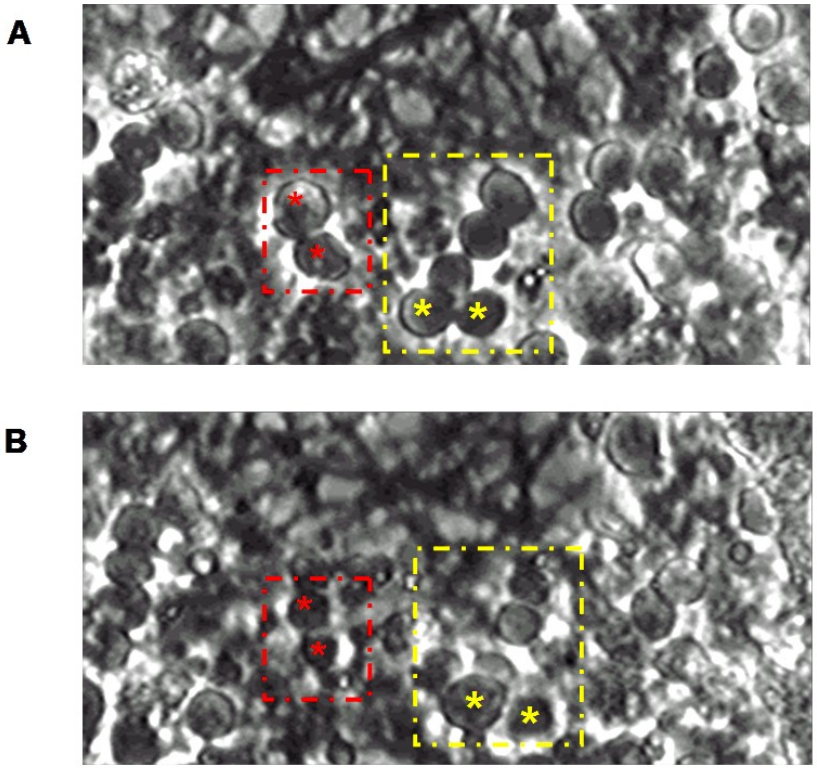

Figure 3.5. **Morphological changes in cultured neurones during the time of maintenance in culture.**

Panels (A) and (B) show the same field of view in one neuronal culture; image in Panel A was taken at DIV 10, whereas image in Panel B was taken at DIV 28. Both the yellow and red boxes highlight neurones which have remained in an almost identical position within the field. The yellow asterisk (*) shows 2 neurones which have not been affected by age and morphologically appear unchanged. The red asterisk (*) show neurones which have undergone a morphological transformation and appear smaller in size.

3.4.3 Assessment of neuronal viability of the primary culture as a function of age.

Apart from the continuous time (age) –dependent decrease in the number of neurones, the other question in assessing these long-term cultures was the status and viability of the neurones present in the culture at the various time points. The establishment of an *in vitro* model for ageing neurones requires an adequate number of neurones which remain viable after weeks of maintenance in culture conditions.

Preliminary experiments showed that the combination of Hoescht 33342 (H33) with propidium iodide (Pi) proved a better alternative than the combination of Calcein and Pi as a method for assessing neuronal viability (For complete method, see *chapter 3.3.2*). This was because the H33/Pi combination was able to distinguish between apoptotic, necrotic and viable neurones (see *figure 3.6*). In comparison, Calcein/Pi only dissociates non-viable from viable neurones, but do not determine whether a non-viable cell died via necrosis or apoptosis (Green and Reed 1998; Toescu 1998; Ward, Rego et al. 2000). Furthermore, H33/Pi was a more efficient method, since it does not require any metabolic transformation and thus has a much shorter loading time; consequently, both dyes were used in combination and loaded simultaneously (10 minutes at 30ºC) whereas, the calcein had to be loaded separate to the Pi (30 minute incubation with the calcein-AM followed by a 30 minute de-esterification period in the absence of the dye) to allow for hydrolysis of the calcein-AM by esterase to produce the fluorescent form of the dye calcein.

The results show that even though the neuronal cell number decreased over time (*Figure 3.4*), neuronal viability was maintained with very little neuronal death for up to 6 weeks: at 42 DIV, 95±1% (S.E.M.) of neurones remaining in the culture were still viable (*Figure 3.8 A and B*). One-way ANOVA analysis showed no significant difference in the percentage of viable neurones as the time in culture increased from DIV 3 to DIV 45 (*F*-statistic=1.21, P-Value>0.05, n=4 [DIV 3], n=13 [7], n=6 [14], n=6 [21], n=4 [35], n=4 [42]). A non-significant decrease of 0.09% in viability per DIV was predicted using linear regression (y= -0.090 xDIV+92.30, R^2=0.027, n=39, *F*-value=1.026, P-value>0.05).

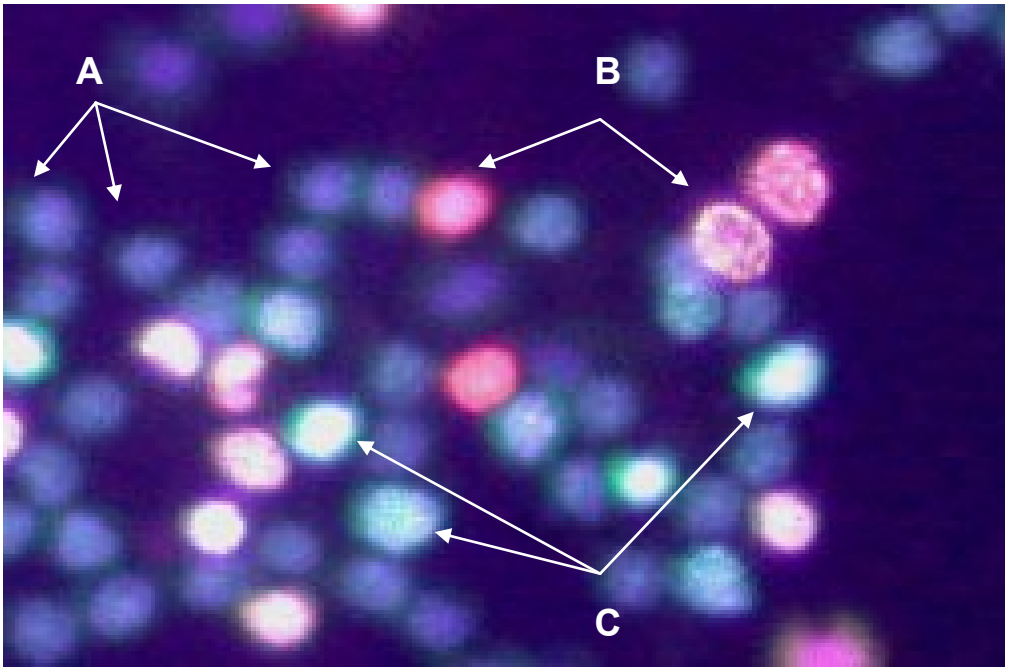

Figure 3.6. **Hoechst (H33) /Propidium iodide (Pi) staining of neuronal cells.**

This demonstrates the staining of cerebellar granular cells with a combination of H33342 and Pi, using the technique described in the *Methods* section. Three different types of neurones can be described and assigned to different states, and a representative of each category is illustrated here: (*A*) Viable cells, with a homogenous and light colouration of the nucleus with H33 (*B*) Necrotic cells, with a red staining of the nucleus with Pi, signifying that the plasma membrane is compromised and leaky, consistent with the necrotic process; (*C*) Apoptotic cells showing a highly fluorescent blue staining of the nucleus, following the condensation of the nuclear DNA, but with a viable plasma membrane.

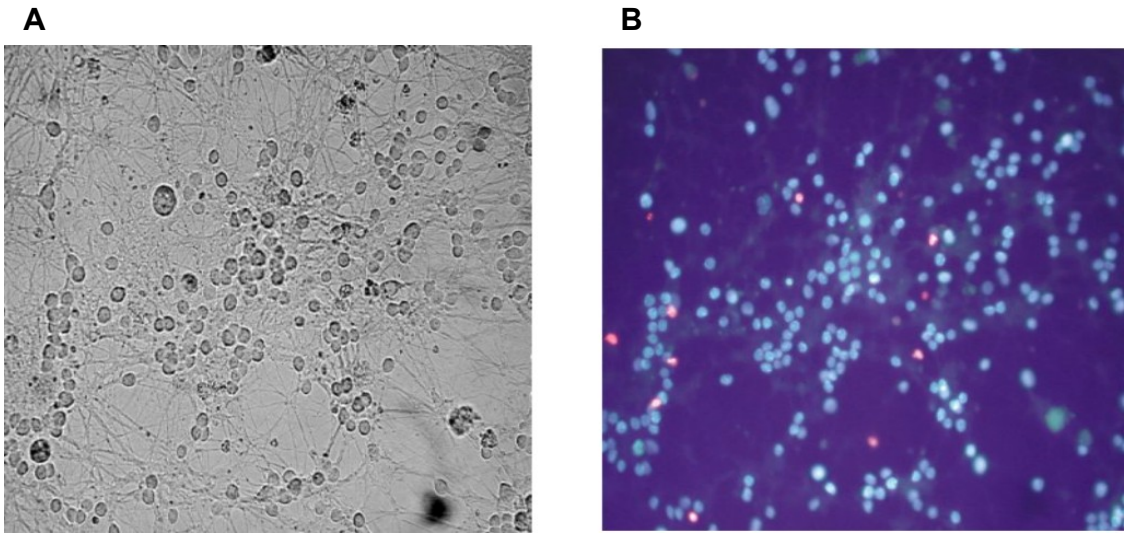

Figure 3.7. **Neuronal viability at 21 days *in vitro*.**

This figure shows the level of viable cells at 21 days *in vitro* (DIV) and maintained in BME. Image (A) shows a bright field image and image (B) shows the same focal field of cells labelled with a combination of the fluorescent dyes Hoechst (H33) and Propidium iodide. The cells stained blue are viable cells and the non-viable cells are labelled either red or highly fluorescent blue.

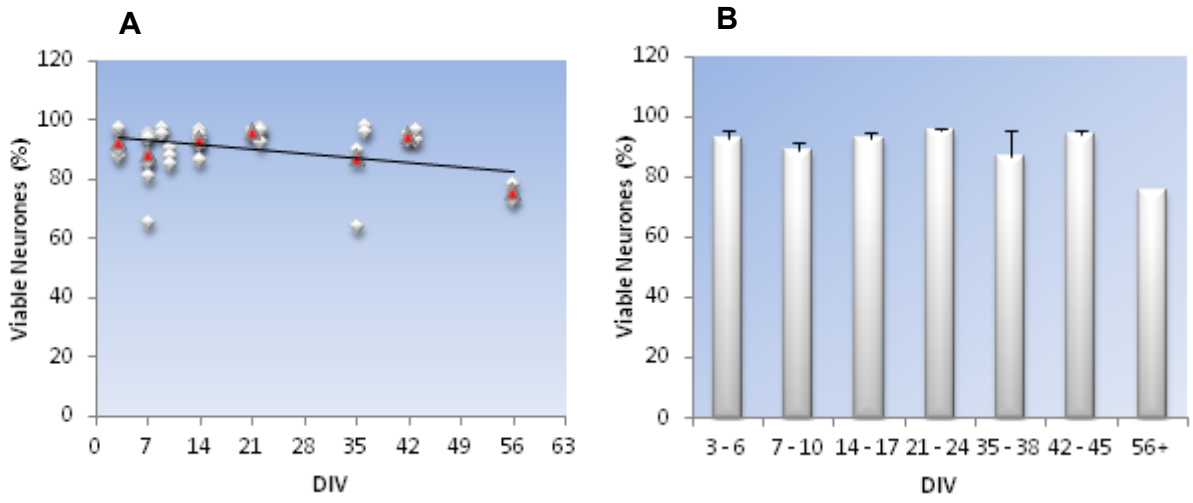

Figure 3.8. **Neuronal viability as a function of the age of the culture.**

Panel *A* shows the data for each individual time point. Each individual point represents the average value of the percentage of PI-negative neurones from 3-5 fields imaged from 1 culture at a particular time point (See *Chapter 3.3.2* for the method used to quantify the number of viable neurones). For clarity, the S.E.M. which ranged between 5-15% for each of the averaged data-points is not illustrated. To facilitate comparison, the data were pooled together in seven age groups, and the resulting average values are presented in a column chart format in Panel *B*. The error bars are the S.E.M. (with the respective 'n' value being: (3-6)=4, (7-10)=13, (14-20)=6, (21-34)=6, (35-41)=4, (42-48)=4 and (50+)=2). A regression line is shown on the graph, suggesting a non-significant decrease in viability of 0.09% with increasing culture time.

3.4.4 Purity – The neuronal culture is a very pure culture of cerebellar granule cells and the contamination with other non-neuronal cells is minimal >1%.

The next stage in characterising this primary cell culture was to explore the number of different cell types found alongside the cerebellar granule cells in the culture. Immunocytochemistry was used as a very simple yet, powerful method of estimating the level of contamination of the cerebellar granule cell culture by astrocytes. (For full method of immunochemistry see *chapter 3.3.3*).

The cellular homogeneity of the primary cerebellar granule culture is illustrated in *figure 3.9*. The nuclei of the neurones were labelled blue by the fluorescent dye Hoechst (H33), their plasma membrane and neurites were labelled red by the primary antibody MAP2. The astrocytes were labelled green by the primary antibody GFAP. In this image a total of 690 cells were counted, with 685 of these cells classified as cerebellar granule neurones and the remaining 5 cells classified as astrocytes. This equates to an overall percentage of 99.3% pure cerebellar granule neurones within this primary culture. Similar observations were made on other cultures at other DIV and in all such images the purity of the culture was similar.

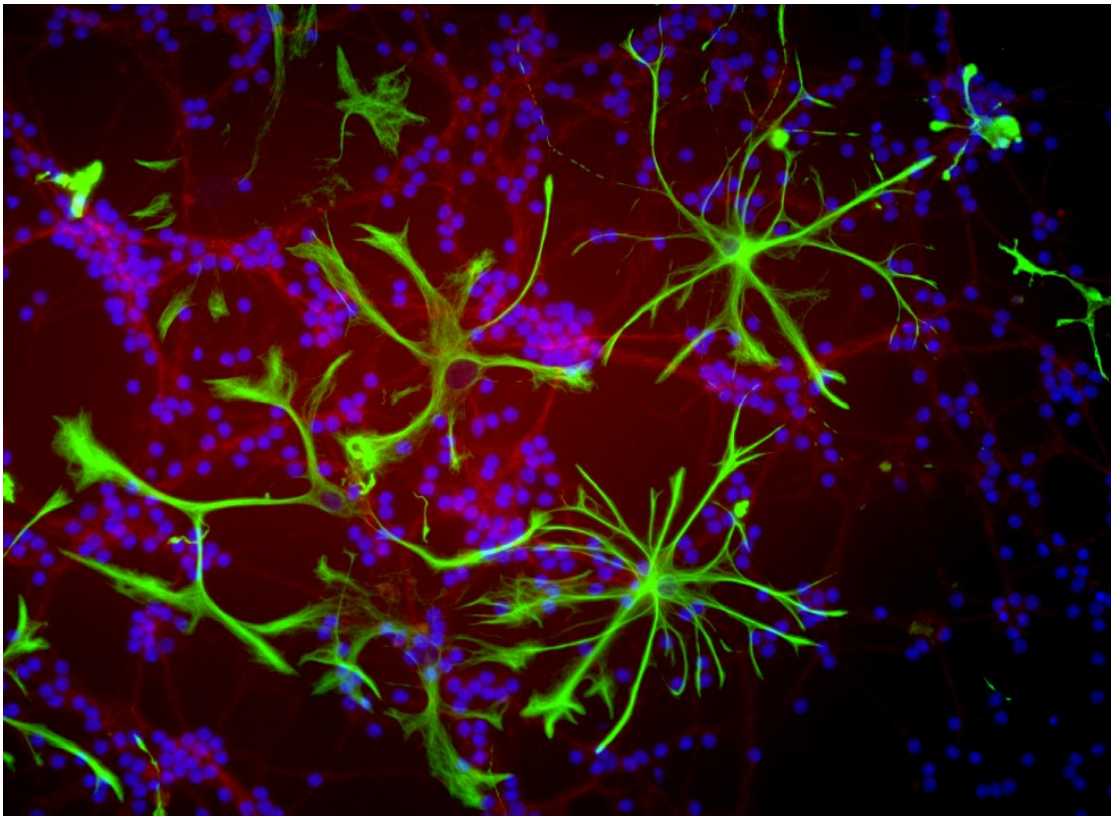

Figure 3.9. **Assessment of glial contamination in the primary cell culture.**

Immunocytochemistry was used to illustrate the low level of non-neuronal contamination of the culture. The primary antibody MAP2 kinase was used in conjunction with the fluorescent label Texas Red to label the neurones and neurites red. The primary antibody GFAP with the fluorescent label FITC was used to label the non-neuronal cells green. To make the viable cerebellar granule neurones more visible, they were labelled with the fluorescent dye Hoechst (H33). Overall, 99.3% of the cells within this population shown in this image are cerebellar granule neurones.

3.5 *Discussion*

There is a wide range of *in vivo* and *in vitro* models (Satrustegui, Villalba et al. 1996; Brewer 1997) which can be used to study the effects of ageing on neuronal cells (Hartmann, Eckert et al. 1996; Satrustegui, Villalba et al. 1996; Verkhratsky and Toescu 1998). The cerebellar granule cell culture has already been widely recognised as a suitable model for studying ageing since it shares similar age-related changes in physiology and metabolic activity as seen in *in vitro* brain slices (Hartmann, Eckert et al. 1996; Kirischuk and Verkhratsky 1996; Toescu and Verkhratsky 2000; Xiong, Camello et al. 2004). In addition it allows numerous experiments to be carried out from the minimal number of animals and enables neurones to be maintained long-term in culture conditions which is impossible to do when using brain slices (Haas, Schaerer et al. 1979). The experiments undertaken in this part of the project were focussed on characterising the cerebellar granule cell culture further and not re-affirming previous findings. In particular the following three factors were thoroughly explored: (1) the number of neurones remaining in culture with increasing *in vitro* age, (2) the percentage of viable neurones in culture with increasing *in vitro* age, (3) the percentage of cerebellar granule neurones defined by their characteristic morphological appearance in comparison to the percentage of astrocytes. Prior to this work, these three criteria were not extensively investigated in the 'ageing in a dish' model (Campbell, Hao et al. 1996; Herman, Chen et al. 1998; Blalock, Porter et al. 1999) or in any other models of ageing over a long duration of time.

The first of the three criteria was investigated by counting the actual numbers of neurones found on a specified region of the culture slip (See *Chapter 3.3.1*) and monitoring any changes in that number with time of maintenance in culture. During the very early stages post-plating, there is a potential risk that the new culture may still contain a combination of post-mitotic granule neurones that are either in the migrating process, or already in their final position in the internal granular layer (IGL) of the cerebellar cortex and mitotic neuronal progenitors from the external granular layer (EGL). This possibility arises since the cerebellar cultures are obtained from pups of postnatal age 5-7 (P5-P7), a time at which the precursor granule cells are still produced in the EGL of the cerebellum (Hatten and Heintz 1995; Goldowitz and Hamre 1998; Sotelo 2004). In addition the newly plated neurones need a short period of time for them to settle in the culture, since neuronal numbers may vary due to some neurones detaching from the culture slip either because of poor adhesion to the actual culture slip or the removal of non-viable neurones from the newly forming network (Aksenova, Aksenov et al. 1999). By allowing a recovery period of 36-48 hours post-plating, allows a much better and confident identification of viable neurones thereby providing a more accurate estimate of initial neuronal numbers.

The results showed no significant difference in the numbers of neurones counted in a fixed field as the culture aged from DIV 2 to DIV 5. As expected, there was a significant decrease in the number of cells with increasing number of days in culture, indicating a 40% decline in neuronal numbers by the end of week 4. This fits in with previous studies which showed a decrease in neuronal numbers in primary long-term rat cerebral cortical cultures after 11 DIV (Robert, Cloix et al.), and between 14-21

DIV (Kim, Oh et al. 2007). More important than the expected decrease in neuronal number is our observation that, within the remaining population, the percentage of viable neurones remained very high (94% of neurones were still viable at DIV 45), with no significant change in viability from DIV 3–DIV 45. The fact that the remaining neurones which have survived the *in vitro* environment are still viable is in agreement with previous investigations which have shown primary cultures of rat cortical neurones surviving up to 30-50 DIV (Robert, Cloix et al.), mouse cortical neurones surviving up to 60 DIV (Lesuisse and Martin 2002), striatal neurones surviving up to 50 DIV and hippocampal neurones surviving up to 35 DIV (Aksenova, Aksenov et al. 1999). This suggests that the neuronal effects associated with the ageing process are not based on the decline of neuronal numbers but due to alterations in the way the existing neurones and their network function.

Proliferation of non-neuronal cell types was reduced by adding 10μM cytosine arabinoside to the cultures 36-48 hours post-plating and maintaining the neurones in 25mM KCL. This is a well established method of reducing the numbers of non-neuronal cells from a primary culture (Gallo, Kingsbury et al. 1987; Daniels and Brown 2002). The neurones were kept slightly depolarised in the presence of KCl since this has been shown to protect the neurones (Gallo, Kingsbury et al. 1987; Toescu 1999; Daniels and Brown 2002) from any toxic effects of the cytosine arabinoside (Toxicity towards cerebellar granule neurones: EC50=60μM (Dessi, Pollard et al. 1995)) (Martin, Wallace et al. 1990; Seil, Drake-Baumann et al. 1992).

The results from the immunocytochemistry studies showed that 99% of the primary cell culture consisted of cerebellar granule neurones which confirms the established view that primary culture of cerebellar granule cells contain very little contamination from other cell types (~5% non-neuronal cells (Gallo, Ciotti et al. 1982; Thangnipon, Kingsbury et al. 1983)).

In summary this work provides further support for using cerebellar granule cell culture as a model for studying the effects of ageing associated with changes in normal physiology and metabolic activity. In the primary cell culture, the neurones are able to 'survive' with very high levels of viability which is essential when studying aged neurones at both the local (cellular) and neuronal network levels. The high percentage of cerebellar granule cells in culture makes it ideal when studying the network as whole (for example the response of all the neurones to different glutamate concentrations) since other cell types will have little influence on the responses. At the very extreme end of *in vitro* conditions (DIV 56+) there is a decline in neuronal numbers and collective measurements of all the neurones may not be ideal. At this stage, experiments focussed at the cellular level would still be justified since individual viable neurones could be selected for experimentation.

4 The effect of age on vulnerability towards glutamate excitotoxicity

4.1 *Neuronal Vulnerability*

In *chapter 3*, further characterisation of primary cultured cerebellar granule neurones provided support for its suitability as an *in vitro* 'ageing in a dish' model that can be used to study the underlying factors of the ageing process. After establishing a suitable experimental model, the next stage of the project was to identify if there was an increase in neuronal vulnerability that could be attributed to the ageing process. Since previous work has shown a link between neuronal age and increased vulnerability towards glutamate-induced cell death (Choi, Maulucci-Gedde et al. 1987; Vergun, Keelan et al. 1999), the effect of glutamate excitotoxicity on neurones at different *in vitro* ages was chosen as the main focus of investigation. In particular, the experiments were designed to assess the effect of the *in vitro* ageing process on the level of neuronal death, the time period for the neuronal death to be initiated and the rate of neuronal death which could indicate a change in neuronal vulnerability.

4.1.1 Glutamate Excitotoxicity

Glutamate is the major excitatory neurotransmitter in the human central nervous system (Brosnan and Brosnan 2012) and is essential for normal neuronal signalling (Mark, Prost et al. 2001). There are two types of glutamate receptor (Michaelis 1998; Dingledine, Borges et al. 1999; Niciu, Kelmendi et al. 2012), the ionotropic glutamate receptors (NMDA receptor (Monaghan and Cotman 1985), AMPA receptor and Kainate receptor) and the metabotropic glutamate receptors (Group I, Group II and Group III). The ionotropic receptors are ligand-gated ion channels that when activated by the binding of glutamate to their receptor, they undergo a conformational change allowing the passage of ions through their central pore. Their respective receptor names derive from their affinity to bind to the specific agonists (ligands): N-methyl-D-aspartate (NMDA), α-amino-3-hydroxy-5-methyl-4-isoxazole proprioninc acid (AMPA) and Kainate. The genes that express the subunits that make up the three types of ionotropic receptor are: NMDA (NR1, NR2A-D and NR3), AMPA (GluR1-4) and Kainate (GluR5-7 and Ka1-2). Of the three ionotropic receptors, the NMDA receptor has the highest permeability of Ca^{2+} with AMPA's permeability of Ca^{2+} dependent upon which of its 4 subunits have combined to form the receptor (Burnashev, Monyer et al. 1992). All three receptors allow the passage of Na^{+} through their pores, which means that both the AMPA and kainate receptors can activate the NMDA receptors by depolarising the membrane resulting in removal of the Mg^{2+} block (Wang and Qin 2010). The metabotropic glutamate receptors are G-protein coupled receptors, classified as Group I, Group II and Group III (Michaelis 1998; Wang and Qin 2010). The genes that express the subunits that make up the

three groups are: mGluR1 and mGluR5 (Group I), mGluR2-3 (Group II) and mGluR4, 6-8 (Group III). These G-protein coupled receptors exert their effects through the formation of IP_3 from phospholipase C,(Group I) and protein kinase C via DAG (Group II and Group III) resulting in the release of Ca^{2+} from intracellular store (Arundine and Tymianski 2004).

Even though glutamate is a crucial part of neuronal signalling, numerous studies over many years have shown that excessive levels of cytosolic glutamate can exert a toxic effect on neurones of the CNS, referred to as glutamate excitotoxicity (Olney 1969). This elevation in cytosolic glutamate leading to excitotoxicity can occur following head trauma, stroke, ischemia (Olney, Collins et al. 1986; Rothman and Olney 1986; Dirnagl, Iadecola et al. 1999; Lee, Zipfel et al. 1999) and has been shown to have a key role in autoimmune demyelination diseases such as multiple sclerosis (Pitt, Werner et al. 2000).

The route of excitotoxicity caused by exposure to high cytosolic glutamate concentrations, has been shown to occur through ionotropic (NMDA receptors in cultured cortical neuronal cells (Choi, Koh et al. 1988; Hartley, Kurth et al. 1993), NMDA receptors in dissociated cell culture from rat spinal cord (Urushitani, Nakamizo et al. 2001) and AMPA/Kainate receptors in a demyelinating mouse model used to study multiple sclerosis (Pitt, Werner et al. 2000)) and metabotropic (Group I metabotropic receptors in hippocampal neuronal cell culture (Attucci, Clodfelter et al. 2002)) glutamate receptors. Even short exposure (5 minute) of primary neocortical neurones to concentrations of glutamate that exceed the normal cellular level were

found to induce neuronal swelling as early as 90 seconds post-glutamate exposure and became more widespread as time progressed (Choi, Maulucci-Gedde et al. 1987).

4.1.2 Delayed Ca^{2+} de-regulation

One of the classic characteristic effects of glutamate excitotoxicity is de-regulation of cytosolic Ca^{2+} following the exposure of the neurones to glutamate. During non-excitotoxic glutamate stimulation, glutamate receptors are activated resulting in an inward movement of Ca^{2+} into the cytosol. This increase in $[Ca^{2+}]_i$ is restored back to normal basal (pre-glutamate) levels by a combination of the following homeostatic mechanisms: (1), the removal of the Ca^{2+} from the cell through the plasma membrane Ca^{2+}-ATPase pump and the Na^{+}/Ca^{2+}-exchanger; (2), through cytosolic buffering of Ca^{2+} by Ca^{2+}-binding proteins; (3), sequestration of the Ca^{2+} by the mitochondria and endoplasmic reticulum. The exposure of neurones to excitotoxic doses of glutamate, even for a short period of time, has been shown to induce a well known phenomenon known as 'delayed Ca^{2+} de-regulation' (DCD) in primary cultured cerebellar granule neurones (Manev, Favaron et al. 1989), cultured embryonic spinal neurones (Tymianski, Charlton et al. 1993) and primary cultured hippocampal neurones (Randall and Thayer 1992). During DCD, three distinct changes in $[Ca^{2+}]_i$ occur: (1), A rapid elevation in $[Ca^{2+}]_i$ followed immediately by a sharp decrease, which does not fully recover to resting (Pre-glutamate) levels; (2), a stabilisation in the $[Ca^{2+}]_i$ again that does not reach basal resting levels; (3), an uncontrolled increase in $[Ca^{2+}]_i$ which does not show any signs of recovery. These three stages

associated with DCD are normally indicators for the subsequent death of the neurones by necrosis (Choi, Maulucci-Gedde et al. 1987), apoptosis (Qin, Wang et al. 1996) or a mixture of both (Ankarcrona, Dypbukt et al. 1995; Martin, Al-Abdulla et al. 1998). The size and duration of the Ca^{2+} influx will depend on various factors including the type of glutamate receptors that are activated. The combination of the aforementioned Ca^{2+} homeostatic mechanisms help the cells to recover from the sudden increase in $[Ca^{2+}]_i$, however desensitisation of the glutamate receptors, delays in mitochondrial Ca^{2+} uptake and slow Ca^{2+} extrusion all could result in incomplete recovery of the $[Ca^{2+}]_i$ back to pre-glutamate levels. A consequence of incomplete recovery of the $[Ca^{2+}]_i$ would be a depletion of ATP as a result of the movement of Ca^{2+} into the mitochondria coupled with an increase in free radical damage.

4.2 *Aim*

This part of the project is focussed on identifying if there is a correlation between vulnerability to the excitotoxic effects of glutamate and neuronal ageing in culture.

4.3 *Methods*

4.3.1 Assessment of neuronal viability using propidium iodide for high throughput measurements.

A 5mg/ml stock solution of propidium iodide (Pi) (Sigma, UK) was prepared by diluting the Pi in dH_2O. For experimental purposes, the Pi stock was further diluted to a final concentration of 50µg/ml, using a 10mM HEPES buffer (pH 7.4) containing 145mM NaCl, 5mM KCl, 1mM $MgCl_2$x6, 1.5mM $CaCl_2$ and 12mM Glucose (Sigma, UK) (referred to as 'experimental' medium). Aluminium foil was used to protect the Pi against direct exposure to light in order to prevent any photobleaching of the Pi, which may reduce the overall fluorescent signal..

Cerebellar granule neurones were plated directly onto the bottom of a 24-well microplate at a plating density of 280,000 cells per well (see *Methods Chapters 2.1.1-2.1.4*). Taking care not to dislodge the cells from the bottom of the microplate, the culture medium from each well was gently removed and replaced with 500µl of the 'experimental' medium containing 50µg/ml Pi (referred to as 'Pi-experimental' medium). Measurements of the Pi's fluorescence were made using a FLUOstar OPTIMA microplate reader (BMG LABTECH) with an excitation wavelength of 544nm and an emission wavelength of 612nm. Four initial measurements of the Pi's fluorescent signal were recorded for each well at 60 second intervals. The mean of these four fluorescence values represented the resting level of Pi fluorescence (pre-

glutamate) which was used to normalise all subsequent recordings for that particular well.(See *figure 4.1*). The 'Pi-experimental' medium was then removed from the microplate wells (stored away from light in a separate 24-well plate for later use) and replaced with 500µl of glutamate (0µM, 12.5µM, 25µM, 50µM, 100µM and 200µM). The glutamate was diluted in 'experimental' medium containing no Mg^{2+} and 10µM glycine (Sigma), referred to as '0Mg^{2+} experimental medium'. The neurones were incubated in the '0Mg^{2+} experimental' medium (with Pi at a final concentration of 50µg/ml) for 60 minutes. Fluorescence measurements were made at 15 minute intervals throughout this 60 minute incubation time (See *figure 4.1*). After removal of the glutamate, the 'Pi-experimental' medium used for the initial reference recordings (pre-glutamate) was returned to its original well and fluorescence measurements were taken at 60 minute intervals for up to 24 hours, allowing a dynamic assessment of the excitotoxic process (See *figure 4.1*). At 24 hours, the 'Pi-experimental' medium was removed from the wells (stored in the second empty microplate) and replaced with 300µl EtOH (100%) or Triton X (0.02%) to induce death of all of the cells in each well. After 10 minutes in the EtOH (or Triton X), the Pi solution was once again returned to its original well and five fluorescence measurements were taken at 30 second intervals (See *figure 4.1*), with the mean of these values representing the maximum (100%) level of neuronal death for that specific well.

Two wells containing only Pi without any cells were used to take background readings, which was subtracted from each of the fluorescence measurements. This background subtracted data obtained from each well was then expressed as a percentage of cell death, using the initial resting reference value for that particular

well, as 0% cell death (resting level of cell death) and the mean fluorescence readings post-EtOH/Triton X as 100% cell death (maximum cell death), for each of their respective wells.

This adapted Pi method was published as an application note for BMG Labtech, which is the company that manufactured the microplate reader. The application note can be found in the *Appendix* section.

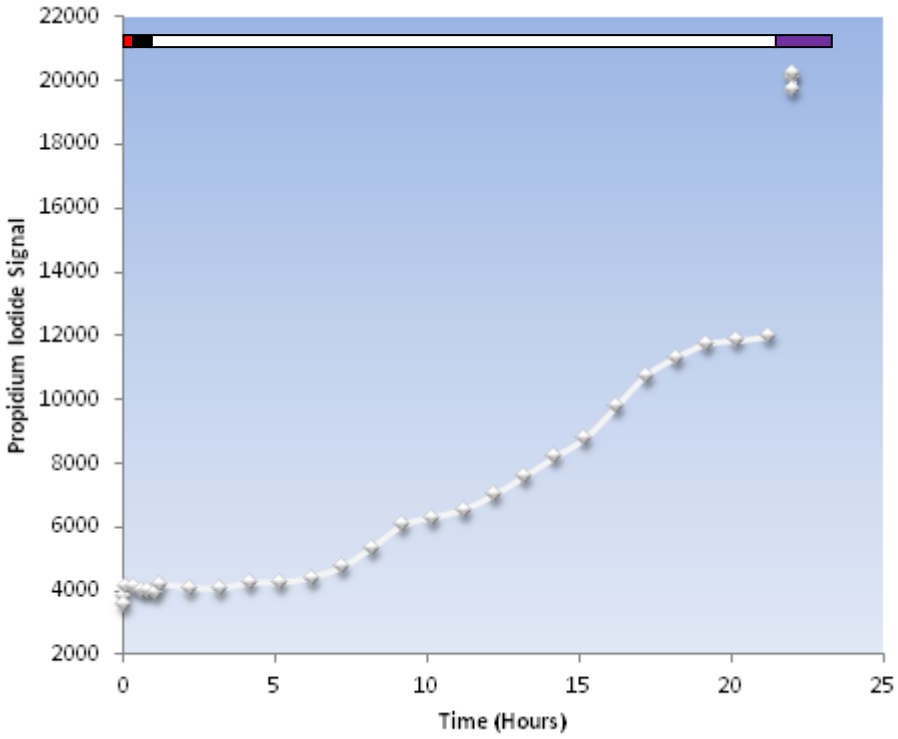

Figure 4.1. **Dynamic propidium iodide measurements.**

This graph shows the propidium iodide (Pi) signal recorded at regular intervals before, during and after a 60 minute glutamate stimulation. In order to obtain a basal Pi signal, four measurements were made pre-glutamate incubation, highlighted by the *red box*. The Pi medium was switched to a Pi solution containing glutamate and measurements were made at 15 minute intervals (*Black box*). After 60 minutes, the glutamate was removed and replaced with the original Pi solution (used pre-glutamate - the *red box*), with measurements recorded at hourly intervals for 24 hours (*White box*). The Pi solution was then removed and the neurones were incubated in 100% EtOH or 0.02% Triton X for 10 minutes. After the removal of the EtOH/Triton X, the Pi solution was again returned to each well and five measurements were made (*Purple box*). In order to express the data as a 'percentage of cell death', the mean of the measurements taken during the resting phase (*Red box*) was used to represent a 'resting level' of death and the mean of the measurements taken after fixation with EtOH or Triton X (*Purple box*) was used as a 'maximum level' of death. All of the data points were normalised using the resting death Pi signal (0% cell death) and the maximum death Pi signal (100% cell death).

4.4 *Results*

4.4.1 Age increases the vulnerability of neurones to the excitotoxic effects of glutamate.

High-throughput dynamic measurements with propidium iodide (Pi) were used to monitor levels of neuronal death caused by exposure to varying concentrations of glutamate. Cerebellar granule neurones which had been maintained *in vitro* for varying lengths of time were incubated in glutamate (0, 12.5μM, 25μM, 50μM, 100μM and 200μM) for 60 minutes and quantitative measurements of cell viability were made at hourly intervals for 24 hours post-glutamate exposure.

The results showed that the greater the *in vitro* age of the culture, the more vulnerable the neurones became towards the excitotoxic effects of glutamate (See *figure 4.2*). Analysis of the data using linear regression showed significant positive correlation between *in vitro* age and neuronal death when the neurones were exposed to 25μM, 50μM and 200μM glutamate. The amount of neuronal death increased by 0.6% per DIV with 25μM glutamate ($y=0.649xDIV+28.305$, $R^2=0.200$, $n=22$, *F*-value=5.000, P-value<0.05), 0.8% per DIV with 50μM glutamate ($y=0.804xDIV+28.521$, $R^2=0.306$, $n=24$, *F*-value=9.700, P-value<0.01) and 0.7% per DIV with 200μM glutamate ($y=0.672xDIV+34.22$, $R^2=0.240$, $n=26$, *F*-value=7.594, P-value<0.05). When the neurones were exposed to lower glutamate concentrations there were no significant correlation (Equation of the line: [0μM] $y=0.195xDIV+15.15$,

R^2=0.036, n=27, *F*-value=0.920, P-value>0.05, [12.5μM] y=0.522xDIV+25.046, R^2=0.1375 n=23, *F*-value=3.347, P-value>0.05 and [100μM] y=0.572xDIV+35.056, R^2=0.142, n=26, *F*-value=3.986, P-value>0.05).

The slopes obtained from each of these graphs were calculated (0μM=0.195, 12.5μM=0.522, 25μM=0.649, 50μM=0.804, 100μM=0.572, 200μM=0.671). The larger the slope, the bigger the difference between the level of neuronal death observed in the cells at the lower DIV (*in vitro* age) in comparison to ones at the higher DIV (*in vitro* age). This difference between the younger and older neurones is shown to increase with glutamate, reaching a peak at 50μM (See *figure 4.2 Panel A-F*).

During the control experiments (0μM glutamate exposure) there was some cell death seen in both the young (DIV 7-15) *in vitro* age group (15.2% ±3.7) and the old (DIV 22-52) *in vitro* age group (23.8% ±4.7) (N.B. This definition of young (DIV 7-15) and old (DIV 22-52) neurones will be used throughout this thesis). One explanation for this rise in non-glutamate cell death is that during the experiments, the cells were maintained in a multi-plate reader at a controlled temperature in a HEPES-based environment. Keeping the neurones in experimental media for 24 hours instead of the nutrient rich culture media can act as a metabolic stressor to the neurones giving rise to some degree of cell death.

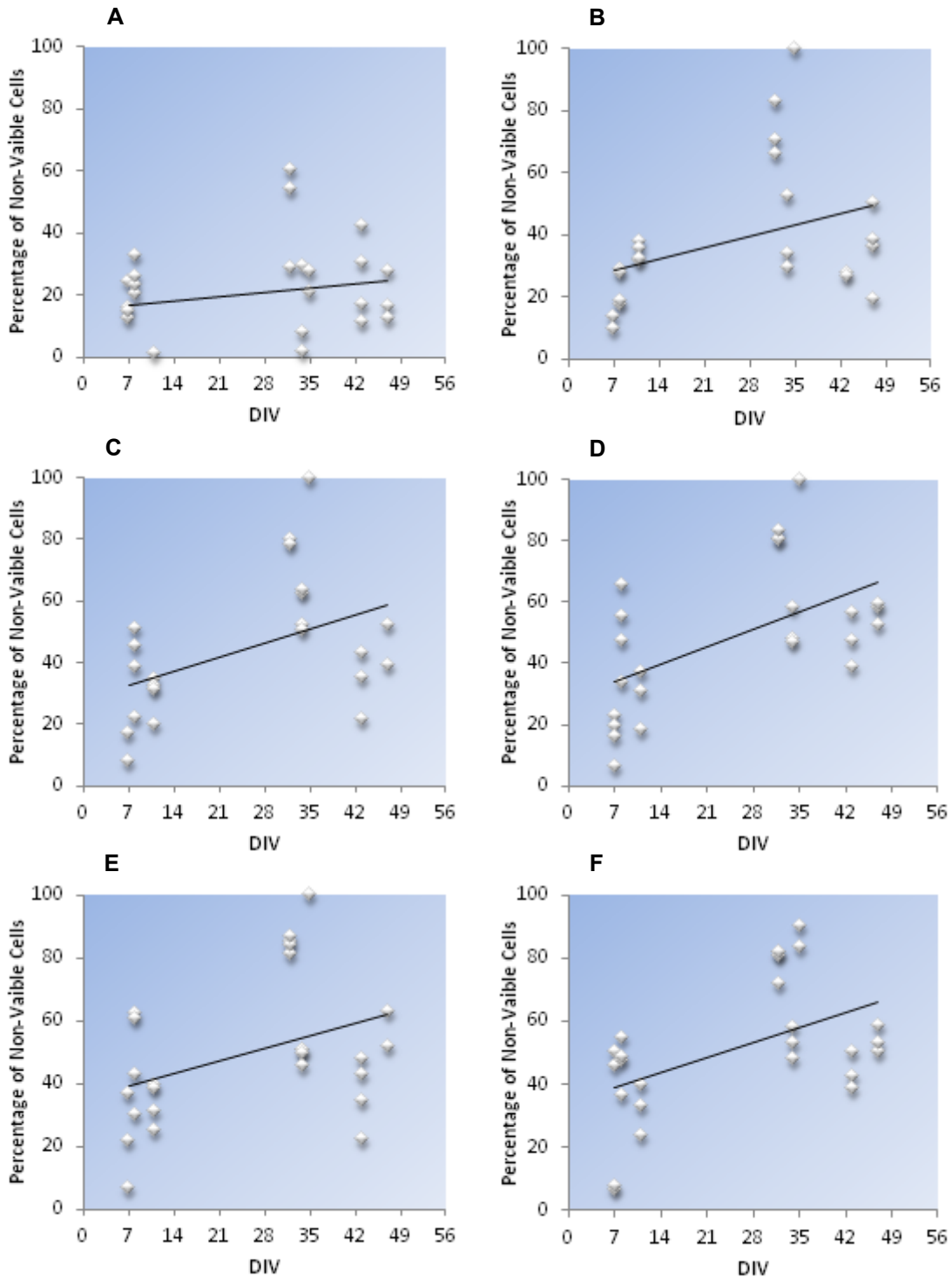

Figure 4.2. **Glutamate excitotoxicity as a function of the age of the culture.**

These graphs show the relationship between DIV and the percentage of non-viable neurones (cell death) 24 hours after a 60 minute exposure to the following glutamate concentrations: (*A*) 0μM, (*B*) 12.5μM, (*C*) 25μM, (*D*) 50μM, (*E*) 100μM and (*F*) 200μM.

4.4.2 The effects of glutamate excitotoxicity on young neurones compared to older neurones.

The linear regression and slope analysis showed an association between older *in vitro* age and increased vulnerability towards glutamate excitotoxicity. In order to better analyse this data, all of the results from section *4.4.1* were reorganised into two groups based on the cell's *in vitro* age. Neurones which had been maintained in culture for between 7-15 days were classified as 'young' neurones and neurones which had been *in vitro* for 22-52 days were deemed as 'old'. The age ranges for the young and old groups were chosen based on previous studies looking at the effect of *in vitro* age on the response of neurones to glutamate (Vergun, Keelan et al. 1999) and KCl stimulation (Toescu and Verkhratsky 2000; Xiong, Camello et al. 2004).

The data was analysed from two separate lines of questioning: (1) Does vulnerability of the neurones towards glutamate excitotoxicity increase as the glutamate concentration increases in each of the two *in vitro* age groups? (2) Does *in vitro* age increase the vulnerability towards glutamate excitotoxicity?

To answer the first question, one-way ANOVA analysis showed a highly significant difference in the percentage of non-viable neurones when each *in vitro* age group was exposed to increasing glutamate concentrations ranging from 0µM to 200µM (One-way ANOVA analysis: Young (DIV 7-15), F-statistic=3.15, $P<0.05$, n=64; Old (DIV 22-52), F-statistic=8.21, $P<0.01$, n=84).

To answer the second question, incubating the neurones in glutamate (0-200μM) did show significant differences in the percentage of cell death (recorded 24 hours post-glutamate stimulation) between the young and old groups of neurones (12.5μM *F*-statistic=7.96, P<0.05, n=10 [Young], n=13 [Old]; 25μM *F*-statistic=11.16, P<0.01, n=10 [Young], n=12 [Old]; 50μM *F*-statistic=16.75, P<0.01, n=11 [Young], n=13 [Old]; 100μM *F*-statistic= 8.81, P<0.01, n=11 [Young], n=15 [Old]; 200μM *F*-statistic=16.08, P<0.01), n=11 [Young], n=15 [Old]. When comparing the percentage of non-viable neurones (recorded 24 hours post-glutamate stimulation) between the young and old *in vitro* age groups, in the absence of any glutamate stimulation, there were no significant differences (*F*-statistic=1.87, P>0.05, n=11 [Young], n=16 [Old]) showing in resting culture conditions age has no significant effect on neuronal viability. Results from these studies are illustrated in *figure 4.3*.

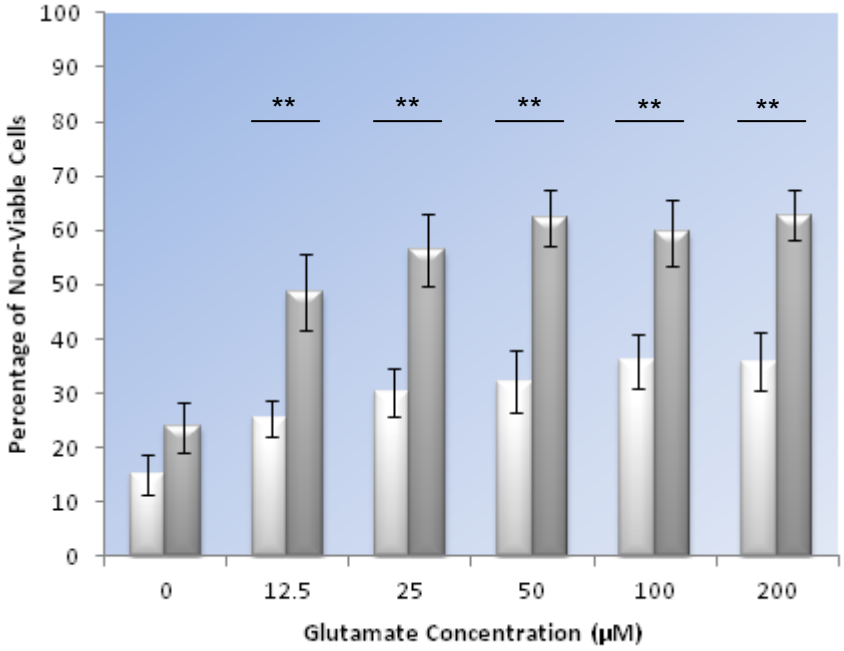

Figure 4.3. **The effect of the glutamate concentration on young and old groups of neurones.**

This graph shows the mean percentage (±S.E.M.) of non-viable neurones (at 24 hours post-glutamate stimulation) from cultures consisting of young (DIV 7-15: Light coloured bars) and old (DIV 22-52: Dark coloured bars) cells, 24 hours after they were incubated in glutamate (0µM, 12.5µM, 25µM, 50µM, 100µM and 200µM) for 60 minutes. Statistically significant differences in the percentage of non-viable cells at 24 hours post-glutamate between the young and old group of neurones are also highlighted on the graph: (*) $P<0.05$ and (**) $P<0.01$.

4.4.3 Dynamics of neuronal death following glutamate incubation and the effect of *in vitro* age.

Up to this point, data from each experiment was analysed using an end-point measurement corresponding to the highest recorded level of propidium iodide (Pi) signal (the highest measure of non-viable neurones) for that particular experiment 24 hours after incubation in the chosen experimental condition (Glutamate). Since the Pi method, which is normally used for end point measurements of cellular viability, was adapted to allow monitoring of neuronal viability over a 24 hour period of time (See *chapter 4.3.1*), the dynamics behind the nature of the neuronal death could be further explored. The first parameter investigated was the time taken for initiation of neuronal death following removal of the glutamate after the 60 minute incubation period (Lag period).

Using the dynamic data from each individual culture slip, graphs were plotted to enable the start point of the neuronal death to be identified. This start point of neuronal death was defined as the time point (after the removal of the glutamate) where there were at least 3 consecutive increases in the percentage on non-viable neurones (See *figure 4.4*.).

In control conditions (in the absence of glutamate), surprisingly the lag period increased with *in vitro* age (linear regression analysis; equation of the line:

y=0.136xDIV+3.883, R^2=0.244, n=22, *F*-value=6.442, P<0.05) (See *figure 4.5 Panel A*). On the introduction of glutamate, this observation in lag period reversed (See *figure 4.5 Panel B-F*), becoming shorter with *in vitro* age as the glutamate concentration increased. Analysis of the data using linear regression showed significant negative correlation between *in vitro* age and the time taken for death to start (post-glutamate stimulation), when the neurones were exposed to 50μM and 100μM glutamate (Equation of the line: [50μM] y= -0.117xDIV+5.536, R^2=0.469, n=24, *F*-value=15.892, P-value<0.0, [100μM] y= -0.081xDIV+3.506, R^2=0.259, n=26, *F*-value=6.622, P-value<0.05). This difference in lag period between the young and old neurones exposed to 50μM glutamate is illustrated in *figure 4.4*. When the neurones were exposed to all of the other glutamate concentrations there were no significant correlation (Equation of the line: [12.5μM] y=0.032xDIV+4.71, R^2=0.03 n=23, *F*-value=0.526, P-value>0.05, [25μM] y= -0.058xDIV+4.72, R^2=0.177, n=22, *F*-value=3.655, P-value>0.05 and [200μM] y= -0.030xDIV+3.108, R^2=0.023, n=26, *F*-value=0.417, P-value>0.05).

As previously described, the data was grouped based on the *in vitro* age of the neurones and classified as young (DIV 7-15) or old (DIV 22-52). In young neurones, there were no significant differences in the measured lag periods regardless of the concentration of glutamate that the neurones were exposed to (One-way ANOVA analysis: *F*-statistic=1.53, P>0.05, n=11[0μM], n=10 [12.5μM], n=10 [25μM], n=11 [50μM], n=11 [100μM], n=11 [200μM]), however older neurones did show significant differences (One-way ANOVA analysis: *F*-statistic=11.80, P<0.01, n=11[0μM], n=9 [12.5μM], n=9 [25μM], n=9 [50μM], n=10 [100μM], n=9 [200μM]).

Comparisons between the lag periods of the young and old groups of neurones showed significant differences when the cells were incubated in resting conditions (One-way ANOVA analysis: *F*-statistic=9.12, P<0.01, n=11[Young], n=11 [Old]), in 50μM glutamate (One-way ANOVA analysis: *F*-statistic=18.56, P<0.01, n=11[Young], n=9 [Old]) and in 100μM glutamate (One-way ANOVA analysis: *F*-statistic=6.91, P<0.05, n=11[Young], n=10 [Old]). No significant differences between the lag period of young and old neurones were shown at glutamate concentrations: 12.5μM (One-way ANOVA analysis: *F*-statistic=0.25, P>0.05, n=10[Young], n=9 [Old]), 25μM (One-way ANOVA analysis: *F*-statistic=1.711, P>0.05, n=10[Young], n=9 [Old]) and 200μM (One-way ANOVA analysis: *F*-statistic=0.78, P>0.05, n=11[Young], n=9 [Old]).

All of the lag periods for each of the experiments were expressed as a mean value (±S.E.M) and plotted against the glutamate concentration (*figure 4.6*). The graph illustrates that the lag period between the end of the glutamate exposure and the start of neuronal death was shortened both with increasing glutamate concentration and with increasing *in vitro* age.

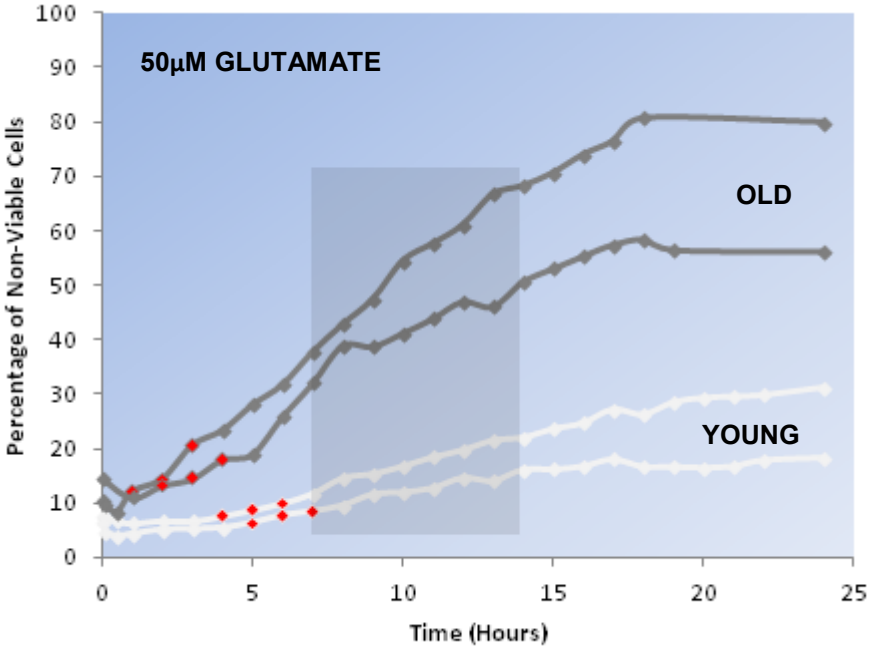

Figure 4.4. **The effect of *in vitro* age on glutamate-induced cell death.**

This graph shows the change in propidium iodide (Pi) signal over 24 hours following a 60 minute incubation in 50µM glutamate from four separate experiments. The 'light coloured' traces are the results from two experiments using 'young' neurones (7-15 DIV) and the dark coloured traces are from two experiments using old neurones (21-52 DIV). The red markers represent three consecutive increases in neuronal death which is defined as the 'lag period'. The shaded box shows the time period (7-14 hours) that the slope of each of the curves was calculated.

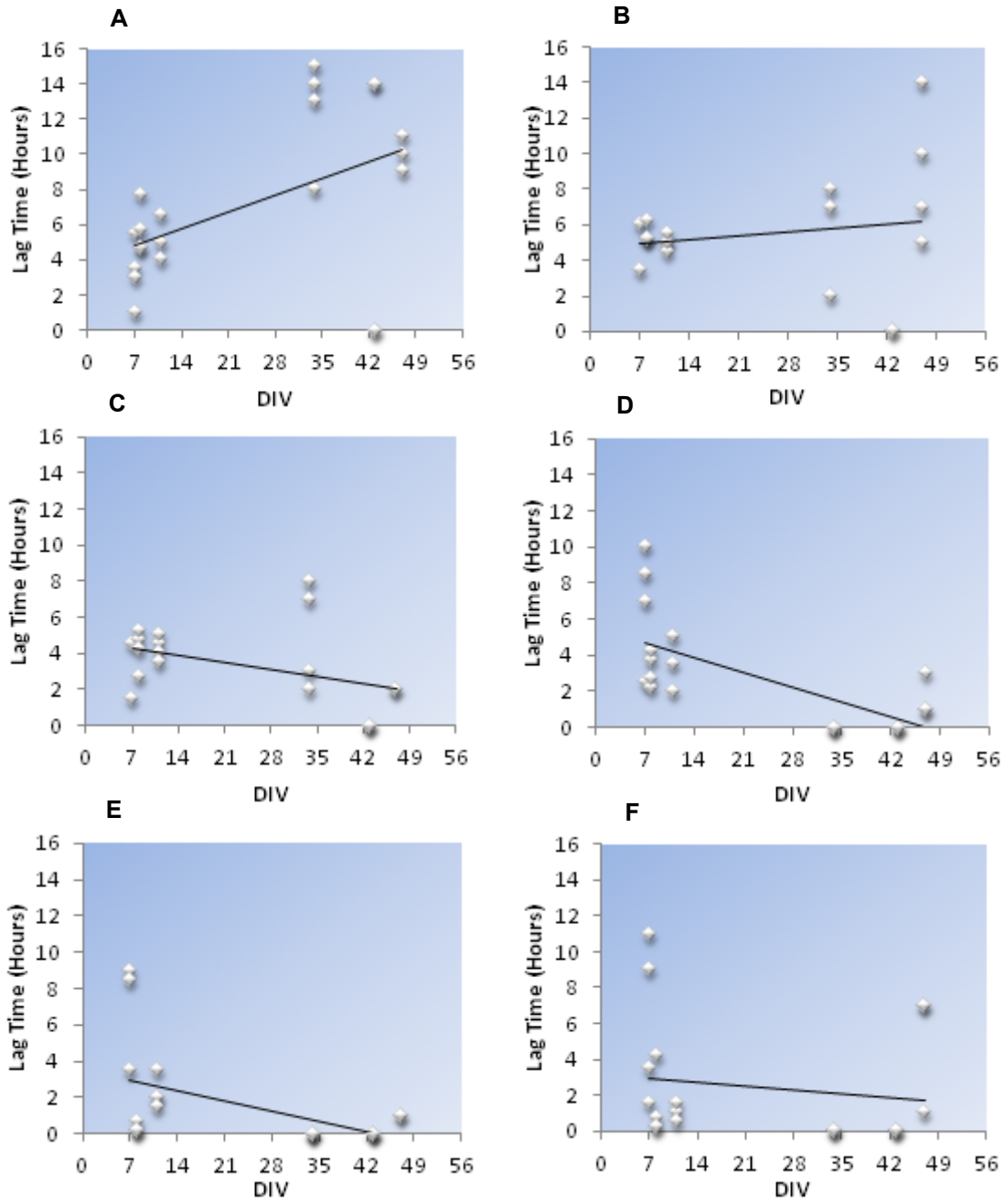

Figure 4.5. **Lag time as a function of the age of the culture.**

These graphs show the relationship between DIV and the time between the removal of glutamate and the start of neuronal death (Lag period). Each graph represents data from a different glutamate concentration with the results of linear regression analysis: (A) 0μM, (B) 12.5μM, (C) 25μM, (D) 50μM, (E) 100μM and (F) 200μM.

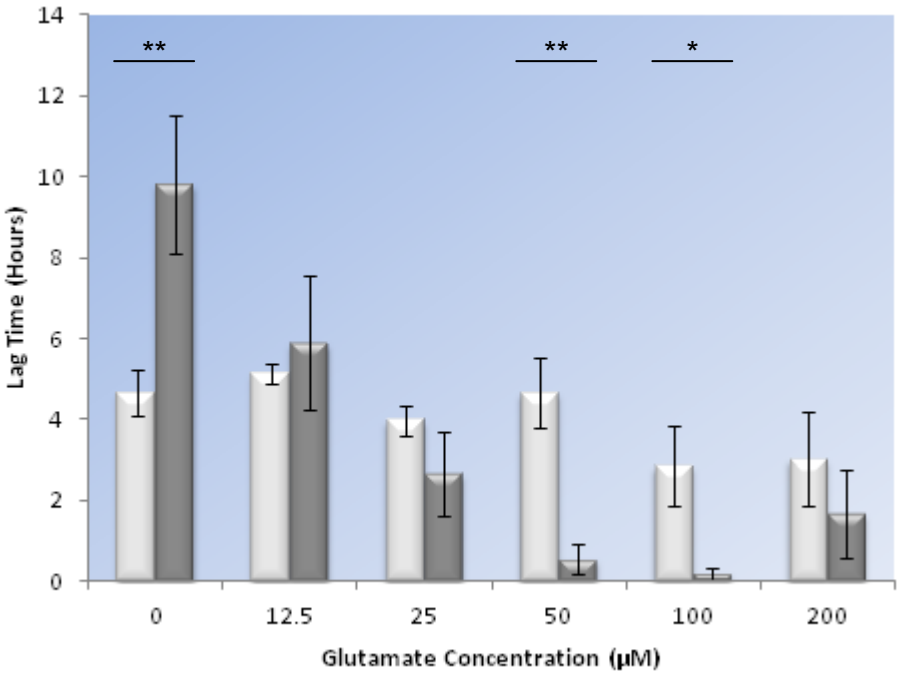

Figure 4.6. **Differences in lag period between young and old groups of neurones.**

This graph shows the mean percentage (±S.E.M.) of lag periods (time from end of 60 minute glutamate incubation to the start of neuronal death) from cultures consisting of young (DIV 7-15: Light coloured bars) and old (DIV 22-52: Dark coloured bars) cells. Statistically significant differences in the lag time between the young and old group of neurones are also highlighted on the graph: (*) $P<0.05$ and (**) $P<0.01$.

4.4.4 The rate of neuronal death resulting from glutamate excitotoxicity increases with *in vitro* age

Using the dynamic Pi data from each of the individual experiments, the slope of the curve during 7-14 hours post-glutamate stimulation was assessed in relation to the culture's *in vitro* age (See *figure 4.4*). This slope measurement represented the rate that the neurones were dying following the 60 minute exposure to glutamate.

As the *in vitro* age increased, the rate of neuronal cell death also increased when the neurones were exposed to the lower concentrations of glutamate (Equation of the line: [0μM] $y=4.536xDIV+101.83$, $R^2=0.294$, n=22, *F*-value=8.308, P-value<0.01, [12.5μM] $y=6.195xDIV+ 120.16$, $R^2=0.655$ n=19, *F*-value=32.303, P-value<0.01 and [25μM] $y=7.424xDIV+149.66$, $R^2=0.326$, n=19, *F*-value=8.225, P-value<0.05). At the higher glutamate concentrations there were no significant correlation between age and rate of neuronal death (Equation of the line: [50μM] $y=2.199xDIV+239.07$, $R^2=0.103$, n=20, *F*-value=2.70, P-value>0.05, [100μM] $y=5.750xDIV+ 194.68$, $R^2=0.185$, n=21, *F*-value=4.303, P-value>0.05 and [200μM] $y=2.304xDIV+246.25$, $R^2=0.144$, n=20, *F*-value=3.032, P-value>0.05) (See *figure 4.7*).

When assessing the young (DIV 7-15) neurones separately (See *figure 4.8*), one-way ANOVA analysis showed that there was a significant difference in the rate of neuronal death with increasing glutamate concentration (*F*-Statistic=6.659, P<0.01,

n=11[0μM], n=10 [12.5μM], n=10 [25μM], n=11 [50μM], n=11 [100μM], n=11 [200μM]). This was not the same for the older neurones (DIV 22-52) which had the same rate of neuronal death irrespective of the glutamate concentration that they were exposed to (*F*-Statistic=0.923, P>0.05, n=11[0μM], n=9 [12.5μM], n=9 [25μM], n=9 [50μM], n=10 [100μM], n=9 [200μM]). When comparing the rate of neuronal death between the young group and old group of neurones for each glutamate concentration, there was a significant difference at glutamate concentrations up to 25μM (One-way ANOVA analysis: 0μM *F*-statistic=7.690, P<0.05, n=11 [Young], n=11 [Old], 12.5μM *F*-Statistic=36.610, P<0.01, n=10 [Young], n=9 [Old] and 25μM *F*-Statistic=8.261, P<0.01, n=10 [Young], n=9 [Old]). At glutamate concentrations of 50μM and above there was no significant difference in the rate at which the neuronal death was occurring between the young and old cultures (One-way ANOVA analysis: 50μM *F*-statistic=1.572, P>0.05, n=11 [Young], n=9 [Old], 100μM *F*-statistic=3.125, P>0.05, n=11 [Young], n=10 [Old], and 200μM *F*-statistic=3.972, P>0.05, n=11 [Young], n=9 [Old]).

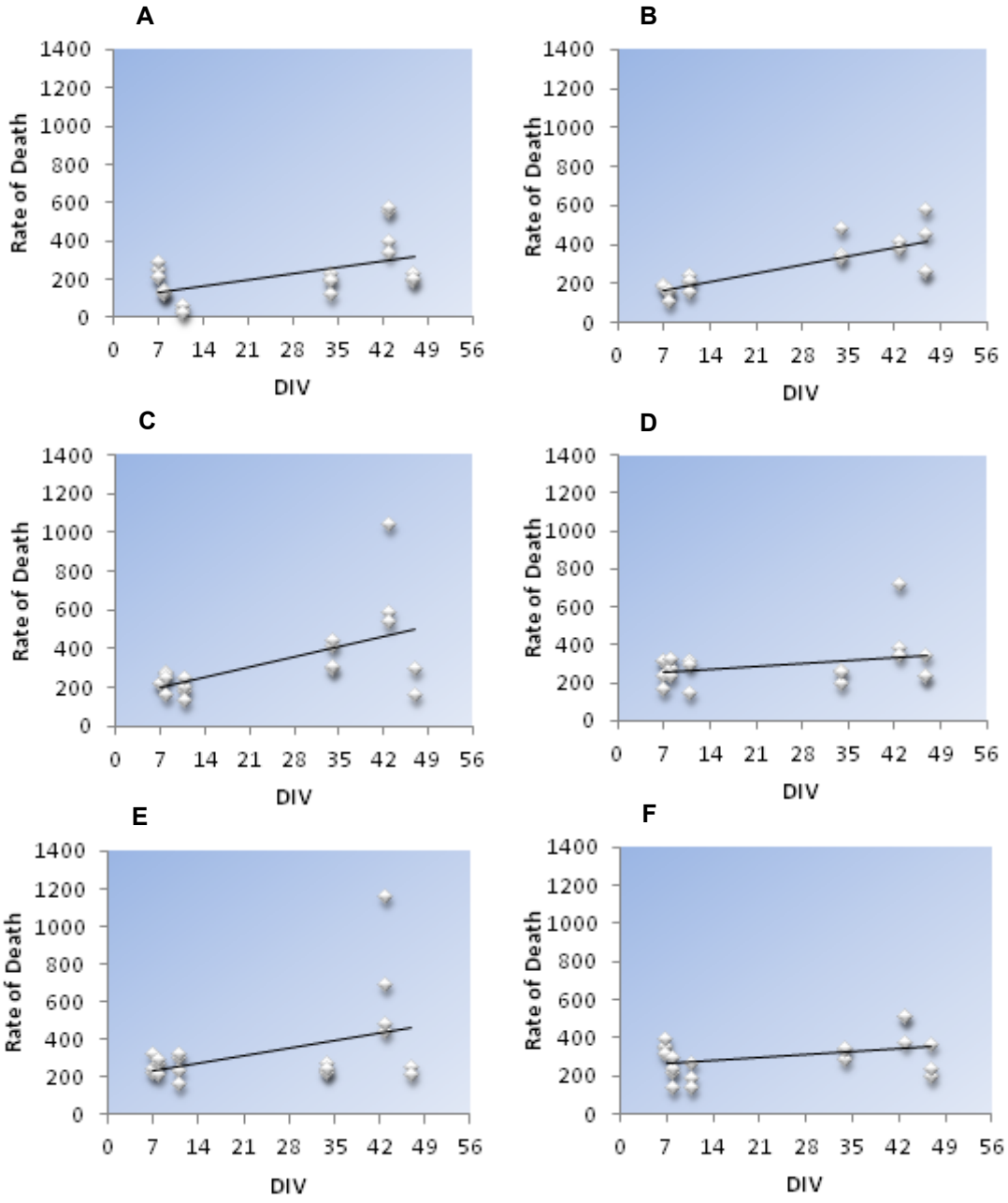

Figure 4.7. **Rate of death as a function of the age of the culture.**

These graphs show the relationship between DIV and the rate of death measured after the 60 minute glutamate incubation. Each graph represents data from a different glutamate concentration: (*A*) 0μM, (*B*) 12.5μM, (*C*) 25μM, (*D*) 50μM, (*E*) 100μM and (*F*) 200μM.

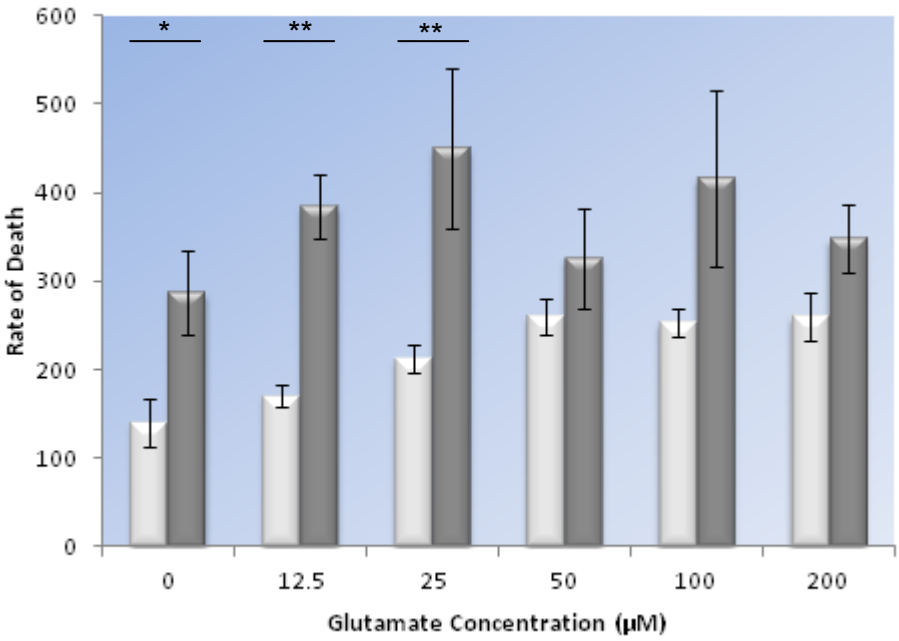

Figure 4.8. **Differences in the rate of cell death, between young and old groups of neurones.**

This graph shows the mean percentage (±S.E.M.) of the rate of death (measured after the 60 minute glutamate incubation) from cultures consisting of young (DIV 7-15: Light coloured bars) and old (DIV 22-52: Dark coloured bars) cells. Statistically significant differences in the rate of death between the young and old group of neurones are also highlighted on the graph: (*) $P<0.05$ and (**) $P<0.01$.

4.5 *Discussion*

This chapter was focused on identifying the changes in neuronal vulnerability towards glutamate-induced excitotoxicity associated with the ageing process. Even though glutamate is an essential neurotransmitter in the CNS, there is a large catalogue of evidence demonstrating the toxic effect of glutamate known as glutamate excitotoxicity (Olney 1969; Olney, Collins et al. 1986; Rothman and Olney 1986; Dirnagl, Iadecola et al. 1999; Lee, Zipfel et al. 1999; Pitt, Werner et al. 2000). .

The results from the viability experiments showed that the vulnerability of cerebellar granule neurones to glutamate excitotoxicity is dependent upon the *in vitro* age of the neurones and the concentration of glutamate applied to the cells. With increasing *in vitro* age, the levels of neuronal death rose significantly, with older neurones consistently having more cell death irrespective of the dose of glutamate applied. The amount of death increased by 0.2%-0.8% per DIV, depending on the concentration of glutamate that the neurones were incubated in. A remarkable 64% of young neurones (DIV 7-15) showed no cell death when incubated in 200μM glutamate for one hour, in contrast to only 37% of old neurones (DIV 22-52) remaining viable after the same exposure to glutamate. This resilience of young neurones to 200μM glutamate was observed in cultured hippocampal neurones, where cells cultured from embryonic rat pups (Day 17) and young rats (9-11 months old) showed little neuronal death in comparison to neurones cultured from old rats (35-37 months old) (Brewer 1998). This age dependent change in neuronal vulnerability has also been demonstrated in cortical neurones exposed to 500μM

glutamate for 5 minutes. As their *in vitro* age aged increased from DIV 5 to DIV17 (Choi, Maulucci-Gedde et al. 1987) there was an increase in vulnerability reflected by changes in the morphological appearance (swelling or cell shrinkage) and by quantitative viability measurements with trypan blue (performing cell counts where non-viable cells stain blue).

Further analysis of the data irrespective of *in vitro* age, showed that significantly larger levels of neuronal death is induced when the neurones are exposed to higher concentrations of glutamate. This glutamate dose-dependent increase in excitotoxicity has also been found in cortical neurones, with 50% neuronal death occurring at a concentration of 50-100μM at DIV 5-7 (Choi, Maulucci-Gedde et al. 1987) and 150-200μM at DIV 14-22 (Hartley, Kurth et al. 1993). In contrast, the data presented here shows that the young cerebellar granule neurones (DIV 7-15) only had a 36% level of death at 200μM (which was the highest glutamate dose tested so an EC_{50} could not be calculated) and the older neurones (DIV 22-52) had an EC_{50} of 12.5-25μM. Since there is such a high degree of discrepancy between the EC_{50} values of the two studies involving cortical neurones, comparisons with the cerebellar granule neurones are less significant. In mixed hippocampal and glia primary cultures at 10-15 DIV, 100μM glutamate induced 62.5% cell death (Abramov and Duchen 2008) which is similar to the level of death observed in the old cerebellar granule neurones (DIV 22-52) when they were exposed to 100μM glutamate (60% death).

There are numerous methods used to quantify levels of cellular death based on various biochemical and molecular principles in order to assess viability. A cell can be deemed as non-viable if it has a compromised plasma membrane or if there it has impaired metabolic functioning. When comparing all of the possible methods for quantifying neuronal death; Lactate dehydrogenase (Nachlas, Margulies et al. 1960; Briere, Preston et al. 1966), MTT assay (Ramsden, Plant et al. 2001; Ramsden, Henderson et al. 2002), WST-1/8 assays (Ishiyama, Tominaga et al. 1996; Maekawa, Yagi et al. 2003; Fotakis and Timbrell 2006), alamar blue assay (White, DiCaprio et al. 1996; O'Brien, Wilson et al. 2000), calcein-AM (Wang, Terasaki et al. 1993), the propidium iodide (Pi) assay (Tanke, van der Linden et al. 1982; Sattler, Charlton et al. 1997) was chosen since it could be adapted to quantify viability dynamically, enabling the entire process of death to be monitored over time. This provided additional information on rates and patterns of death which some of the other methods could not produce.

Using this adapted dynamic Pi method, the lag period (time between the end of the glutamate stimulation and the start of neuronal death) and the rate of death (gradient in the viability curve) were assessed in relation to *in vitro* age. During resting and low glutamate concentrations (12.5μM) the lag period in the old neurones (22-52) was longer that the young (DIV7-15) neurones, however, once the glutamate concentration reached 25μM, the lag period of the old neurones became shorter than the young neurones, with significant differences at 50μM and 100μM glutamate concentrations. This supports the idea that there is an increase in vulnerability to glutamate excitotoxicity, with increasing *in vitro* age. The older neurones were also

more sensitive to the glutamate, with significantly shorter lag periods as the glutamate concentration progressively increased, whereas the lag period in the young neurones remained constant irrespective of the glutamate concentration. The shortest lag time observed in the young neurones was 2.85 hours (100μM glutamate) and in the old neurones, there was almost immediate cell death following removal of glutamate (0.56 hours at 50μM and 0.20 hours at 100μM). A lag period of 2 hours was observed in another study involving 8 day old cerebellar granule neurones exposed to 50μM glutamate for 15 minutes (Manev, Favaron et al. 1989) which is slightly shorter than the results seen in this study (50μM 4.7 hours).

A significantly faster rate of neuronal death was also observed in older neurones in comparison to the younger ones, when exposed to glutamate concentrations of between 0μM and 25μM. Again this shows that the older neurones are more sensitive to the glutamate insult, particularly at the lower doses. Interestingly, the rate of death in the younger neurones increased with glutamate concentration however, in the old neurones, the rate remained constant. This may suggest that since the older neurones are more sensitive to the glutamate, so death may already be occurring at the maximum rate.

There are numerous factors which may underlie this elevated susceptibility to glutamate-induced cell death, most of these based around the impairment in Ca^{2+} homeostasis (Toescu and Verkhratsky 2003). Studies have focussed on the importance of both the movement of Ca^{2+} into the cell and the removal of the

excessive Ca^{2+} from the cytosol, in trying to find the cause of neuronal vulnerability associated with aged neurones.

Glutamate can activate both ionotropic receptors and metabotropic receptors leading to intracellular rises in Ca^{2+} (Michaelis 1998; Dingledine, Borges et al. 1999; Niciu, Kelmendi et al. 2012) (See *chapter 4.1.1)*. Different studies have focussed on the importance of each type of receptor in glutamate excitotoxicity. NMDA has been cited by many as a major player in excitotoxicity since inhibition of the receptor with an antagonist such as DL-2-amino-5-phoshonovalerate (APV), its active isomer D-APV (Choi, Koh et al. 1988; Attucci, Clodfelter et al. 2002) or MK-801 (Hartley, Kurth et al. 1993) has been shown to prevent neuronal death following glutamate exposure. In addition, studies have shown age-dependent differences in the expression of various NMDA receptor subunits with age (Arundine and Tymianski 2003; Fu, Logan et al. 2005) e.g. increased NR1 expression in cerebellar granule neurones with age (Xia, Ragan et al. 1995), increased NR2B in hippocampal slices (Zhou and Baudry 2006) and decrease of NR3A in rat brain (Wong, Liu et al. 2002) which could all play a role in increasing vulnerability. A higher density in the NMDA receptors with age has been shown (Xia, Ragan et al. 1995; Fogal, Trettel et al. 2005), resulting in greater influxes of Ca^{2+} that could remain elevated for a longer period of time. Furthermore, NMDA receptor activation can also lead to secondary Ca^{2+} increases via the release of Ca^{2+} from intracellular stores (Clodfelter, Porter et al. 2002; Solovyova, Veselovsky et al. 2002). Apart from the ionotropic glutamate receptors, the Group I metabotropic receptors have also been found to play a role in excitotoxicity (Attucci, Clodfelter et al. 2002).

Elevations in $[Ca^{2+}]_i$ can be restored to normal basal levels by sequestration of the Ca^{2+} by the mitochondria (Ward, Rego et al. 2000). There is extensive evidence for the role of the mitochondria in glutamate excitotoxicity (Stout, Raphael et al. 1998) with many experiments showing that the Ca^{2+} unloaded from the mitochondria (after stimulation with glutamate) by addition of the protonophore, carbonyl cyanide m-chlorophenyl-hydrazone (CCCP) corresponds to the amount of $[Ca^{2+}]_i$ that initially entered into the cytosol (during glutamate stimulation) (White and Reynolds 1997; Keelan, Vergun et al. 1999; Brocard, Tassetto et al. 2001). Preventing the uptake of Ca^{2+} into the mitochondria by inhibiting the Ca^{2+} uniporter with ruthenium red or, by depolarising the mitochondria prior to exposing the neurones to glutamate, significantly decreases the amount of neuronal death (Khodorov, Pinelis et al. 1999; Kannurpatti, Joshi et al. 2000; Khodorov, Storozhevykh et al. 2002; Khodorov 2004). Since uptake of the Ca^{2+} into the mitochondria not only leads to depletion of ATP as a result of the mitochondria becoming depolarised, but also can lead to the opening of the mitochondrial permeability transition pore (MPTP) which results in the total irreversible disruption of the mitochondrial membrane potential leading to death of the cell (Friberg and Wieloch 2002). A consequence of depleted ATP would be less extrusion of the Ca^{2+} via the plasma membrane Ca^{2+}-ATPase pump.

Overload of calmodulin with Ca^{2+} has also been suggested as a cause of excitotoxicity, via the stimulated production of Ca^{2+}/calmodulin dependent enzymes such as NOS (Dawson, Dawson et al. 1993) and proteolysis of fodrin by calpain (Johnson, Litersky et al. 1991). A study in cortical neurones found calmodulin to be

protective glutamate exposure (Shirasaki, Kanazawa et al. 2006). Other factors include impaired Ca^{2+} extrusion by the plasma membrane Ca^{2+}-ATPase pump and the Na^{+}/Ca^{2+}-exchanger; sequestration of the Ca^{2+} by the endoplasmic reticulum and ROS production (Budd and Nicholls 1996; Vergun, Sobolevsky et al. 2001; Parihar and Brewer 2007).

Overall this work provides detailed information on the dynamics associated with increased vulnerability of aged neurones to glutamate excitotoxicity. In conclusion cerebellar granule neurones do show an age-dependent increase in vulnerability to the excitotoxic effects of glutamate. The possible factors responsible for increased vulnerability are investigated in the following chapter.

5 The functional parameters involved in glutamate excitotoxicity.

5.1 *Calcium homeostasis*

In order to determine the underlying mechanisms that lead to the increased vulnerability of aged neurones to glutamate excitotoxicity, investigations into the relationship between the increases in intracellular Ca^{2+} concentration ($[Ca^{2+}]_i$) and buffering of the Ca^{2+} by the mitochondria were explored.

Calcium is an important signalling molecule and it is crucial that its cellular levels are maintained, which is why there are many homeostatic mechanisms to deal with increases in $[Ca^{2+}]_i$. There are three main types of channels allowing the influx of Ca^{2+} into the cytosol (Carafoli, Santella et al. 2001). The first are the voltage-gated Ca^{2+} channels (VGCC) which open in response to depolarisation of the plasma membrane once they reach the threshold of the channel. There are 6 types of these channels (L, P, Q, N, R and T) with P,Q (High voltage) and R-types (Intermediate voltage) located in cerebellar granule cells. These types of channel allow Ca^{2+}, Ba^{2+} and Sr^{2+} to pass through however, they do not permit the passage of monovalent ions such as Na^{+} (Carafoli 1987). They are found in both excitatory cells such as neurones, skeletal muscle and heart as well as non-excitatory cells. For a complete

review on this type of Ca^{2+} channel refer to (Catterall 2000). The second mechanism of Ca^{2+} entry into the cell is through ligand-gated Ca^{2+} channels, which open in response to the binding of specific ligands to the receptor on the channel. The ionotropic and metabotropic glutamate receptors (Michaelis 1998; Dingledine, Borges et al. 1999; Niciu, Kelmendi et al. 2012) fall within this category and are discussed further in *Chapter 4.1.1*. This group also includes the ryanodine receptors, which are Ca^{2+}-induced Ca^{2+}-release receptors, that release Ca^{2+} from endoplasmic reticulum stores when activated by large $[Ca^{2+}]_i$ concentrations (Fagni, Chavis et al. 2000). The third type of channel are 'store operated Ca^{2+} channels' (SOCC) which are dependent upon the Ca^{2+} levels in the endoplasmic reticulum (ER) stores. As the levels of Ca^{2+} stored in the ER diminish, the SOCC open inducing a Ca^{2+} influx into the cytosol. The exact connection between the ER and SOCC is still undefined.

In order to regulate the $[Ca^{2+}]_i$ it is important to have various extrusion mechanisms for removing Ca^{2+} out of the cell. The Na^+/Ca^{2+} exchanger is a membrane protein located within the plasma membrane. It allows three Na^+ ions to enter into the cytosol in exchange for one Ca^{2+} ion leaving the cytosol. The Na^+ ions diffuse into the cytosol down a concentration gradient and the energy harvested from this movement is used to drive the Ca^{2+} out of the cytosol against its concentration gradient. The Na^+/Ca^{2+} exchanger has a low affinity for Ca^{2+} however it allows a large capacity of Ca^{2+} to move across it at a fast rate. The plasma membrane Ca^{2+}-ATPase (PMCA) uses ATP to pump Ca^{2+} out of the cytosol against its natural concentration gradient. The PMCA has a higher affinity for Ca^{2+} than the Na^+/Ca^{2+} exchanger but a lower capacity for extruding Ca^{2+}. Therefore even though it is less

effective at removing Ca^{2+} it is initiated at a lower Ca^{2+} threshold making its role more important in tweaking the level of cytosolic Ca^{2+} as apposed to responding to large Ca^{2+} influxes.

During elevations in $[Ca^{2+}]_i$ an alternative to extrusion of the Ca^{2+} out of the cell, is the move sequestration of the Ca^{2+} by the endoplasmic reticulum and the mitochondria. Movement into the mitochondria is via the mitochondrial Ca^{2+} uniporter which moves Ca^{2+} down its electrochemical gradient (Duzenli, Bakuridze et al. 2005). The mitochondria is able to buffer large amounts of Ca^{2+} (Duchen 1999) and is able to slowly release the Ca^{2+} back into the cytosol, which can then be removed by another homeostatic mechanism (Khodorov, Pinelis et al. 1999). The endoplasmic reticulum (ER) takes in Ca^{2+} via the endoplasmic reticulum ATPase.

5.2 *Aim*

The aim of this part of the project was to explore the relationship between the glutamate-induced Ca^{2+} load and the unloading of the mitochondria with CCCP with regards to *in vitro* age.

5.3 *Methods*

5.3.1 Assessing $[Ca^{2+}]_i$ changes: use of Fura-2-AM

In order to monitor changes in $[Ca^{2+}]_i$ the ratiometric fluorescent dye Fura–2 was used (Roe, Lemasters et al. 1990; Barreto-Chang and Dolmetsch 2009). A 10mM stock of Fura-2-AM (Invitrogen, UK) was made up by diluting it with dimethyl sulfoxide (DMSO) (Sigma, UK). Next, 2ml of a 10mM HEPES buffer (pH 7.4) containing 145mM NaCl, 5mM KCl, 1mM $MgCl_2$x6, 1.5mM $CaCl_2$ and 12mM Glucose (Sigma, UK) referred to as 'experimental' medium was transferred into a 20ml centrifuge tube (Falcon) and 2µl of the detergent pluronic (Invitrogen, UK) was added. The 'experimental' medium containing the pluronic detergent was mixed using a vortex-mixer. Whilst still being mixed on the vortex-mixer, 0.5µl Fura-2AM from the Fura-2-AM stock solution was added to the centrifuge tube giving a final Fura-2-AM concentration of 2.5µM. Due to the light sensitive nature of the dye the centrifuge tube was completely covered in aluminium foil.

Cover-slips were transferred to a 4-well micro-plate (Falcon) and incubated in 0.5ml of the 2.5µM Fura-2-AM solution for 30 minutes at a temperature of 30ºC. At the end of the incubation time, the Fura-2-AM was removed and replaced with 'experimental' medium and the cells incubated for another 30 minutes (this time at room temperature) to allow de-esterification of the Fura-2-AM.

Fluorescence measurements were carried out using a fluorescence microscope connected to an intensified GenIV camera (Roper Instruments, UK). The monochromator (Cairn Research Ltd., UK) and computer software MetaFluor (Universal Imaging, USA) was used for controlling the capturing/wavelength settings. The x20 water immersion lens was used for the experiments. Using the software, 20 neurones and three background regions (darkened areas of the field not containing or affected by the fluorescence of any neurones) were specified and monitored for any changes in Ca^{2+}. The 25ND DIC filter (excludes 75% of the fluorescent light) was used to reduce photobleaching of the Fura-2-AM. Two excitation wavelengths were used: 340nm and 380nm, the emission filter was a 520nm bandpass filter and a ratio of the two excitation images was calculated.

The cover-slip was placed into a glass petri dish containing the 'experimental' medium. A perfusion and extrusion system was set up to add/remove the experimental solutions in which the neurones are exposed to. The perfusion system consisted of a syringe connected to a 2-way tap (open/close) to control the flow rate of the solution, narrow tubing and a hypodermic needle. The extrusion system consisted of a hypodermic needle, narrow tubing and a pump to provide the suction to remove the solution from the petri dish. This was done so that measurements could be constantly made from the same highlighted neurones without moving the focal field. The average flow rate for the perfusion system was 2.8ml/min when using a 20ml syringe and 2.7ml/min when using a 50ml syringe. The overall average is 2.7ml/min with an average of 29drops/min.

5.3.2 The experimental procedure.

Initial resting $[Ca^{2+}]_i$ measurements were made during the first 300 seconds pre-stimulation. This was followed by 180 second stimulation with glutamate, using the perifusion system to remove the 'experimental' medium and introduce the glutamate to the neurones. On completion of the 180 seconds, the extrusion pump was used to remove the glutamate and replaced with the 'experimental' medium. Following 300 second incubation in the 'experimental' medium, the perifusion system was used to replace the 'experimental' medium with 10μM carbonyl cyanide *m*-chlorophenylhydrazone (CCCP) (Sigma, UK) and recording were made for a further 300 seconds.

The various phases of this experimental procedure are illustrated in *figure 5.1*. In order to assess the overall change in $[Ca^{2+}]_i$ homeostasis, the area under the curve (AUC) was determined for each phase of the curve (i.e. resting, glutamate stimulation, recovery and CCCP stimulation). This AUC was taken to represent an integrated assessment of the level of $[Ca^{2+}]_i$ challenge and for these experiments it was considered to be more relevant than the simple measurement of the amplitude of the 340/380nm signal.

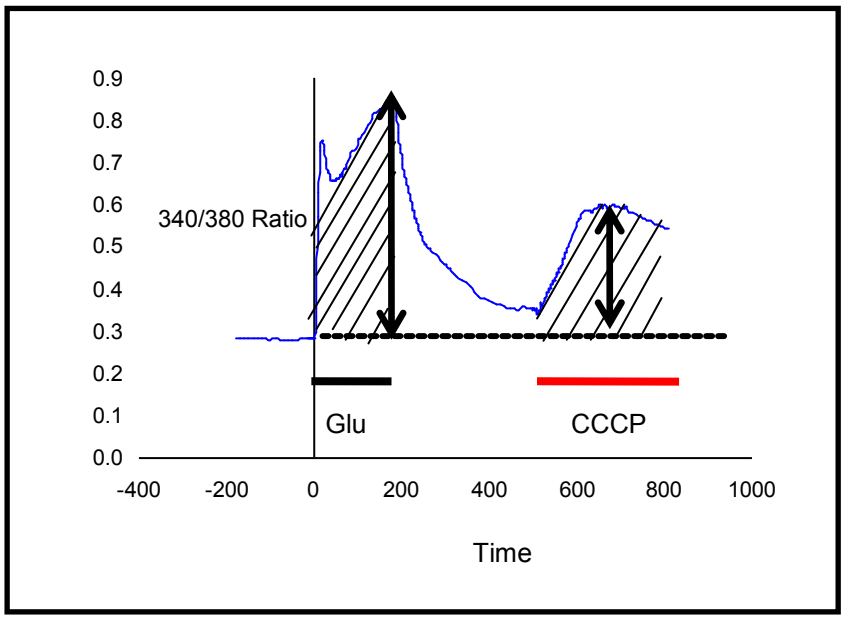

Figure 5.1. **The two functional parameters chosen to be assessed.**

This figure illustrates the different phases in the experimental procedure. A 180 second stimulation with glutamate (represented by the thick black line on the graph), followed by a 300 second recovery period and then completed by a 300 second incubation in CCCP (thick red line on graph). The shaded regions on the graph represent the section of the graph that was used to calculate the 'area under the cure' (AUC).

5.4 *Results*

5.4.1 Excessive cytosolic Ca^{2+} following glutamate exposure is sequestered by the mitochondria.

The first stage in this section of the project was to establish a basal measure of the amount of Ca^{2+} that is normally stored inside the mitochondria, at normal physiological cytosolic Ca^{2+} concentrations ($[Ca^{2+}]_i$) and without any prior stimulation of the cell with glutamate or any depolarising agent such as KCl, which may affect $[Ca^{2+}]_i$. Cerebellar granule neurones were labelled with Fura-2-AM (see *methods section 5.3.1*) and the normal experimental procedure described in *Methods Section 5.3.2* was carried out, with a 180 second exposure to zero-Mg^{2+} (without any glutamate). The CCCP (10μM) was then added after the 5 minute recovery period with no increase in $[Ca^{2+}]_i$ seen, (See *figure 5.2.A*). For the purpose of visual comparison, the results of 20 neurones exposed to 200μM glutamate for 180 seconds, is represented in *figure 5.2.B*. It shows that the addition of CCCP after the 300 second recovery period, induces a large rise in $[Ca^{2+}]_i$ as the mitochondria unloads its contents.

Even though all of the 20 neurones from the experiment in *figure 5.2* were cultured on the same culture slip, there was a high degree of variability in the response of the neurones to the glutamate. Based on this observation, neurones were defined as

being independent in terms of their physiological behaviour, even though they share the same neuronal network within the same culture.

5.4.2 The size of the initial glutamate induced Ca^{2+} influx and the mitochondrial Ca^{2+} load shows dose dependency.

The results showed that increasing the dose of glutamate applied to the neurones, increased the size of the initial Ca^{2+} elevation. This glutamate-induced rise in $[Ca^{2+}]_i$ was associated with a second increase in Ca^{2+}, following the addition of CCCP, which represents the unloading of Ca^{2+} from the mitochondria. Therefore, the higher the concentration of glutamate applied to the cerebellar granule neurones, the more Ca^{2+} entered into the cytosol from the extracellular medium, which resulted in a greater movement of Ca^{2+} into the mitochondria. This is clearly demonstrated in *figure 5.3* when comparing the changes in $[Ca^{2+}]_i$ induced by 2μM glutamate with 200μM glutamate.

A further observation made from studying the dynamics of the changes in the $[Ca^{2+}]_i$ was that some of the neurones appeared to have a twin peak during their initial response to the glutamate stimulation (See *figure 5.4*). This double peak, consisting of a repeated pattern of 'increase in $[Ca^{2+}]_i$ followed by a decrease', was mainly observed in the neurones exposed to higher concentrations of glutamate (200μM). This twin peak was not investigated further.

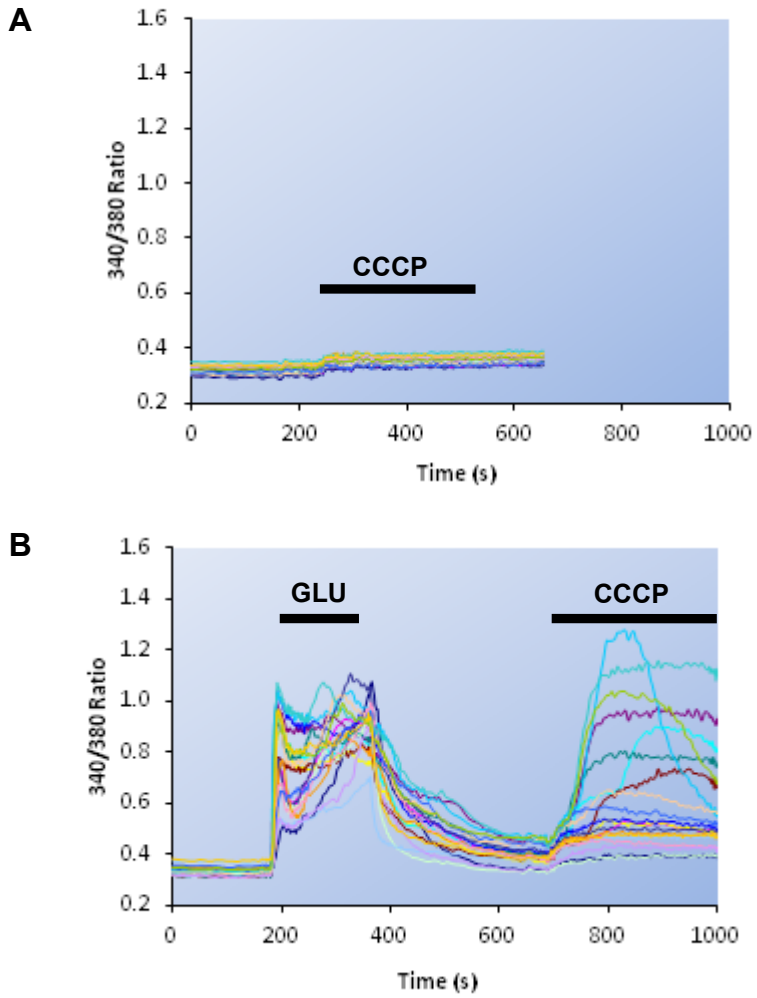

Figure 5.2. **Unloading of the mitochondria's Ca^{2+} with and without exposure to glutamate.**

The first trace (*Panel A*) represents the changes in cytosolic Ca^{2+} ($[Ca^{2+}]_i$) from 20 neurones when stimulated with CCCP for 300 seconds (in the absence of glutamate stimulation). The second trace (*Panel B*) is for the purpose of visual comparison, showing the change in $[Ca^{2+}]_i$ from 20 neurones induced by a 200μM glutamate exposure for 180 seconds followed by addition of CCCP for 300 seconds. All neurones were loaded with Fura-2-AM and the graphs show the ratio of the 340/380nm signal.

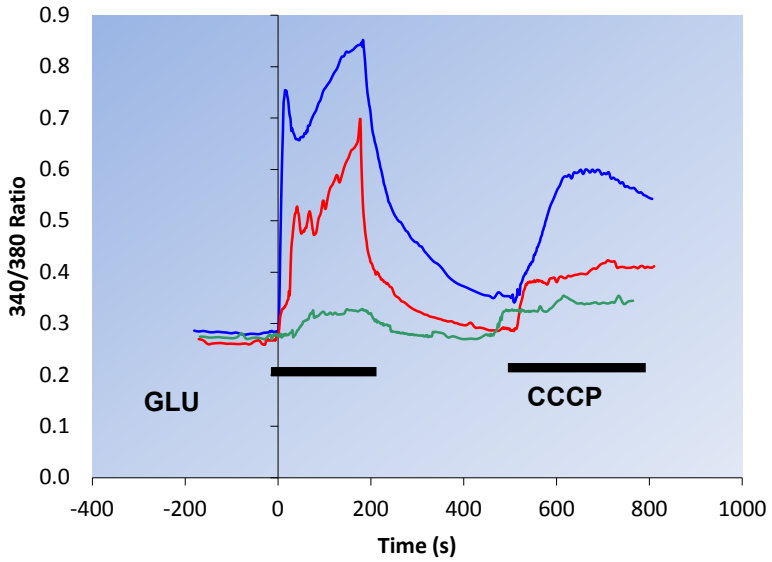

Figure 5.3. **A comparison of the averaged responses of neurones to varying concentrations of glutamate, followed by unloading of the mitochondria with CCCP.**

This graph shows the mean changes in cytosolic Ca^{2+} during a 180 second stimulation with glutamate (2μM, 20μM or 200μM) followed by a 300 second wash period (recovery), then a 300 second incubation in 10μM CCCP. Each of the traces represent the average change in $[Ca^{2+}]_i$, expressed as a ratio of the 340/380nm Fura-2 signal, obtained from 15-21 neurones. The blue trace represents the averaged response to 200μM glutamate, the red trace represents the response to 20μM and the green trace represents exposure to 2μM. The 0-timepoint on the x-axis corresponds to the start of the glutamate stimulation.

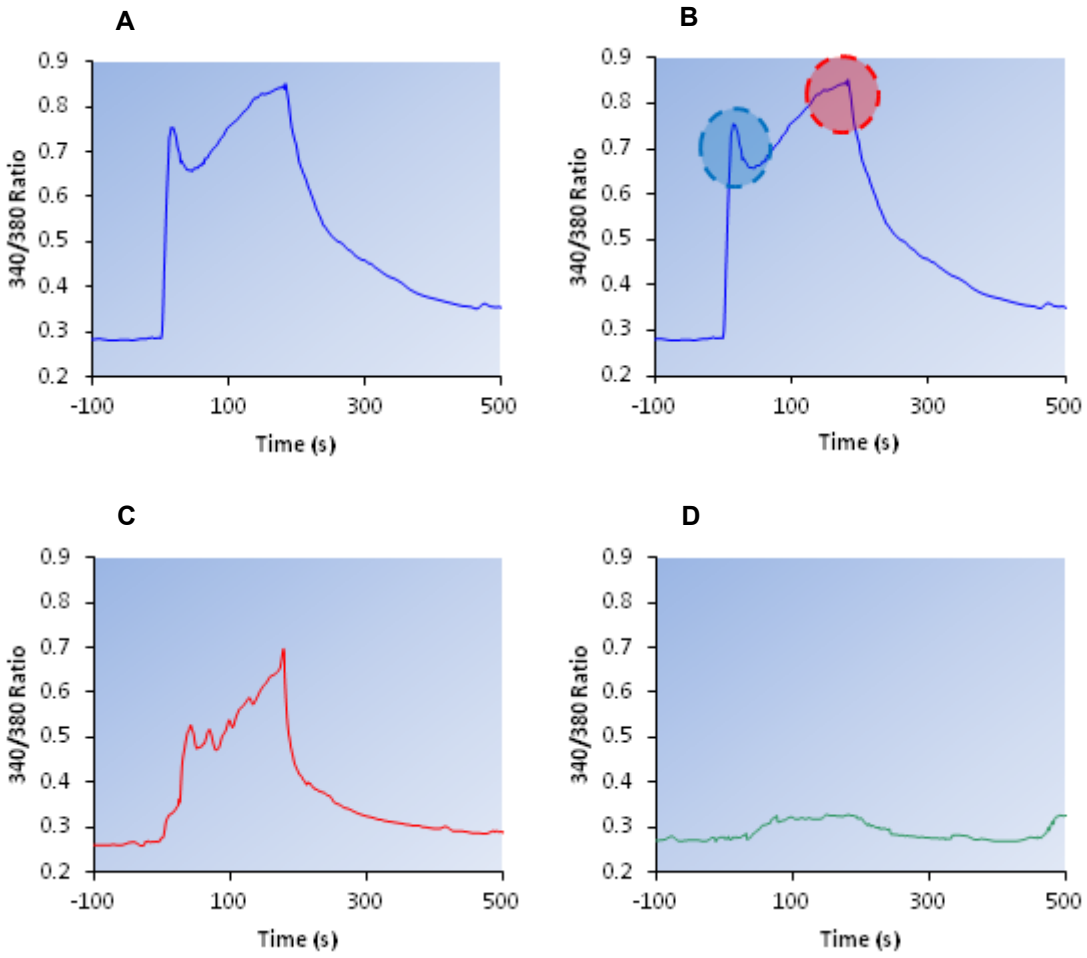

Figure 5.4. **The twin peak observed during the initial $[Ca^{2+}]_i$ rise.**

In *Panel A*, the highlighted blue and red regions on the graph illustrate the twin peak observed during the initial elevation in $[Ca^{2+}]_i$ during stimulation of the neurones stimulation with glutamate. *Panels B-D*, show the data from *figure 5.3*, separated by glutamate concentration: 200μM (*B*), 20μM (*C*) and 2μM (*D*). This has been done to allow the dynamics of the response (twin peak) to be viewed more easily, showing that the double peak is more pronounced at higher glutamate concentrations.

5.4.3 The effect of *in vitro* age on the initial increase in $[Ca^{2+}]_i$ induced by stimulation with glutamate.

The size of the initial elevation in cytosolic Ca^{2+} (expressed as an 'area under the curve' - AUC) following the 180 second glutamate incubation, was the first aspect of the neuronal response to glutamate stimulation investigated. Using linear regression analysis, an equation of the line, R^2-value, *F*-value and P-value were determined for all of the data represented in *figure 5.5.A-C*. The results show that at the lowest glutamate concentration,(2µM) there was a significant negative correlation between the size of the initial Ca^{2+} load induced by glutamate and the *in vitro* age (Equation of the line: [2µM] y=-0.081xDIV+7.362, R^2=0.140, n=104, *F*-value=16.753, P<0.001). At the higher glutamate concentrations, a significant positive correlation was shown, with larger $[Ca^{2+}]_i$ elevations associated with increasing *in vitro* age (Equation of the line: [20µM] y = 2.068xDIV+8.096, R^2=0.574, n=172, *F*-value=228.762, P<0.001 and [200µM] y=1.6312xDIV+61.903, R^2=0.252, n=255, *F*-value= 85.318, P<0.001).

The data was separated into two *in vitro* age groups: Young (DIV 7-15) and old (DIV 21-52) (See *figure 5.5.D*). One-way ANOVA analysis showed a significant difference between the young and old neurones at 2µM (*F*-statistic=52.062, P<0.001, n=55 [Young], n=50 [Old]), 20µM (*F*-statistic=238.506, P<0.001, n=95 [Young], n=77 [Old]) and 200µM (*F*-statistic=226.02, P<0.001, n=78 [Young], n=177 [Old]) with the older neurones having larger Ca^{2+} elevations at the higher glutamate doses (20µM and 200µM). The statistical analysis also showed that the $[Ca^{2+}]_i$ increased as the

glutamate concentration increased in both the young neurones (*F*-statistic=82.383, P<0.001, n=55 [2μM], n=95 [20μM], n=78 [200μM]) and old (*F*-statistic=287.721, P<0.001, n=51 [2μM], n=78 [20μM], 178 [200μM]).

5.4.4 The effect of *in vitro* age on the second increase in $[Ca^{2+}]_i$ induced by stimulation with CCCP.

The second aspect of the response of individual neurones to glutamate stimulation investigated, was the level $[Ca^{2+}]_i$ change during the 300 second incubation in 10μM CCCP. The addition of CCCP was after the glutamate stimulation (followed by the 300 second recovery wash period) and represented the unloading of the Ca^{2+} from the mitochondria. Using linear regression analysis, an equation of the line, R^2-value, *F*-value and P-value were determined for all of the data represented in *figure 5.6.A-C*. The results showed a significant positive correlation between the size of the $[Ca^{2+}]_i$ elevation induced by CCCP and the *in vitro* age of the neurones when they were exposed to higher concentrations of glutamate (Equation of the line: [20μM] y=2.06xDIV+10.21, R^2=0.317, n=172, *F*-value=78.781, P<0.001 and [200μM] y=2.05xDIV+72.21, R^2=0.138, n=255, *F*-value=40.477, P<0.001). At the lowest concentration of glutamate, the correlation was negative between the size of the initial Ca^{2+} load and the *in vitro* age (Equation of the line: y =-0.2837xDIV+25.388, R^2=0.250, n=105, *F*-value=34.271, P<0.001).

The data was then separated into two *in vitro* age groups: Young (DIV 7-15) and old (DIV 21-52) (See *figure 5.6.D*). One-way ANOVA analysis showed a significant difference between the young and old neurones at 2μM (*F*-statistic=5.753, P<0.05, n=55 [Young], n=50 [Old]), 20μM (*F*-statistic=34.297, P<0.001, n=95 [Young], n=77 [Old] and 200μM (*F*-statistic=116.677, P<0.001, n=78 [Young], n=177[Old]). The statistical analysis also showed that CCCP induced a significant rise in the $[Ca^{2+}]_i$ that was associated with increasing glutamate concentration for both young (*F*-statistic=17.024, P<0.001, n=55 [2μM], n=95 [20μM] and n=78 [200μM]) and old neurones (*F*-statistic=103.227, P<0.001, n=51 [2μM], n=78 [20μM], n=178 [200μM]).

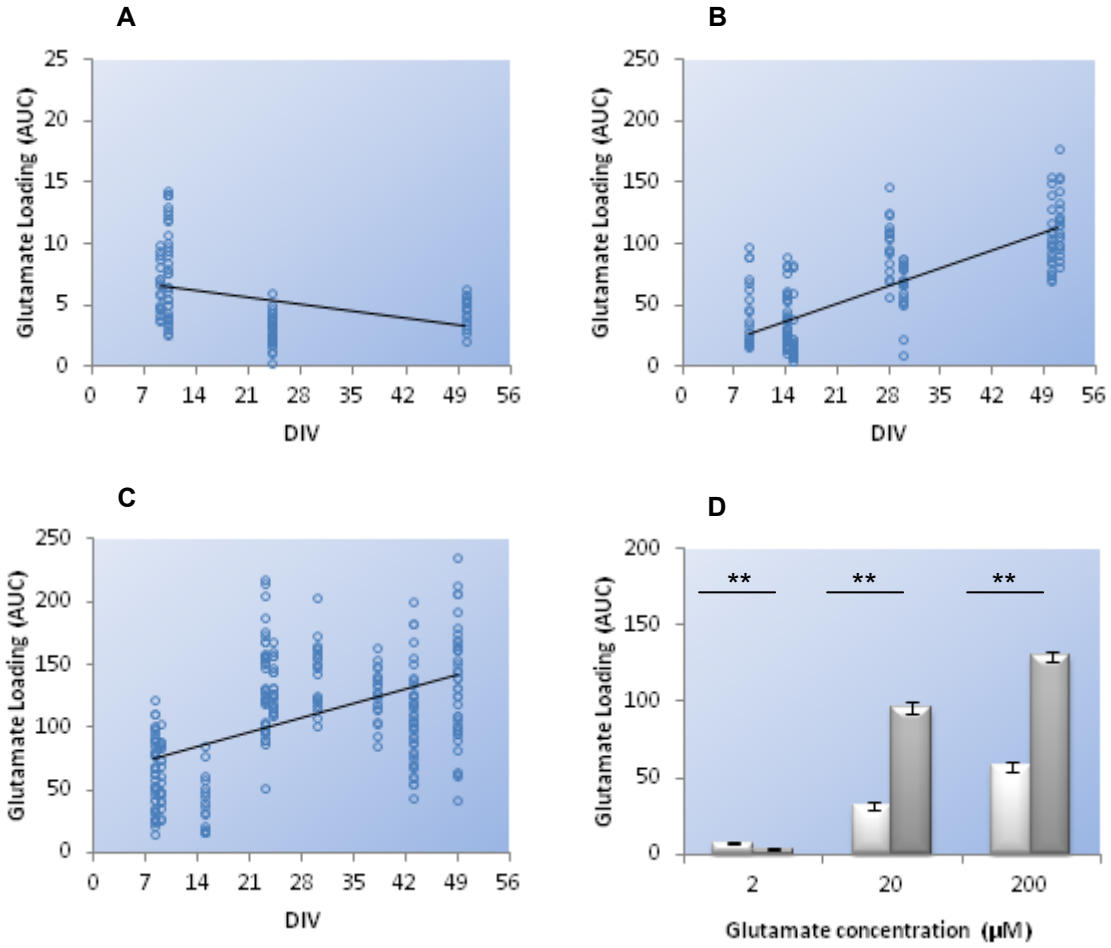

Figure 5.5. **The effect of *in vitro* age on glutamate-induced Ca^{2+} elevations.**

These graphs show the effect of *in vitro* age (DIV) on the cytosolic Ca^{2+} concentration following a 180 second stimulation with glutamate: (*A*) 2µM, (*B*) 20µM and (*C*) 200µM. This glutamate-induced elevation in $[Ca^{2+}]_i$ is referred to as 'glutamate loading' and is derived from calculating the area under the curve. Each data point on the graph represents a measurement taken from one neurone. Graph *D* shows the mean glutamate load (±S.E.M.) for each glutamate concentration. The light coloured bars represent neurones at 7-15 DIV and the dark coloured bars represent neurones at 21-52 DIV. Statistically significant differences in the mean glutamate loading (AUC) between the young and old group of neurones are also highlighted on the graph: (**) P<0.01.

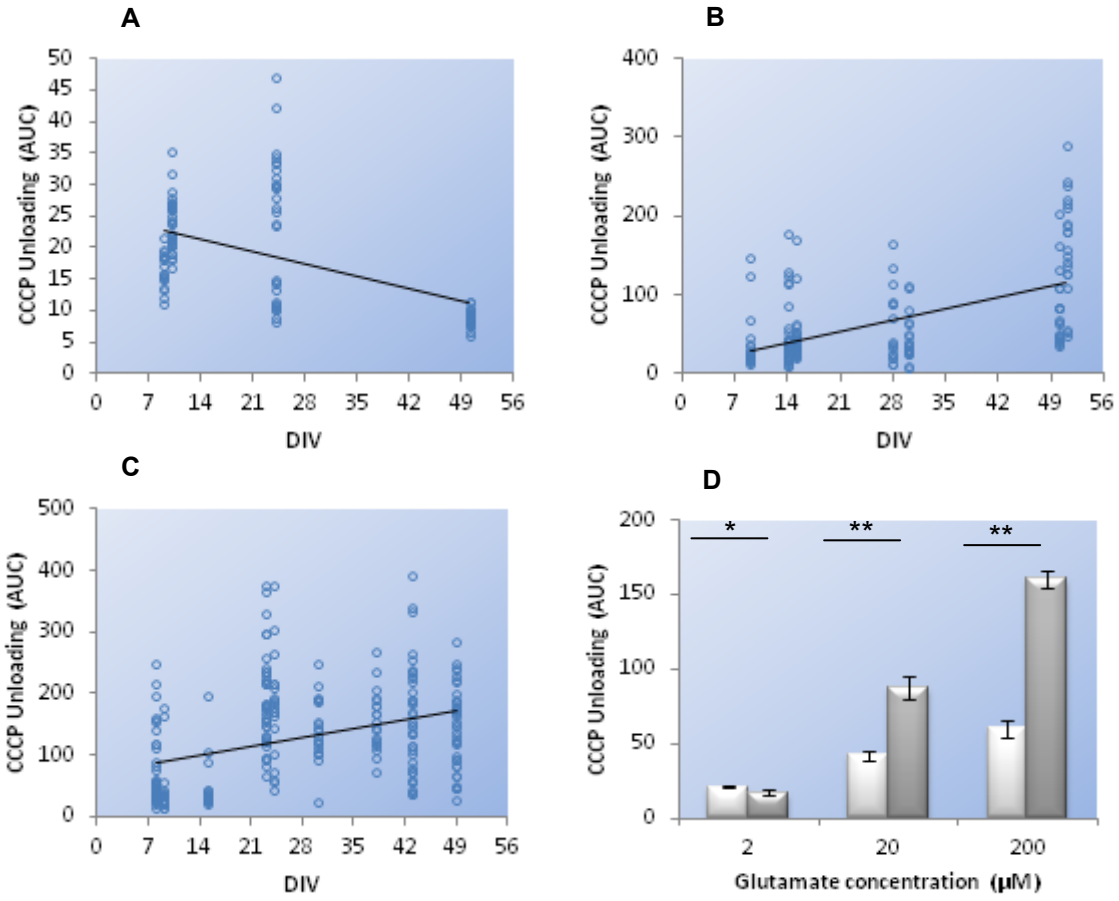

Figure 5.6. **The effect of *in vitro* age on the change in $[Ca^{2+}]_i$ induced by CCCP post-glutamate stimulation.**

These graphs show the effect of *in vitro* age (DIV) on the cytosolic Ca^{2+} concentration following a 300 second stimulation with CCCP. The neurones were exposed to 10µM CCCP after a prior stimulation with glutamate (180 seconds) followed by a 300 second recovery period (*Panel A*=2µM, *panel B*=20µM and *panel C*=200µM). This CCCP-induced elevation in $[Ca^{2+}]_i$ is referred to as the 'CCCP Unloading' and is expressed as the area under the curve (AUC). Each data point on the graph represents a measurement taken from one neurone. Graph *D* shows the mean (±S.E.M.) CCCP unloading for each glutamate concentration. The light coloured bars represent neurones at 7-15 DIV and the dark coloured bars represent neurones at 21-52 DIV. Statistically significant differences in the mean CCCP unloading (AUC) between the young and old group of neurones are also highlighted on the graph: (*) $P<0.05$ and (**) $P<0.01$.

5.4.5 The relationship between the change in $[Ca^{2+}]_i$ induced by glutamate and the change in $[Ca^{2+}]_i$ induced by CCCP.

The relationship between the increase in $[Ca^{2+}]_i$ induced by the glutamate stimulation (loading of the neurone) and the rise on $[Ca^{2+}]_i$ following the addition of CCCP (unloading of the mitochondria) was assessed by plotting each parameter against each other and using linear regression to analyse the correlation. An equation of the line, R^2-value, *F*-value and P-value were determined for all of the data represented in *figure 5.7.A-C*. The results showed a significant positive correlation between the unloading of the mitochondria with CCCP and the loading of the neurone by 20μM glutamate ($y=0.85xDIV+ 11.26$, $R^2=0.398$, $n=172$, *F*-value=112.349, $P<0.001$) and 200μM glutamate ($y=1.11xDIV+10.49$, $R^2=0.424$, $n=255$, *F*-value=185.965, $P<0.001$), with insignificant correlation with 2μM glutamate ($y=0.39xDIV+17.16$, $R^2=0.022$, $n=105$, *F*-value=2.289, $P>0.05$).

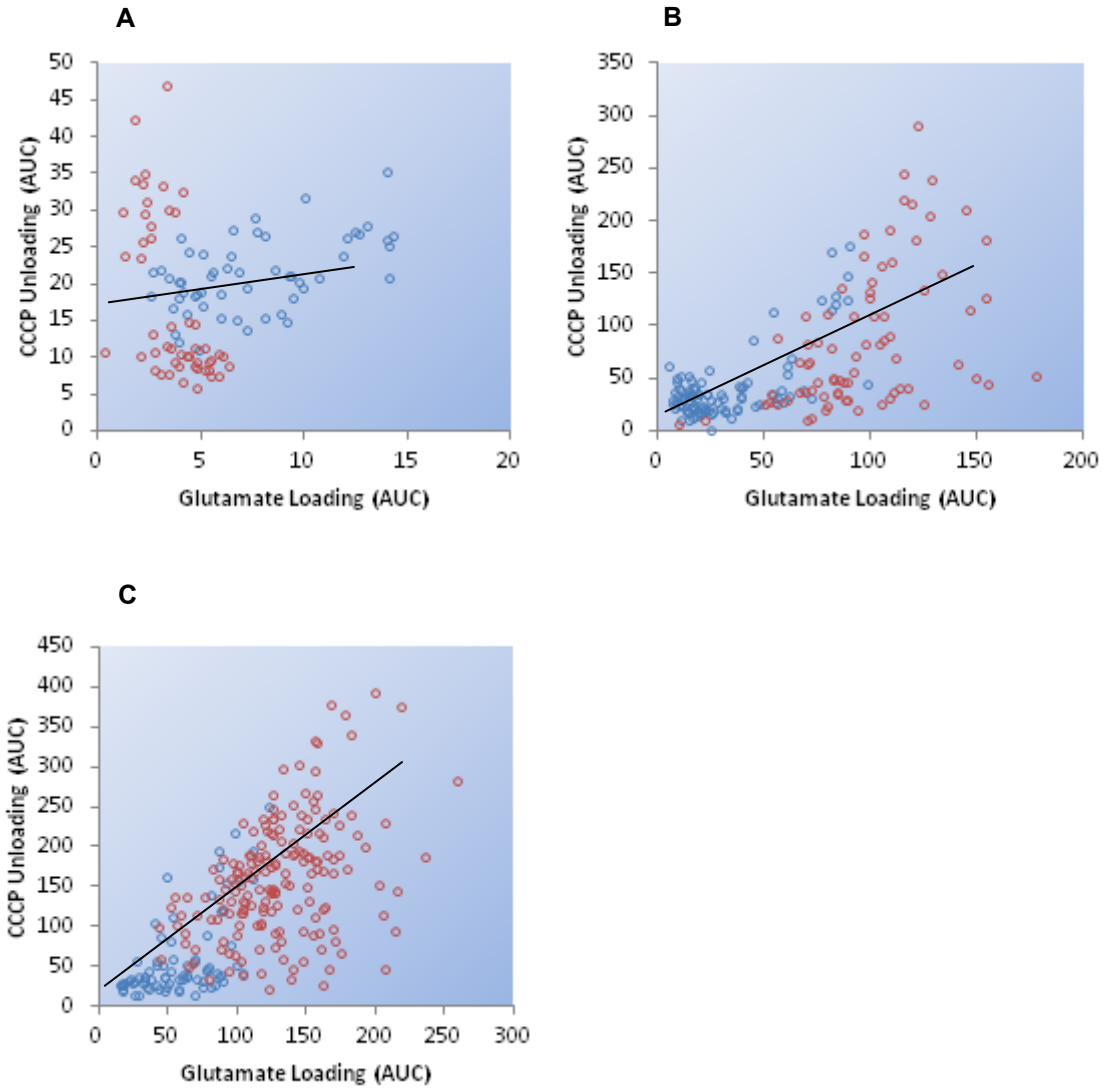

Figure 5.7. **The relationship between the glutamate loading of the neurone and the CCCP unloading.**

These graphs show the $[Ca^{2+}]_i$ after a 180 second glutamate stimulation (Loading of the neurone), against the $[Ca^{2+}]_i$ following a 300 second stimulation with CCCP (Unloading of the mitochondria). The graphs represent the area under the curve data from the following glutamate stimulations: (A) 2μM, (B) 20μM and (C) 200μM. Each data point on the graph represents a measurement taken from one neurone, with the blue circles coming from neurones at DIV 7-15 (Young) and the red circles from neurones at DIV 21-52 (Old).

5.4.6 The ability of the neurones to recovery to glutamate-induced rises in $[Ca^{2+}]_i$ and how this is affected by *in vitro* ageing.

The next stage of the analysis involved the period of time starting at the end of the 180 second glutamate and finishing just before the start of the CCCP incubation. This phase of the response was termed the 'recovery 'period' since the neurones were only exposed to the 'experimental' medium allowing time for the cells to try to restore their $[Ca^{2+}]_i$ back to normal cellular levels. Using linear regression, an equation of the line, R^2-value, *F*-value and P-value were determined for all of the data represented in *figure 5.8.A-C*. The results showed significant positive correlation between the *in vitro* age of neurones and the amount of recovery at: [2μM] Equation of the line: y=0.08xDIV+1.23, R^2=0.235, n=105, *F*-value=31.688, P<0.001, [20μM] y=1.84xDIV+2.99, R^2=0.531, n=172, *F*-value=192.579, P<0.001, [200μM] (y=1.800xDIV+45.328, R^2=0.294).

The data was then separated into two *in vitro* age groups: Young (DIV 7-15) and old (DIV 21-52) (See *figure 5.8.D*). One-way ANOVA analysis showed a significant difference between the young and old neurones at 2μM (*F*-statistic=4.103, P<0.05, n=55 [Young], n=50 [Old]), 20μM (*F*-statistic=179.557, P<0.001, n=95 [Young], n=77 [Old]) and 200μM (*F*-statistic=148.179, $P=3.85x10^{-27}$, n=78 [Young], n=177 [Old]). The statistical analysis also showed more elevation in the $[Ca^{2+}]_i$ during the recovery phase with increasing glutamate concentration in both the young (*F*-statistic=64.825, P<0.001, n=55 [2μM], n=95 [20μM], n=78 [200μM]) and old (*F*-statistic=197.629, P<0.001, n=51 [2μM], n=78 [20μM], n=178 [200μM]) neurones.

5.4.7 How the duration of glutamate exposure affects cytosolic Ca^{2+}.

To further investigate the relationship between the glutamate-induced Ca^{2+} increase and the unloading of Ca^{2+} from the mitochondria, experiments where carried out following the same experimental procedure described in *chapter 5.3.2*, but this time the duration of the glutamate stimulation was varied (60 seconds, 180 seconds and 540 seconds). Only one glutamate dose (20μM) was used for each experiment and all of the neurones in this part of the study were at an *in vitro* age of between 7 and 15 DIV.

Using one-way ANOVA analysis, significant differences were found between the glutamate loading of the neurones ($[Ca^{2+}]_i$ elevation induced by glutamate), the recovery period (time between the end of the glutamate stimulation and before the CCCP incubation) and the CCCP unloading (unloading of the Ca^{2+} from the mitochondria by CCCP) for all three lengths of glutamate stimulation: 60 seconds (*F*-statistic=16.625, P<0.001, n=77 [Glutamate load], n=77 [recovery] n=77 [CCCP Unloading], 180 seconds (*F*-statistic=12.784, P<0.001, n=100 [Glutamate load], n=100 [recovery], n=100 [CCCP Unloading] and 540 seconds (*F*-statistic=350.491, P<0.001, n=120 [Glutamate load], n=120 [recovery], n=120 [CCCP unloading]). There was a significantly larger increase in the initial cytosolic Ca^{2+} increase (glutamate loading) as the duration of the glutamate stimulation was lengthened (One-way ANOVA analysis: *F*-statistic=1873.529, P<0.001, n=77 [60 seconds], n=100 [180 seconds], n=120 [540 seconds]). When exposing the neurones to the shorter durations of glutamate stimulation (60 seconds and 180 seconds), there were

no significant differences in the CCCP unloading of the mitochondria (One-way ANOVA analysis: *F*-statistic=0.593, P>0.05, n=77 [60 seconds], n=100 [180 seconds]), however lengthening the glutamate exposure to 540 seconds showed a significantly larger mitochondrial unloading (One-way ANOVA analysis: *F*-statistic=295.393, P<0.001, n=77 [60 seconds], n=100 [180 seconds], n=120 [540 seconds]). The same pattern was found in the AUC for the recovery period, with no significant differences at the shorter glutamate exposures (One-way ANOVA analysis: *F*-statistic=0.586, P>0.05, n=77 [60 seconds], n=100 [180 seconds]), but a significant difference when incubated in glutamate for 540 seconds (One-way ANOVA analysis: *F*-statistic=208.940, P<0.001, n=77 [60 seconds], n=100 [180 seconds], n=120 [540 seconds]).

The graph of the mean (±S.E.M.) change in $[Ca^{2+}]_i$ expressed as an area under the curve (AUC) for the glutamate load, recovery and CCCP unloading is shown in *figure 5.9.A.* Linear regression analysis was used to explore the relationship between the glutamate load and the CCCP unloading of the mitochondria (*Figure 5.9.B-D*). The analysis showed a positive correlation between glutamate stimulation and the CCCP unloading when exposed to shorter lengths of glutamate ([60 seconds] y=1.35xglutamate loading+17.70, R^2=0.163, n=77, *F*-value=14.548, P<0.001; [180 seconds] y=1.15xglutamate loading+14.72, R^2=0.451, n=100, *F*-value=80.509, P<0.001) but no correlation when exposed to 540 seconds glutamate (y=-0.14xDIV+226.55, R^2=0.010, n=120, *F*-value=1.142, P>0.05).

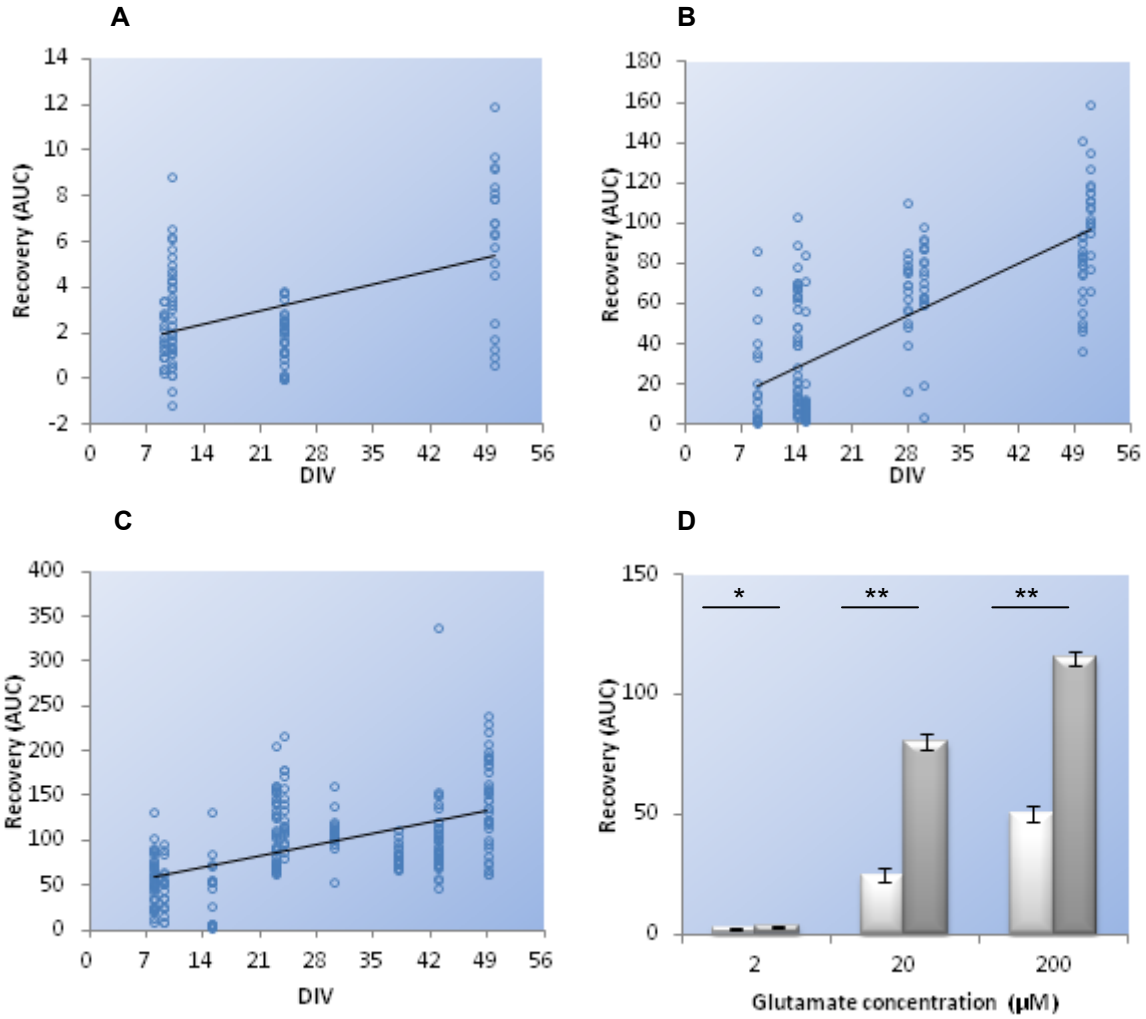

Figure 5.8. **The effect of *in vitro* age on glutamate-induced Ca^{2+} influx.**

These graphs show the effect of *in vitro* age (DIV) on the cytosolic Ca^{2+} concentration during the 300 second recovery period following glutamate exposure: (A) 2µM, (B) 20µM and (C) 200µM. This measure of $[Ca^{2+}]_i$ during the recovery period is derived from calculating the area under the curve. Each data point on the graph represents one measurement taken from a single neurone. Graph *D* shows the mean recovery (±S.E.M.) for each glutamate concentration. The light coloured bars represent neurones at 7-15 DIV and the dark coloured bars represent neurones at 21-52 DIV. Statistically significant differences in the mean recovery (AUC) between the young and old group of neurones are also highlighted on the graph: (*) $P<0.05$ and (**) $P<0.01$.

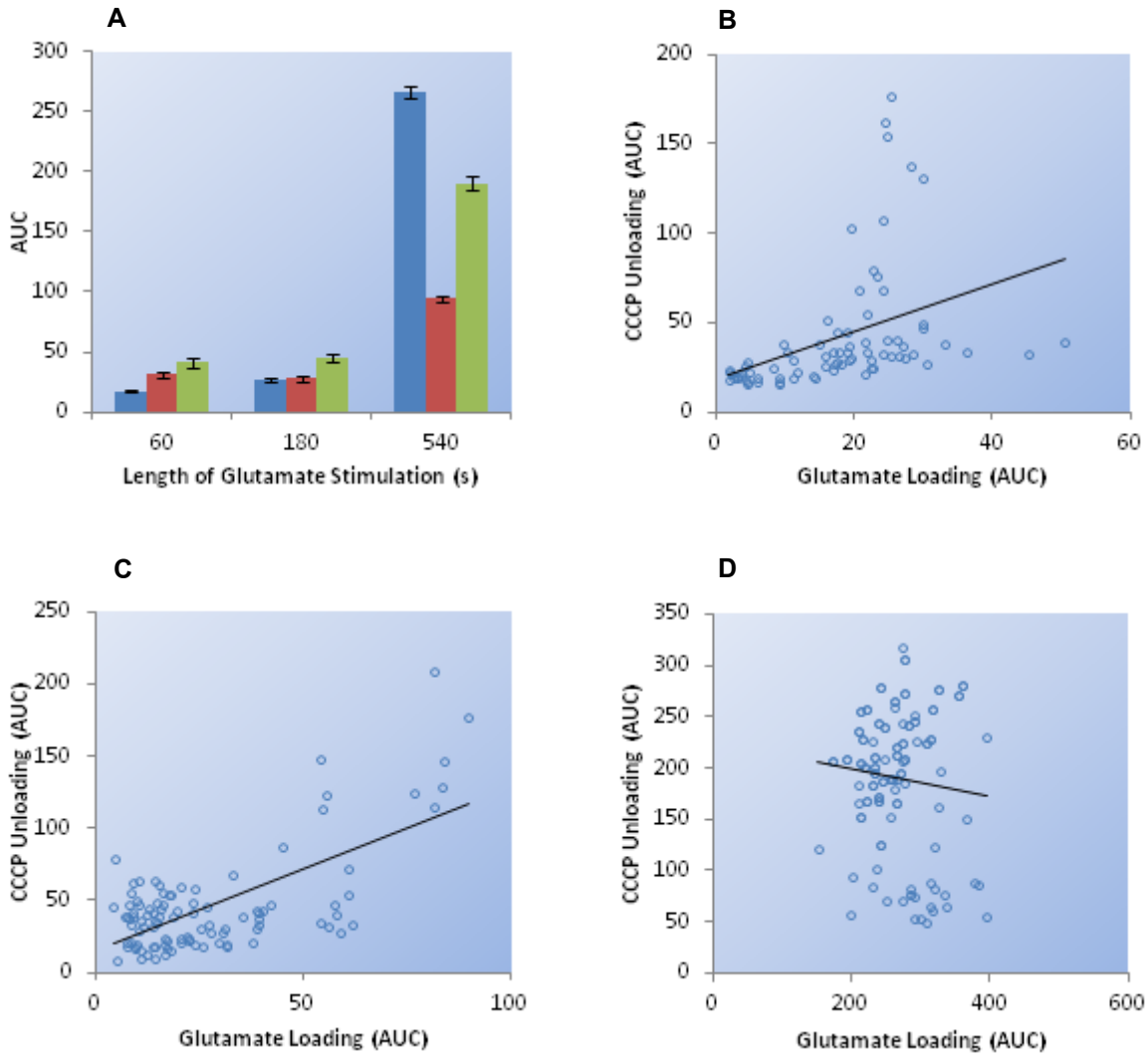

Figure 5.9. **The relationship between the duration of the glutamate stimulation and the unloading of Ca^{2+} from the mitochondria.**

These graphs show the effect of varying the length of the glutamate stimulation on the $[Ca^{2+}]_i$. The mean (±S.E.M.) change in $[Ca^{2+}]_i$ expressed as an area under the curve (AUC) is shown in *Panel A*. The blue bar on the graph represents the AUC for the glutamate stimulation, the red bar is the AUC for the recovery period and the green bar is the AUC for the unloading of the mitochondria by CCCP. *Panels B-D* show the AUC for the glutamate stimulation (Loading of the neurone), against the $[Ca^{2+}]_i$ following 300 second stimulation with CCCP (Unloading of the mitochondria). The graphs represent the AUC data from experiments using the following lengths of glutamate stimulations: (*B*) 60 seconds, (*C*) 180 seconds and (*D*) 540 seconds. Each data point on the graph represents a measurement taken from one neurone (DIV 7-15).

5.4.8 How the recovery period following glutamate exposure affects cytosolic Ca^{2+}.

Following on from the investigations into the affect of varying the duration of the glutamate incubation, the next stage of the project was to look at how increasing the recovery period (time starting at the end of the glutamate incubation and ending just before the CCCP exposure) affects the release of Ca^{2+} from the mitochondria (termed CCCP unloading). The three lengths of recovery period investigated were 100 seconds, 300 seconds and 900 seconds, each following a 20μM glutamate exposure for 180 seconds. All of the neurones in these experiments had an *in vitro* age of between 7 and 15 DIV.

Using one-way ANOVA analysis, a significant difference was shown between the CCCP unloading and the length of the recovery period, with a smaller $[Ca^{2+}]_i$ elevation associated with longer recovery duration (*F*-statistic=17.508, P<0.001, n=55 [100 seconds], n=99 [300 seconds] n=35 [900 seconds]).

Linear regression analysis was used to explore the relationship between the glutamate load and the CCCP unloading of the mitochondria and how this was affected by increasing the length of the recovery period (*Figure 5.10.B-D*). The analysis showed a positive correlation between the size of the glutamate load and the unloading of the mitochondria with CCCP, when exposed to each of the lengths of recovery duration, with a decrease in the slope of the response as the recovery period lengthens ([100 seconds] y=2.52xglutamate loading-26.82, R^2=0.796, n=60, *F*-value=226.879, P<0.001; [300 seconds] y=1.15xglutamate loading+14.72, R^2= 0.451,

n=100, *F*-value=80.509, P<0.001 and [900 seconds] y=0.19xglutamate loading+7.92, R^2=0.345, n=39, *F*-value= 19.485, P<0.001).

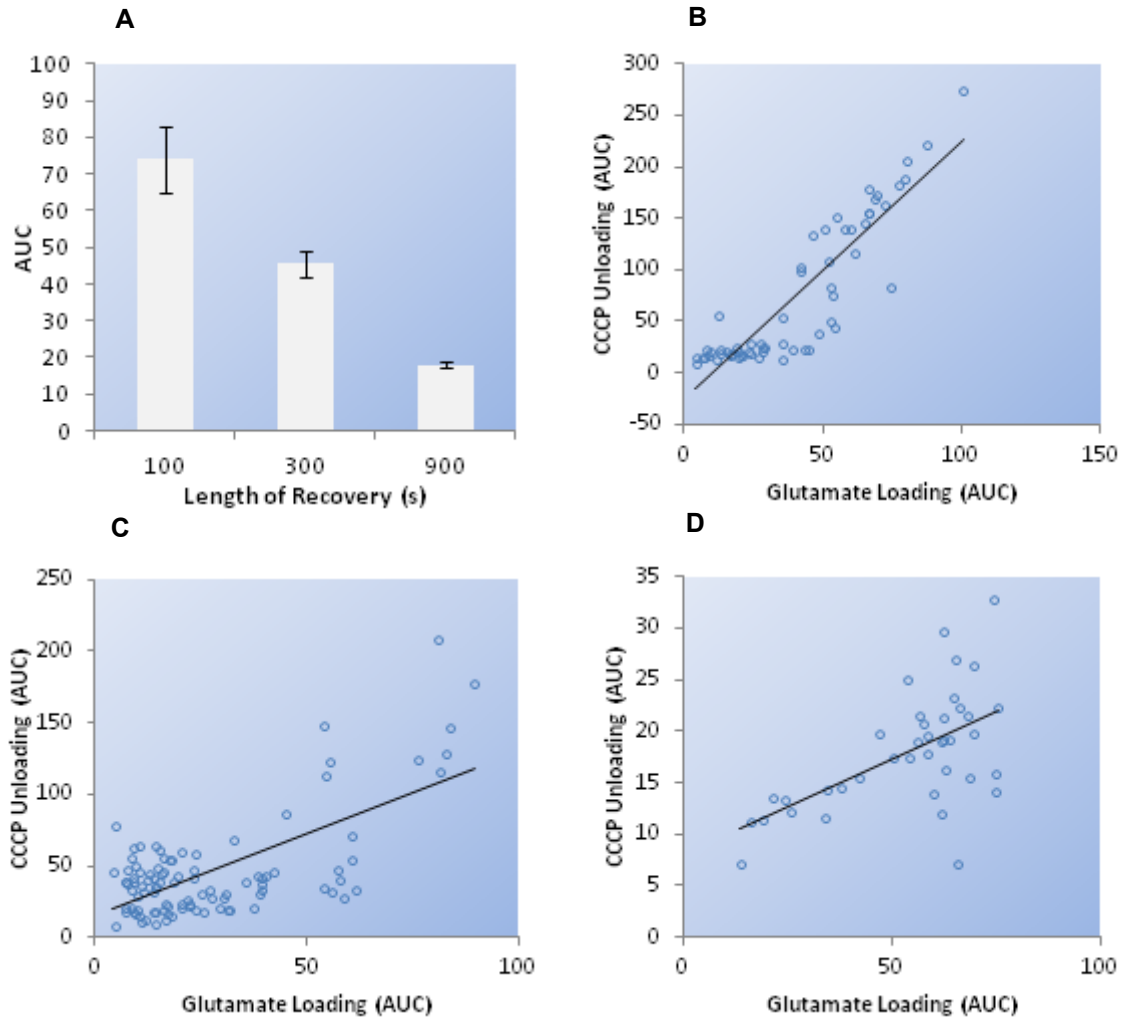

Figure 5.10. **The effect of the duration of the recovery period on the unloading of Ca^{2+} from the mitochondria.**

These graphs show the effect of increasing the length of the recovery period on the release of Ca^{2+} from the mitochondria (CCCP unloading). The mean (±S.E.M.) change in $[Ca^{2+}]_i$ expressed as an area under the curve (AUC) is shown in *Panel A*. *Panels B-D* show the AUC for the glutamate stimulation (loading of the neurones), against the AUC for the CCCP unloading, with the following durations of recovery: (*B*) 100 seconds, (*C*) 300 seconds and (*D*) 900 seconds. Each data point on the graph represents a measurement taken from one neurone (DIV 7-15).

5.5 *Discussion*

The work from the previous chapter showed that with increasing *in vitro* age, neurones became more vulnerable to the excitotoxic effects of glutamate. In order to try to find the possible mechanisms that may underlie this age-associated risk to excitotoxicity, this final part of the project was focussed on the changes in cytosolic Ca^{2+} concentration ($[Ca^{2+}]_i$) induced by glutamate and the role of the mitochondria in leading to neuronal death.

Many studies have shown that the addition of glutamate to rat cortical neurones (Brocard, Tassetto et al. 2001), hippocampal neurones (Connor, Wadman et al. 1988; Randall and Thayer 1992; Keelan, Vergun et al. 1999), cerebellar Purkinje neurones (Connor and Tseng 1988), rat forebrain neurones (White and Reynolds 1997) and cortical brain slices (Kannurpatti, Joshi et al. 2000) all lead to increases in $[Ca^{2+}]_i$. This study using cerebellar granule neurones supports those findings and shows the important effect of age (*in vitro* age) on the sensitivity of the neurones towards glutamate and therefore towards glutamate excitotoxicity. Significantly larger elevations in $[Ca^{2+}]_i$ following stimulation of cerebellar granule neurones with glutamate (20μM and 200μM) were positively correlated with *in vitro* age. Linear regression showed an increase in the area under the curve (AUC) of 2 per DIV when exposed to 20μM and 200μM glutamate concentrations. A similar finding was shown in primary cultured hippocampal neurones (containing glia) where neurones at 14 DIV had significantly larger glutamate-induced $[Ca^{2+}]_i$ rises in comparison to neurones at 9 DIV (Keelan, Vergun et al. 1999).

This was not the same when stimulating the neurones with 2μM, with older neurones appearing less sensitive to the glutamate than the younger neurones reflected in the smaller change in their $[Ca^{2+}]_i$. This may be due to the glutamate activating a non-NMDA response in the older neurones, since the NMDA has been shown to show a larger Ca^{2+} influx when stimulated with glutamate in comparison to the AMPA and Kainate (Brocard, Tassetto et al. 2001).

The size of the $[Ca^{2+}]_i$ increase was dependent on the glutamate concentration applied to the neurones, with significantly larger rises in $[Ca^{2+}]_i$ when stimulated with successively higher glutamate concentrations, irrespective of whether the neurones were classified as being young (7-15 DIV) or old (21-52 DIV). This glutamate dose-dependent change in $[Ca^{2+}]_i$ was shown in rat cortical neurones exposed to glutamate concentrations ranging from 1μM to 300μM (Brocard, Tassetto et al. 2001) and in cultured rat forebrain neurones when exposed to concentrations of 3μM to 300μM glutamate (White and Reynolds 1997).

The addition of the protonophore CCCP to the cerebellar granule neurones, following glutamate stimulation (20μM and 200μM), induced an increase in the $[Ca^{2+}]$, which also showed a significant positive correlation between the *in vitro* age of the neurones and the size of the rise in $[Ca^{2+}]_i$. When comparing the increase in $[Ca^{2+}]_i$ induced by the glutamate with the increase in $[Ca^{2+}]_i$ induced by the CCCP, the two were shown to be significantly correlated. The $[Ca^{2+}]_i$ following CCCP stimulation was increased with successively higher concentrations of glutamate, with the AUC increasing from a rate of 0.85 per DIV at 20μM, to a rate of 1.11 per DIV at 200μM.

This correlation between the glutamate-induced Ca^{2+} rise and the CCCP-induced Ca^{2+} rise has been shown in hippocampal neurones mixed with glia (Keelan, Vergun et al. 1999; Abramov and Duchen 2008), cultured cortical neurones (Brocard, Tassetto et al. 2001) and cortical brain slices (Kannurpatti, Joshi et al. 2000).

The protonophore CCCP is an ionophore that allows protons to move across the inner mitochondrial membrane, dissipating the mitochondrial membrane potential and leading to the release of Ca^{2+} from the mitochondria to the cytosol (Duchen 1990; Kiedrowski and Costa 1995). The rise in $[Ca^{2+}]_i$ following stimulation with CCCP is therefore due to unloading of the Ca^{2+} from the mitochondria. The mitochondria are capable of buffering large amounts of Ca^{2+} and therefore play an important role in Ca^{2+} homeostasis (Duchen 1999). When glutamate induces an increase in $[Ca^{2+}]_i$, some of this Ca^{2+} is sequestered by the mitochondria (Khodorov, Pinelis et al. 1999) resulting in a decrease in $[Ca^{2+}]_i$. The experiments exposing neurones to CCCP, without any previous glutamate stimulation, showed no increase in $[Ca^{2+}]_i$ which supports the idea that the CCCP-induced increase in $[Ca^{2+}]_i$ is due to the release of Ca^{2+} that was sequestered by the mitochondria (Thayer and Wang 1995; Budd and Nicholls 1996; Wang and Thayer 1996; Brocard, Tassetto et al. 2001).

The older neurones took a significantly longer time to recover to stimulation of glutamate at all three concentrations, ranging from 0.1-1.8 increases in AUC per DIV, which is similar to findings in hippocampal neurones (Keelan, Vergun et al. 1999; Vergun, Keelan et al. 1999). Since there was a clear vulnerability of the older neurones towards the glutamate excitotoxicity, the next stage of the project was

focussed on exploring the effect of the length of the glutamate stimulation. This results showed that when cerebellar granule neurones were exposed to shorter glutamate stimulations, (20μM: 60 seconds and 180 seconds) the glutamate-induced loading of the cell with Ca^{2+} was significantly smaller than the release of the Ca^{2+} from the mitochondria. However when exposed to the 20μM glutamate for 540 seconds, the mitochondrial Ca^{2+} release was significantly smaller than the glutamate load. A similar finding was shown in cortical neurones, with shorter glutamate stimulations (≤600 seconds with 30μM) having smaller $[Ca^{2+}]_i$ rises in comparison to the Ca^{2+} released from the mitochondria (Brocard, Tassetto et al. 2001). A further finding was that a three-fold increase in the length of the stimulation (from 60 seconds to 180 seconds) only showed a small significant increase in the glutamate loading of the cell and the mitochondrial unloading, illustrating how the neurones of all *in vitro* ages were less sensitive to shorter glutamate stimulation, perhaps not reaching the threshold to activate the NMDA receptors.

The final parameter assessed was the effect of the duration of the recovery period on the release of Ca^{2+}. This data showed that as the length of time between the glutamate exposure and the addition of CCCP increased, the amount of Ca^{2+} unloaded from the mitochondria significantly dropped which support findings in cortical neurones (Brocard, Tassetto et al. 2001). This suggests that the mitochondria first sequestered the Ca^{2+} from the cytosol and then slowly unloaded the Ca^{2+} over time.

The larger elevations of $[Ca^{2+}]_i$ in response to glutamate in the older neurones, could result from more activation of the ionotropic NMDA receptors which have been shown to induce the largest glutamate-induced Ca^{2+} load in relation to the AMPA and kainite receptors (Brocard, Tassetto et al. 2001). In addition, numerous studies have shown an age-dependent shift in the expression of the various subunits forming the ionotropic NMDA receptors (Xia, Ragan et al. 1995; Wong, Liu et al. 2002; Arundine and Tymianski 2003; Fu, Logan et al. 2005; Zhou and Baudry 2006) and the Group I metabotropic receptors (Attucci, Clodfelter et al. 2002), both been associated with glutamate excitotoxicity (Choi, Koh et al. 1988; Hartley, Kurth et al. 1993; Attucci, Clodfelter et al. 2002). This change in receptor subunit composition in the older neurones could result in greater permeability of the glutamate receptors to Ca^{2+}.

The density of L-type voltage-gated Ca^{2+} channels (VGCC) has also been shown to increase with *in vitro* age in hippocampal CA1 pyramidal neurones (Thibault and Landfield 1996; Thibault, Porter et al. 1998). Larger influxes of Na^+ and Ca^{2+} through the glutamate ionotropic receptors would depolarise the plasma membrane quicker, activating the VGCC at a faster rate. The suggestion that there are more VGCC in older neurones for the Ca^{2+} to move through, would result in greater Ca^{2+} influxes, which in turn could trigger more Ca^{2+}-induced Ca^{2+}-release from the endoplasmic reticulum (ryanodine receptors), further amplifying the change in $[Ca^{2+}]_i$ (Fagni, Chavis et al. 2000). Another aspect to consider is the role of the endoplasmic reticulum in sequestering Ca^{2+} from the cytosol, since it has been shown that the aged neurones have a smaller capacity to sequester cytosolic Ca^{2+} (Kirischuk and

Verkhratsky 1996). This would result in older neurones relying more heavily on mitochondrial sequestration and the other Ca^{2+} homeostatic mechanisms.

A final link between *in vitro* age and the change in $[Ca^{2+}]_i$ induced by glutamate, in particular when considering their delayed recovery, could be a result of accumulative damage to the extrusion pathways by ROS. It has been shown that the effects of accumulative damage from ROS contribute to the vulnerabilities associated with ageing (Harman 1956; Barnard, Robertson et al. 1997; Barja 2004). In particular, these ROS could induce lipid peroxidation, effecting key Ca^{2+} homeostatic mechanisms such as the plasma-membrane Ca^{2+}-ATPase and the endoplasmic reticulum Ca^{2+}-ATPase. Interference of either of these mechanisms would affect the restoration of Ca^{2+} back to normal cellular levels.

In the previous chapter the increased susceptibility of older neurones towards glutamate excitotoxicity was discussed with a suggestion that Ca^{2+} may lie at the route of the increased vulnerability. This chapter has followed on from the findings of *chapter 4* and focussed on the dynamics and mechanisms which underlie the neuronal response to glutamate stimulation. Evidence was provided to demonstrate the association of the glutamate-induced Ca^{2+} influx into the cytosol with the sequestration of this Ca^{2+} by the mitochondria, which was affected by the glutamate concentration, the length of the glutamate stimulation and the duration of the recovery period. In addition it has shown that as neurones age, they become more sensitive towards glutamate stimulation, resulting in greater sequestration of the Ca^{2+} by the mitochondria through the mitochondrial Ca^{2+}-uniporter. The consequences of

this glutamate-induced elevation in $[Ca^{2+}]_i$ and the subsequent movement of the Ca^{2+} into the mitochondria will be discussed in relation to the increased age-dependent vulnerability of the neurones to glutamate excitotoxicity in *chapter 6*.

6 Discussion

Ageing of the brain is a multi-factorial process which affects every living organism in a multitude of ways. It can result in age-associated memory impairment (Crook, Bahar et al. 1987; Coria, Gomez de Caso et al. 1993; Larrabee and Crook 1994; Barker, Jones et al. 1995; Koivisto, Reinikainen et al. 1995), age-associated cognitive decline, (Levy 1994; Hanninen, Koivisto et al. 1996; Rosenzweig and Barnes 2003) and the association of age with the incidence of neurodegenerative disease is well documented (Cleveland and Rothstein 2001; Mattson 2004; Cookson 2005; Moore, West et al. 2005). This increase in age-dependent vulnerability in neurones of the central nervous system, illustrates the importance of trying to understand the underlying mechanisms of the ageing process (Keelan, Vergun et al. 1999; Toescu, Verkhratsky et al. 2004; Mattson and Magnus 2006). The focus of this project was to try to assess the increased vulnerability of aged neurones and to provide insight into what causes these changes to occur at the cellular level.

The first stage of this project was to characterise and assess the suitability of primary cultured cerebellar granule neurones, as an *in vitro* 'ageing in a dish' model for studying the effects of *in vitro* age on vulnerability (Hartmann, Eckert et al. 1996; Kirischuk and Verkhratsky 1996; Toescu and Verkhratsky 2000; Xiong, Verkhratsky et al. 2002; Xiong, Camello et al. 2004). Completion of the investigation into this 'ageing in a dish' model shows that even though there were expected losses in neuronal numbers with increasing time maintained in culture (Kim, Oh et al. 2007; Robert, Cloix et al. 2012), the vast majority of the remaining neurones were still

viable at 45 DIV (94% of neurones still viable), which is consistent with other *in vitro* models using different neuronal cell types (Aksenova, Aksenov et al. 1999; Lesuisse and Martin 2002; Robert, Cloix et al. 2012). In addition, the model was shown to consist of >95% cerebellar granule neurones, which reconfirmed other studies and demonstrated the homogeneity of the culture (Gallo, Ciotti et al. 1982; Thangnipon, Kingsbury et al. 1983). This cerebellar granule neuronal culture had a relatively high 'survival' rate (where neuronal numbers were reasonably maintained over time), a consistently high level of neuronal viability for up to 8 weeks in culture and had very little contamination with other non-neuronal cells. These three criteria when combined, demonstrate the suitability of this experimental model for exploring cellular changes associated with the ageing process.

Using this *in vitro* model, the age-dependent vulnerability (Choi, Maulucci-Gedde et al. 1987; Vergun, Keelan et al. 1999) towards glutamate excitotoxicity (Lucas and Newhouse 1957; Olney 1969; Rothman and Olney 1986) was explored. This study showed that increases in *in vitro* age were associated with a higher susceptibility of the neurones to glutamate excitotoxicity. Older neurones (21-52 DIV) were shown to have more neuronal death in comparison to younger cells (7-15 DIV) exposed to the same glutamate concentrations (0.2-0.8% death per DIV - at all glutamate concentrations), which supports studies in cultured cortical neurones (Choi, Maulucci-Gedde et al. 1987) and cultured hippocampal neurones (Brewer 1998). Using an adapted propidium iodide method (See *chapter 4.3.1*), this study was able to investigate the dynamics of the glutamate-induced neuronal death which has not been previously explored to the same extent. The results showed that older

neurones had a shorter lag period (defined as the time taken for neuronal death to start following glutamate exposure) when stimulated with glutamate concentrations ≥50μM and a steeper rate of death when exposed to glutamate concentrations ≤50μM.

This age-dependent increase in vulnerability was associated with an age-dependent increase in sensitivity of the neurones to glutamate stimulation, with older neurones having larger glutamate-induced elevations in $[Ca^{2+}]_i$ in comparison to the younger cells. This increase in $[Ca^{2+}]_i$ was directly correlated with an increase in sequestration of the Ca^{2+} by the mitochondria, agreeing with studies in various cell types (Keelan, Vergun et al. 1999; Kannurpatti, Joshi et al. 2000; Brocard, Tassetto et al. 2001; Abramov and Duchen 2008). The size of the mitochondrial Ca^{2+} load was dependent on the concentration of glutamate applied, the duration of the glutamate stimulation and the length of the recovery period (time between glutamate-induced Ca^{2+} loading of the cell and CCCP-induced mitochondrial unloading), which supports similar findings in cortical neurones (Brocard, Tassetto et al. 2001).

From this study, it appears that the two key components of the increased vulnerability of the aged neurones to glutamate excitotoxicity, are the $[Ca^{2+}]_i$ and the mitochondrial sequestration of Ca^{2+}. The data has shown a clear age-dependent rise in vulnerability towards glutamate excitotoxicity, which is associated with a larger glutamate induced Ca^{2+} load that is significantly correlated with uptake of the Ca^{2+} by the mitochondria.

Factors which may contribute towards the high levels of glutamate-induced elevations in $[Ca^{2+}]_i$ found in the older neurones include: the age-dependent changes in expression of the various types of subunits which make-up the NMDA receptor (Xia, Ragan et al. 1995; Wong, Liu et al. 2002; Arundine and Tymianski 2003; Fu, Logan et al. 2005; Zhou and Baudry 2006) and Metabotropic receptors (Attucci, Clodfelter et al. 2002); the increase in density of L-type voltage-gated Ca^{2+} channels (VGCC) associated with age (Thibault and Landfield 1996; Thibault, Porter et al. 1998); an age-dependent reduction in the sequestering capacity of the endoplasmic reticulum (Kirischuk and Verkhratsky 1996) and the cumulative effect of reactive oxygen species (ROS) damage to the cell which may result in impaired Ca^{2+} homeostasis (Harman 1956; Barnard, Robertson et al. 1997; Barja 2004).

Small rises in $[Ca^{2+}]_i$, induce less mitochondrial Ca^{2+} uptake, resulting in a brief depolarisation of the mitochondrial membrane, which has been shown to enhance oxidative phosphorylation, resulting in a faster rate of ATP synthesis (Nicholls and Budd 2000; Toescu 2000). This may at first seem like a benefit to the neurone however, increased activity of the electron transport chain is associated with a greater risk of producing ROS at Complex I (Turrens and Boveris 1980; Kudin, Bimpong-Buta et al. 2004) and Complex III (Turrens, Alexandre et al. 1985; Turrens 1997). These ROS have been widely shown to contribute to cellular damage, leading to more genetic mutations which accumulate over time (Harman 1956; Barnard, Robertson et al. 1997; Barja 2004). In addition, production of ROS can initiate apoptosis by increasing the Ca^{2+} uptake into the mitochondria, eventually

leading to the release of cytochrome c, or by activating pro-apoptotic factors such as BAX and p53 (Toescu 1998; Brookes, Yoon et al. 2004; Mattson and Magnus 2006).

In contrast, excessive increases in $[Ca^{2+}]_i$ resulting in greater mitochondrial sequestration of the Ca^{2+}, disrupts the mitochondrial membrane potential, reducing the proton motive force (Nicholls and Akerman 1982; Gunter, Gunter et al. 1994). Since the entire concept of oxidative phosphorylation is based on the mitochondrial membrane potential, disruption of this membrane potential would not only lead to a halt in the respiratory chain, but would also result in the reversal of the ATP-synthase enzyme (Budd and Nicholls 1996; Dimroth, Kaim et al. 2000; Nicholls and Budd 2000; Schultz and Chan 2001). This would mean that instead of the ATP-synthase being used to produce ATP via oxidative phosphorylation, it would instead be used like an ATPase pump, using the energy harvested from the de-phosphorylation of ATP, to pump Ca^{2+} out of the mitochondria, in an attempt to restore the mitochondrial membrane potential. This increased use of ATP by the reversed action of the ATP-synthase coupled with the increased demand in ATP required by the plasma membrane Ca^{2+}-ATPase (for the extrusion of Ca^{2+} from the cytosol) and endoplasmic reticulum Ca^{2+}-ATPase (for movement of the Ca^{2+} into the endoplasmic reticulum), would result in rapid depletion of the cells ATP stores (Nicholls and Budd 2000). In addition, depolarisation of the mitochondria with Ca^{2+} has been shown to induce opening of the mitochondrial permeability transition pore (Green and Reed 1998; Kowaltowski, Naia-da-Silva et al. 1998; Friberg and Wieloch 2002) which could result in permanent disruption of the mitochondrial membrane potential leading to the release of cytochrome c and apoptosis inducing factors leading to inevitable death of the cell (Mattson and Kroemer 2003; Brookes, Yoon et al. 2004). This is consistent

with the data showing that the larger glutamate-induced Ca^{2+} increases are associated with more neuronal death as seen in the older neurones and in all neurones when applying larger concentrations of glutamate, or when lengthening the duration of the glutamate stimulation.

In order to provide more evidence for the importance of the mitochondrial sequestration of Ca^{2+} in age-dependent vulnerability, further experiments need to be carried out. Firstly Fura-2-AM could be co-loaded with the fluorescent dye R123, enabling simultaneous measurements of the $[Ca^{2+}]_i$ and the changes in the mitochondrial membrane potential (Castilho, Hansson et al. 1998; Xiong, Camello et al. 2004; Abramov and Duchen 2008). This would further correlate the rise in $[Ca^{2+}]_i$ with sequestration of the Ca^{2+}, since movement of the Ca^{2+} into the mitochondria would result in a depolarisation of the mitochondrial membrane (Khodorov, Pinelis et al. 1996; Vergun, Keelan et al. 1999). Secondly, various mitochondrial modulators could be tested as protective agents against glutamate excitotoxicity, including ruthenium red, which reduces uptake of Ca^{2+} through the mitochondrial uniporter, therefore preventing Ca^{2+} sequestration by the mitochondria (Duzenli, Bakuridze et al. 2005). Other modulators include inhibitors of the mitochondrial Na^+/Ca^{2+}-exchanger which in normal cellular conditions removes one Ca^{2+} out of the cell in exchange for three Na^+ into the cell, however activation of glutamate ionotropic receptors leads to large influxes of Na^+ into the cytosol, which causes a reversal in the direction of the Na^+/Ca^{2+}-exchanger, further increasing the $[Ca^{2+}]_i$. Addition of an inhibitor of this channel would prevent reversal of the exchanger during glutamate stimulation, allowing the Ca^{2+} extrusion to continue as normal (White and Reynolds

1996). Also inhibitors of the mitochondrial permeability transition pore (MPTP) could be used to explore its role in the excitotoxic neuronal death, since studies have shown an increased susceptibility of MPTP pore formation in aged neurones (Toescu, Myronova et al. 2000).

Thirdly, the importance of oxidative phosphorylation could be investigated further and compared between young and old neurones since previous work has suggested that inhibition of oxidative phosphorylation may be a protective mechanism for the cell (Castilho, Hansson et al. 1998; Castilho, Ward et al. 1999). Finally the impact of ATP depletion could be assessment by quantifying ATP in young and old neurones during stimulation with glutamate and comparing this with the observed levels of neuronal death (Budd and Nicholls 1996).

In summary, this project has demonstrated that there is an increased neuronal vulnerability with age. In this study, the focus of attention was the neuronal vulnerability to glutamate stimulation, since this is the major excitatory neurotransmitter and the major factor in various processes associated with excitotoxic damage (e.g., stroke). As mentioned earlier, it is well established that ageing is a major risk factor for all neurodegenerative diseases and normal ageing; however, the key difference is that the ageing brain does not show the drastic and significant neuronal loss typical of neurodegenerative diseases (West, Coleman et al. 1994; Morrison and Hof 1997). This observation of fact suggests that the process of normal brain ageing may involve only a mild impairment of Ca^{2+} homeostasis, inducing smaller levels of mitochondrial Ca^{2+} sequestration, generating less ROS, all

at levels too small to induce neuronal death, but still able to affect the neuronal network activity. With the activation of pathogenic mechanisms that might be specific for each neurodegenerative diseases, the balance of this inter-linked trio (Ca^{2+}, mitochondria and ROS) will become disturbed, with elevations in Ca^{2+} leading to greater mitochondrial sequestration, more ROS production, and this combination would result in neuronal death. What the current set of data indicates is that ageing leads to a slight shift in neuronal vulnerability, which is probably enough to compromise the defence of neuronal cells when faced with the extra neurodegenerative load. The data presented here clearly show lower levels of glutamate-induced neuronal death in the young neurones in comparison to the old. The younger neurones are far better at handling the increase in $[Ca^{2+}]_i$ and also have far less oxidative damage which results in their survival. As the neurones age, the ability to respond to excessive elevated $[Ca^{2+}]_i$ is reduced, making the cell more prone to neuronal death each day. But, since the aged neurones are still present in the brain, a better understanding of the metabolic and energetic changes that are induced by the ageing process can provide future means of earlier or effective interventions that will reduce the cognitive burden of the older age, and even more importantly, reduce or delay further the incidence of neurodegenerative processes.

7 References

Abdel-Hamid, K. M. and M. Tymianski (1997). "Mechanisms and effects of intracellular calcium buffering on neuronal survival in organotypic hippocampal cultures exposed to anoxia/aglycemia or to excitotoxins." J Neurosci **17**(10): 3538-53.

Abramov, A. Y. and M. R. Duchen (2008). "Mechanisms underlying the loss of mitochondrial membrane potential in glutamate excitotoxicity." Biochim Biophys Acta **1777**(7-8): 953-64.

Aksenova, M. V., M. Y. Aksenov, et al. (1999). "Aging in a dish: age-dependent changes of neuronal survival, protein oxidation, and creatine kinase BB expression in long-term hippocampal cell culture." J Neurosci Res **58**(2): 308-17.

Ali, S. T., J. R. Coggins, et al. (1997). "The study of cell-death proteins in the outer mitochondrial membrane by chemical cross-linking." Biochem J **325 (Pt 2)**: 321-4.

Ankarcrona, M., J. M. Dypbukt, et al. (1995). "Glutamate-induced neuronal death: a succession of necrosis or apoptosis depending on mitochondrial function." Neuron **15**(4): 961-73.

Arundine, M. and M. Tymianski (2003). "Molecular mechanisms of calcium-dependent neurodegeneration in excitotoxicity." Cell Calcium **34**(4-5): 325-37.

Arundine, M. and M. Tymianski (2004). "Molecular mechanisms of glutamate-dependent neurodegeneration in ischemia and traumatic brain injury." Cell Mol Life Sci **61**(6): 657-68.

Attucci, S., G. V. Clodfelter, et al. (2002). "Group I metabotropic glutamate receptor inhibition selectively blocks a prolonged Ca(2+) elevation associated with age-dependent excitotoxicity." Neuroscience **112**(1): 183-94.

Baffy, G., T. Miyashita, et al. (1993). "Apoptosis induced by withdrawal of interleukin-3 (IL-3) from an IL-3-dependent hematopoietic cell line is associated with repartitioning of intracellular calcium and is blocked by enforced Bcl-2 oncoprotein production." J Biol Chem **268**(9): 6511-9.

Baines, C. P., R. A. Kaiser, et al. (2005). "Loss of cyclophilin D reveals a critical role for mitochondrial permeability transition in cell death." Nature **434**(7033): 658-62.

Bannon, M. J. and C. J. Whitty (1997). "Age-related and regional differences in dopamine transporter mRNA expression in human midbrain." Neurology **48**(4): 969-77.

Barinaga, M. (1998). "Stroke-damaged neurons may commit cellular suicide." Science **281**(5381): 1302-3.

Barja, G. (2004). "Free radicals and aging." Trends Neurosci **27**(10): 595-600.

Barker, A., R. Jones, et al. (1995). "A prevalence study of age-associated memory impairment." Br J Psychiatry **167**(5): 642-8.

Barnard, M. L., B. Robertson, et al. (1997). "Role of nitric oxide and superoxide anion in spontaneous lung chemiluminescence." Am J Physiol **272**(2 Pt 1): L262-7.

Barreto-Chang, O. L. and R. E. Dolmetsch (2009). "Calcium imaging of cortical neurons using Fura-2 AM." J Vis Exp(23).

Basanez, G. and J. Zimmerberg (2001). "HIV and apoptosis death and the mitochondrion." J Exp Med **193**(4): F11-4.

Beal, M. F. (2005). "Mitochondria take center stage in aging and neurodegeneration." Ann Neurol **58**(4): 495-505.

Bernardi, P. (1999). "Mitochondrial transport of cations: channels, exchangers, and permeability transition." Physiol Rev **79**(4): 1127-55.

Birgbauer, E., T. S. Rao, et al. (2004). "Lysolecithin induces demyelination in vitro in a cerebellar slice culture system." J Neurosci Res **78**(2): 157-66.

Blalock, E. M., N. M. Porter, et al. (1999). "Decreased G-protein-mediated regulation and shift in calcium channel types with age in hippocampal cultures." J Neurosci **19**(19): 8674-84.

Bodhinathan, K., A. Kumar, et al. (2010). "Redox sensitive calcium stores underlie enhanced after hyperpolarization of aged neurons: role for ryanodine receptor mediated calcium signaling." J Neurophysiol **104**(5): 2586-93.

Brewer, G. J. (1997). "Isolation and culture of adult rat hippocampal neurons." J Neurosci Methods **71**(2): 143-55.

Brewer, G. J. (1998). "Age-related toxicity to lactate, glutamate, and beta-amyloid in cultured adult neurons." Neurobiol Aging **19**(6): 561-8.

Brocard, J. B., M. Tassetto, et al. (2001). "Quantitative evaluation of mitochondrial calcium content in rat cortical neurones following a glutamate stimulus." J Physiol **531**(Pt 3): 793-805.

Brookes, P. S., Y. Yoon, et al. (2004). "Calcium, ATP, and ROS: a mitochondrial love-hate triangle." Am J Physiol Cell Physiol **287**(4): C817-33.

Brosnan, J. T. and M. E. Brosnan (2012). "Glutamate: a truly functional amino acid." Amino Acids.

Bruno, A. M., J. Y. Huang, et al. (2011). "Altered ryanodine receptor expression in mild cognitive impairment and Alzheimer's disease." Neurobiol Aging **33**(5): 1001 e1-6.

Brustovetsky, N. and J. M. Dubinsky (2000). "Limitations of cyclosporin A inhibition of the permeability transition in CNS mitochondria." J Neurosci **20**(22): 8229-37.

Budd, S. L. and D. G. Nicholls (1996). "Mitochondria, calcium regulation, and acute glutamate excitotoxicity in cultured cerebellar granule cells." J Neurochem **67**(6): 2282-91.

Budd, S. L. and D. G. Nicholls (1996). "A reevaluation of the role of mitochondria in neuronal Ca2+ homeostasis." J Neurochem **66**(1): 403-11.

Burnashev, N., H. Monyer, et al. (1992). "Divalent ion permeability of AMPA receptor channels is dominated by the edited form of a single subunit." Neuron **8**(1): 189-98.

Camandola, S. and M. P. Mattson (2010). "Aberrant subcellular neuronal calcium regulation in aging and Alzheimer's disease." Biochim Biophys Acta **1813**(5): 965-73.

Campbell, L. W., S. Y. Hao, et al. (1996). "Aging changes in voltage-gated calcium currents in hippocampal CA1 neurons." J Neurosci **16**(19): 6286-95.

Canzoniero, L. M., A. Rossi, et al. (1992). "The Na(+)-Ca2+ exchanger activity in cerebrocortical nerve endings is reduced in old compared to young and

mature rats when it operates as a Ca2+ influx or efflux pathway." Biochim Biophys Acta **1107**(1): 175-8.
Carafoli, E. (1987). "Intracellular calcium homeostasis." Annu Rev Biochem **56**: 395-433.
Carafoli, E., L. Santella, et al. (2001). "Generation, control, and processing of cellular calcium signals." Crit Rev Biochem Mol Biol **36**(2): 107-260.
Castilho, R. F., O. Hansson, et al. (1998). "Mitochondrial control of acute glutamate excitotoxicity in cultured cerebellar granule cells." J Neurosci **18**(24): 10277-86.
Castilho, R. F., M. W. Ward, et al. (1999). "Oxidative stress, mitochondrial function, and acute glutamate excitotoxicity in cultured cerebellar granule cells." J Neurochem **72**(4): 1394-401.
Catterall, W. A. (2000). "Structure and regulation of voltage-gated Ca2+ channels." Annu Rev Cell Dev Biol **16**: 521-55.
Chen, Q. and E. J. Lesnefsky (2006). "Depletion of cardiolipin and cytochrome c during ischemia increases hydrogen peroxide production from the electron transport chain." Free Radic Biol Med **40**(6): 976-82.
Cho, S., A. Wood, et al. (2007). "Brain slices as models for neurodegenerative disease and screening platforms to identify novel therapeutics." Curr Neuropharmacol **5**(1): 19-33.
Choi, D. W., J. Y. Koh, et al. (1988). "Pharmacology of glutamate neurotoxicity in cortical cell culture: attenuation by NMDA antagonists." J Neurosci **8**(1): 185-96.
Choi, D. W., M. Maulucci-Gedde, et al. (1987). "Glutamate neurotoxicity in cortical cell culture." J Neurosci **7**(2): 357-68.
Cleveland, D. W. and J. D. Rothstein (2001). "From Charcot to Lou Gehrig: deciphering selective motor neuron death in ALS." Nat Rev Neurosci **2**(11): 806-19.
Cocco, T., P. Sgobbo, et al. (2005). "Tissue-specific changes of mitochondrial functions in aged rats: effect of a long-term dietary treatment with N-acetylcysteine." Free Radic Biol Med **38**(6): 796-805.
Connor, J. A. and H. Y. Tseng (1988). "Measurement of intracellular Ca2+ in cerebellar Purkinje neurons in culture: resting distribution and response to glutamate." Brain Res Bull **21**(3): 353-61.
Connor, J. A., W. J. Wadman, et al. (1988). "Sustained dendritic gradients of Ca2+ induced by excitatory amino acids in CA1 hippocampal neurons." Science **240**(4852): 649-53.
Cookson, M. R. (2005). "The biochemistry of Parkinson's disease." Annu Rev Biochem **74**: 29-52.
Coria, F., J. A. Gomez de Caso, et al. (1993). "Prevalence of age-associated memory impairment and dementia in a rural community." J Neurol Neurosurg Psychiatry **56**(9): 973-6.
Cotman, C. W. and A. J. Anderson (1995). "A potential role for apoptosis in neurodegeneration and Alzheimer's disease." Mol Neurobiol **10**(1): 19-45.
Cragg, S., M. E. Rice, et al. (1997). "Heterogeneity of electrically evoked dopamine release and reuptake in substantia nigra, ventral tegmental area, and striatum." J Neurophysiol **77**(2): 863-73.

Crook, T., H. Bahar, et al. (1987). "Age-associated memory impairment: diagnostic criteria and treatment strategies." Int J Neurol **21-22**: 73-82.

Daniels, M. and D. R. Brown (2002). "High extracellular potassium protects against the toxicity of cytosine arabinoside but is not required for the survival of cerebellar granule cells in vitro." Mol Cell Neurosci **19**(2): 281-91.

Dejean, L. M., S. Martinez-Caballero, et al. (2005). "Oligomeric Bax is a component of the putative cytochrome c release channel MAC, mitochondrial apoptosis-induced channel." Mol Biol Cell **16**(5): 2424-32.

Dejean, L. M., S. Martinez-Caballero, et al. (2006). "Is MAC the knife that cuts cytochrome c from mitochondria during apoptosis?" Cell Death Differ **13**(8): 1387-95.

Dessi, F., H. Pollard, et al. (1995). "Cytosine arabinoside induces apoptosis in cerebellar neurons in culture." J Neurochem **64**(5): 1980-7.

Dimroth, P., G. Kaim, et al. (2000). "Crucial role of the membrane potential for ATP synthesis by F(1)F(o) ATP synthases." J Exp Biol **203**(Pt 1): 51-9.

Dingledine, R., K. Borges, et al. (1999). "The glutamate receptor ion channels." Pharmacol Rev **51**(1): 7-61.

Dirnagl, U., C. Iadecola, et al. (1999). "Pathobiology of ischaemic stroke: an integrated view." Trends Neurosci **22**(9): 391-7.

Duchen, M. R. (1990). "Effects of metabolic inhibition on the membrane properties of isolated mouse primary sensory neurones." J Physiol **424**: 387-409.

Duchen, M. R. (1999). "Contributions of mitochondria to animal physiology: from homeostatic sensor to calcium signalling and cell death." J Physiol **516 (Pt 1)**: 1-17.

Duzenli, S., K. Bakuridze, et al. (2005). "The effects of ruthenium red, dantrolene and nimodipine, alone or in combination, in NMDA induced neurotoxicity of cerebellar granular cell culture of rats." Toxicol In Vitro **19**(5): 589-94.

Edinger, A. L. and C. B. Thompson (2004). "Death by design: apoptosis, necrosis and autophagy." Curr Opin Cell Biol **16**(6): 663-9.

Eguchi, Y., S. Shimizu, et al. (1997). "Intracellular ATP levels determine cell death fate by apoptosis or necrosis." Cancer Res **57**(10): 1835-40.

Fagni, L., P. Chavis, et al. (2000). "Complex interactions between mGluRs, intracellular Ca2+ stores and ion channels in neurons." Trends Neurosci **23**(2): 80-8.

Finkel, T. and N. J. Holbrook (2000). "Oxidants, oxidative stress and the biology of ageing." Nature **408**(6809): 239-47.

Freeman, S. H., R. Kandel, et al. (2008). "Preservation of neuronal number despite age-related cortical brain atrophy in elderly subjects without Alzheimer disease." J Neuropathol Exp Neurol **67**(12): 1205-12.

Friberg, H. and T. Wieloch (2002). "Mitochondrial permeability transition in acute neurodegeneration." Biochimie **84**(2-3): 241-50.

Fu, Z., S. M. Logan, et al. (2005). "Deletion of the NR2A subunit prevents developmental changes of NMDA-mEPSCs in cultured mouse cerebellar granule neurones." J Physiol **563**(Pt 3): 867-81.

Gallo, V., M. T. Ciotti, et al. (1982). "Selective release of glutamate from cerebellar granule cells differentiating in culture." Proc Natl Acad Sci U S A **79**(24): 7919-23.

Gallo, V., A. Kingsbury, et al. (1987). "The role of depolarization in the survival and differentiation of cerebellar granule cells in culture." J Neurosci **7**(7): 2203-13.

Gerace, E., T. Scartabelli, et al. (2012). "Mild activation of poly(ADP-ribose) polymerase (PARP) is neuroprotective in rat hippocampal slice models of ischemic tolerance." Eur J Neurosci.

Goldowitz, D. and K. Hamre (1998). "The cells and molecules that make a cerebellum." Trends Neurosci **21**(9): 375-82.

Green, D. R. and J. C. Reed (1998). "Mitochondria and apoptosis." Science **281**(5381): 1309-12.

Guerrieri, F., G. Capozza, et al. (1992). "Age-related changes of mitochondrial F0F1 ATP synthase." Ann N Y Acad Sci **671**: 395-402.

Gunter, T. E., K. K. Gunter, et al. (1994). "Mitochondrial calcium transport: physiological and pathological relevance." Am J Physiol **267**(2 Pt 1): C313-39.

Guo, L., D. Pietkiewicz, et al. (2004). "Effects of cytochrome c on the mitochondrial apoptosis-induced channel MAC." Am J Physiol Cell Physiol **286**(5): C1109-17.

Haas, H. L., B. Schaerer, et al. (1979). "A simple perfusion chamber for the study of nervous tissue slices in vitro." J Neurosci Methods **1**(4): 323-5.

Hanninen, T., K. Koivisto, et al. (1996). "Prevalence of ageing-associated cognitive decline in an elderly population." Age Ageing **25**(3): 201-5.

Haripriya, D., M. A. Devi, et al. (2004). "Age-dependent alterations in mitochondrial enzymes in cortex, striatum and hippocampus of rat brain -- potential role of L-Carnitine." Biogerontology **5**(5): 355-64.

Harman, D. (1956). "Aging: a theory based on free radical and radiation chemistry." J Gerontol **11**(3): 298-300.

Hartley, D. M., M. C. Kurth, et al. (1993). "Glutamate receptor-induced 45Ca2+ accumulation in cortical cell culture correlates with subsequent neuronal degeneration." J Neurosci **13**(5): 1993-2000.

Hartmann, H., A. Eckert, et al. (1996). "Down-regulation of free intracellular calcium in dissociated brain cells of aged mice and rats." Life Sci **59**(5-6): 435-49.

Hatten, M. E. and N. Heintz (1995). "Mechanisms of neural patterning and specification in the developing cerebellum." Annu Rev Neurosci **18**: 385-408.

Herman, J. P., K. C. Chen, et al. (1998). "Up-regulation of alpha1D Ca2+ channel subunit mRNA expression in the hippocampus of aged F344 rats." Neurobiol Aging **19**(6): 581-7.

Hickey, M. A. and M. F. Chesselet (2003). "Apoptosis in Huntington's disease." Prog Neuropsychopharmacol Biol Psychiatry **27**(2): 255-65.

Ito, S., S. Ohta, et al. (1999). "Functional integrity of mitochondrial genomes in human platelets and autopsied brain tissues from elderly patients with Alzheimer's disease." Proc Natl Acad Sci U S A **96**(5): 2099-103.

Kannurpatti, S. S., P. G. Joshi, et al. (2000). "Calcium sequestering ability of mitochondria modulates influx of calcium through glutamate receptor channel." Neurochem Res **25**(12): 1527-36.

Katsuki, H. and A. Akaike (2004). "Excitotoxic degeneration of hypothalamic orexin neurons in slice culture." Neurobiol Dis **15**(1): 61-9.

Keelan, J., O. Vergun, et al. (1999). "Excitotoxic mitochondrial depolarisation requires both calcium and nitric oxide in rat hippocampal neurons." J Physiol **520 Pt 3**: 797-813.

Kerr, J. F., A. H. Wyllie, et al. (1972). "Apoptosis: a basic biological phenomenon with wide-ranging implications in tissue kinetics." Br J Cancer **26**(4): 239-57.
Khachaturian, Z. S. (1987). "Hypothesis on the regulation of cytosol calcium concentration and the aging brain." Neurobiol Aging **8**(4): 345-6.
Khachaturian, Z. S. (1991). "Calcium and the aging brain: upsetting a delicate balance?" Geriatrics **46**(11): 78-9, 83.
Khachaturian, Z. S. (1994). "Calcium hypothesis of Alzheimer's disease and brain aging." Ann N Y Acad Sci **747**: 1-11.
Khodorov, B. (2004). "Glutamate-induced deregulation of calcium homeostasis and mitochondrial dysfunction in mammalian central neurones." Prog Biophys Mol Biol **86**(2): 279-351.
Khodorov, B., V. Pinelis, et al. (1996). "Dominant role of mitochondria in protection against a delayed neuronal Ca2+ overload induced by endogenous excitatory amino acids following a glutamate pulse." FEBS Lett **393**(1): 135-8.
Khodorov, B., V. Pinelis, et al. (1999). "Blockade of mitochondrial Ca2+ uptake by mitochondrial inhibitors amplifies the glutamate-induced calcium response in cultured cerebellar granule cells." FEBS Lett **458**(2): 162-6.
Khodorov, B. I., D. A. Fayuk, et al. (1996). "Effect of a prolonged glutamate challenge on plasmalemmal calcium permeability in mammalian central neurones. Mn2+ as a tool to study calcium influx pathways." Int J Neurosci **88**(3-4): 215-41.
Khodorov, B. I., T. P. Storozhevykh, et al. (2002). "The leading role of mitochondrial depolarization in the mechanism of glutamate-induced disruptions in Ca2+ homeostasis." Neurosci Behav Physiol **32**(5): 541-7.
Kiedrowski, L. and E. Costa (1995). "Glutamate-induced destabilization of intracellular calcium concentration homeostasis in cultured cerebellar granule cells: role of mitochondria in calcium buffering." Mol Pharmacol **47**(1): 140-7.
Kim, M. J., S. J. Oh, et al. (2007). "Neuronal loss in primary long-term cortical culture involves neurodegeneration-like cell death via calpain and p35 processing, but not developmental apoptosis or aging." Exp Mol Med **39**(1): 14-26.
Kirischuk, S. and A. Verkhratsky (1996). "Calcium homeostasis in aged neurones." Life Sci **59**(5-6): 451-9.
Koivisto, K., K. J. Reinikainen, et al. (1995). "Prevalence of age-associated memory impairment in a randomly selected population from eastern Finland." Neurology **45**(4): 741-7.
Kowaltowski, A. J., R. F. Castilho, et al. (1996). "Opening of the mitochondrial permeability transition pore by uncoupling or inorganic phosphate in the presence of Ca2+ is dependent on mitochondrial-generated reactive oxygen species." FEBS Lett **378**(2): 150-2.
Kowaltowski, A. J., E. S. Naia-da-Silva, et al. (1998). "Ca2+-stimulated mitochondrial reactive oxygen species generation and permeability transition are inhibited by dibucaine or Mg2+." Arch Biochem Biophys **359**(1): 77-81.
Krajewski, S., S. Tanaka, et al. (1993). "Investigation of the subcellular distribution of the bcl-2 oncoprotein: residence in the nuclear envelope, endoplasmic reticulum, and outer mitochondrial membranes." Cancer Res **53**(19): 4701-14.
Krebs, H. A. (1970). "The history of the tricarboxylic acid cycle." Perspect Biol Med **14**(1): 154-70.
Kroemer, G. and J. C. Reed (2000). "Mitochondrial control of cell death." Nat Med **6**(5): 513-9.

Ku, H. H., U. T. Brunk, et al. (1993). "Relationship between mitochondrial superoxide and hydrogen peroxide production and longevity of mammalian species." Free Radic Biol Med **15**(6): 621-7.

Kudin, A. P., N. Y. Bimpong-Buta, et al. (2004). "Characterization of superoxide-producing sites in isolated brain mitochondria." J Biol Chem **279**(6): 4127-35.

Kujoth, G. C., A. Hiona, et al. (2005). "Mitochondrial DNA mutations, oxidative stress, and apoptosis in mammalian aging." Science **309**(5733): 481-4.

Larrabee, G. J. and T. H. Crook, 3rd (1994). "Estimated prevalence of age-associated memory impairment derived from standardized tests of memory function." Int Psychogeriatr **6**(1): 95-104.

Larrabee, G. J. and W. J. McEntee (1995). "Age-associated memory impairment: sorting out the controversies." Neurology **45**(4): 611-4.

Lee, J. M., G. J. Zipfel, et al. (1999). "The changing landscape of ischaemic brain injury mechanisms." Nature **399**(6738 Suppl): A7-14.

Lesnefsky, E. J. and C. L. Hoppel (2006). "Oxidative phosphorylation and aging." Ageing Res Rev **5**(4): 402-33.

Lesuisse, C. and L. J. Martin (2002). "Long-term culture of mouse cortical neurons as a model for neuronal development, aging, and death." J Neurobiol **51**(1): 9-23.

Levy, R. (1994). "Aging-associated cognitive decline. Working Party of the International Psychogeriatric Association in collaboration with the World Health Organization." Int Psychogeriatr **6**(1): 63-8.

Li, P., D. Nijhawan, et al. (1997). "Cytochrome c and dATP-dependent formation of Apaf-1/caspase-9 complex initiates an apoptotic protease cascade." Cell **91**(4): 479-89.

Li, V., T. Brustovetsky, et al. (2009). "Role of cyclophilin D-dependent mitochondrial permeability transition in glutamate-induced calcium deregulation and excitotoxic neuronal death." Exp Neurol **218**(2): 171-82.

Liao, C. Y., B. A. Rikke, et al. (2012). "Genetic variation in the murine lifespan response to dietary restriction: from life extension to life shortening." Aging Cell **9**(1): 92-5.

Lucas, D. R. and J. P. Newhouse (1957). "The toxic effect of sodium L-glutamate on the inner layers of the retina." AMA Arch Ophthalmol **58**(2): 193-201.

Manev, H., M. Favaron, et al. (1989). "Delayed increase of Ca2+ influx elicited by glutamate: role in neuronal death." Mol Pharmacol **36**(1): 106-12.

Mark, L. P., R. W. Prost, et al. (2001). "Pictorial review of glutamate excitotoxicity: fundamental concepts for neuroimaging." AJNR Am J Neuroradiol **22**(10): 1813-24.

Martin, D. P., T. L. Wallace, et al. (1990). "Cytosine arabinoside kills postmitotic neurons in a fashion resembling trophic factor deprivation: evidence that a deoxycytidine-dependent process may be required for nerve growth factor signal transduction." J Neurosci **10**(1): 184-93.

Martin, L. J., N. A. Al-Abdulla, et al. (1998). "Neurodegeneration in excitotoxicity, global cerebral ischemia, and target deprivation: A perspective on the contributions of apoptosis and necrosis." Brain Res Bull **46**(4): 281-309.

Marzo, I., C. Brenner, et al. (1998). "The permeability transition pore complex: a target for apoptosis regulation by caspases and bcl-2-related proteins." J Exp Med **187**(8): 1261-71.

Mata, A. M. and M. R. Sepulveda (2010). "Plasma membrane Ca-ATPases in the nervous system during development and ageing." World J Biol Chem **1**(7): 229-34.

Mattson, M. P. (2004). "Pathways towards and away from Alzheimer's disease." Nature **430**(7000): 631-9.

Mattson, M. P., B. Cheng, et al. (1992). "beta-Amyloid peptides destabilize calcium homeostasis and render human cortical neurons vulnerable to excitotoxicity." J Neurosci **12**(2): 376-89.

Mattson, M. P. and G. Kroemer (2003). "Mitochondria in cell death: novel targets for neuroprotection and cardioprotection." Trends Mol Med **9**(5): 196-205.

Mattson, M. P. and T. Magnus (2006). "Ageing and neuronal vulnerability." Nat Rev Neurosci **7**(4): 278-94.

Melov, S., J. Ravenscroft, et al. (2000). "Extension of life-span with superoxide dismutase/catalase mimetics." Science **289**(5484): 1567-9.

Merry, B. J. (2002). "Molecular mechanisms linking calorie restriction and longevity." Int J Biochem Cell Biol **34**(11): 1340-54.

Michaelis, E. K. (1998). "Molecular biology of glutamate receptors in the central nervous system and their role in excitotoxicity, oxidative stress and aging." Prog Neurobiol **54**(4): 369-415.

Michaelis, M. L., D. J. Bigelow, et al. (1996). "Decreased plasma membrane calcium transport activity in aging brain." Life Sci **59**(5-6): 405-12.

Michaelis, M. L., K. Johe, et al. (1984). "Age-dependent alterations in synaptic membrane systems for Ca2+ regulation." Mech Ageing Dev **25**(1-2): 215-25.

Michinaga, S., A. Hisatsune, et al. (2010). "Inhibition of neural activity depletes orexin from rat hypothalamic slice culture." J Neurosci Res **88**(1): 214-21.

Mitchell, P. (1976). "Possible molecular mechanisms of the protonmotive function of cytochrome systems." J Theor Biol **62**(2): 327-67.

Mitchell, P. and J. Moyle (1967). "Chemiosmotic hypothesis of oxidative phosphorylation." Nature **213**(5072): 137-9.

Mitchell, P. and J. Moyle (1969). "Estimation of membrane potential and pH difference across the cristae membrane of rat liver mitochondria." Eur J Biochem **7**(4): 471-84.

Monaghan, D. T. and C. W. Cotman (1985). "Distribution of N-methyl-D-aspartate-sensitive L-[3H]glutamate-binding sites in rat brain." J Neurosci **5**(11): 2909-19.

Moore, D. J., A. B. West, et al. (2005). "Molecular pathophysiology of Parkinson's disease." Annu Rev Neurosci **28**: 57-87.

Morrison, J. H. and P. R. Hof (1997). "Life and death of neurons in the aging brain." Science **278**(5337): 412-9.

Nakagawa, T., S. Shimizu, et al. (2005). "Cyclophilin D-dependent mitochondrial permeability transition regulates some necrotic but not apoptotic cell death." Nature **434**(7033): 652-8.

Newell, D. W., A. Barth, et al. (1995). "Glutamate and non-glutamate receptor mediated toxicity caused by oxygen and glucose deprivation in organotypic hippocampal cultures." J Neurosci **15**(11): 7702-11.

Nicholls, D. and K. Akerman (1982). "Mitochondrial calcium transport." Biochim Biophys Acta **683**(1): 57-88.

Nicholls, D. G. and S. L. Budd (2000). "Mitochondria and neuronal survival." Physiol Rev **80**(1): 315-60.

Niciu, M. J., B. Kelmendi, et al. (2012). "Overview of glutamatergic neurotransmission in the nervous system." Pharmacol Biochem Behav **100**(4): 656-64.

Ojaimi, J., C. L. Masters, et al. (1999). "Mitochondrial respiratory chain activity in the human brain as a function of age." Mech Ageing Dev **111**(1): 39-47.

Olney, J. W. (1969). "Brain lesions, obesity, and other disturbances in mice treated with monosodium glutamate." Science **164**(880): 719-21.

Olney, J. W., R. C. Collins, et al. (1986). "Excitotoxic mechanisms of epileptic brain damage." Adv Neurol **44**: 857-77.

Papa, S. (1996). "Mitochondrial oxidative phosphorylation changes in the life span. Molecular aspects and physiopathological implications." Biochim Biophys Acta **1276**(2): 87-105.

Parihar, M. S. and G. J. Brewer (2007). "Simultaneous age-related depolarization of mitochondrial membrane potential and increased mitochondrial reactive oxygen species production correlate with age-related glutamate excitotoxicity in rat hippocampal neurons." J Neurosci Res **85**(5): 1018-32.

Pavlov, E. V., M. Priault, et al. (2001). "A novel, high conductance channel of mitochondria linked to apoptosis in mammalian cells and Bax expression in yeast." J Cell Biol **155**(5): 725-31.

Pinton, P., D. Ferrari, et al. (2000). "Reduced loading of intracellular Ca(2+) stores and downregulation of capacitative Ca(2+) influx in Bcl-2-overexpressing cells." J Cell Biol **148**(5): 857-62.

Pitt, D., P. Werner, et al. (2000). "Glutamate excitotoxicity in a model of multiple sclerosis." Nat Med **6**(1): 67-70.

Puzianowska-Kuznicka, M. and J. Kuznicki (2009). "The ER and ageing II: calcium homeostasis." Ageing Res Rev **8**(3): 160-72.

Qin, Z. H., Y. Wang, et al. (1996). "Stimulation of N-methyl-D-aspartate receptors induces apoptosis in rat brain." Brain Res **725**(2): 166-76.

Randall, R. D. and S. A. Thayer (1992). "Glutamate-induced calcium transient triggers delayed calcium overload and neurotoxicity in rat hippocampal neurons." J Neurosci **12**(5): 1882-95.

Robert, F., J. F. Cloix, et al. (2012). "Ultrastructural characterization of rat neurons in primary culture." Neuroscience **200**: 248-60.

Roe, M. W., J. J. Lemasters, et al. (1990). "Assessment of Fura-2 for measurements of cytosolic free calcium." Cell Calcium **11**(2-3): 63-73.

Rosenzweig, E. S. and C. A. Barnes (2003). "Impact of aging on hippocampal function: plasticity, network dynamics, and cognition." Prog Neurobiol **69**(3): 143-79.

Rothman, S. M. and J. W. Olney (1986). "Glutamate and the pathophysiology of hypoxic--ischemic brain damage." Ann Neurol **19**(2): 105-11.

Ruan, H., X. D. Tang, et al. (2002). "High-quality life extension by the enzyme peptide methionine sulfoxide reductase." Proc Natl Acad Sci U S A **99**(5): 2748-53.

Rytter, A., T. Cronberg, et al. (2003). "Mouse hippocampal organotypic tissue cultures exposed to in vitro "ischemia" show selective and delayed CA1 damage that is aggravated by glucose." J Cereb Blood Flow Metab **23**(1): 23-33.

Satrustegui, J., M. Villalba, et al. (1996). "Cytosolic and mitochondrial calcium in synaptosomes during aging." Life Sci **59**(5-6): 429-34.

Sattler, R., M. P. Charlton, et al. (1997). "Determination of the time course and extent of neurotoxicity at defined temperatures in cultured neurons using a modified multiwell plate fluorescence scanner." J Cereb Blood Flow Metab **17**(4): 455-63.

Schriner, S. E., N. J. Linford, et al. (2005). "Extension of murine life span by overexpression of catalase targeted to mitochondria." Science **308**(5730): 1909-11.

Schultz, B. E. and S. I. Chan (2001). "Structures and proton-pumping strategies of mitochondrial respiratory enzymes." Annu Rev Biophys Biomol Struct **30**: 23-65.

Seil, F. J., R. Drake-Baumann, et al. (1992). "Cytosine arabinoside effects in mouse cerebellar cultures in the presence of astrocytes." Neuroscience **51**(1): 149-58.

Sotelo, C. (2004). "Cellular and genetic regulation of the development of the cerebellar system." Prog Neurobiol **72**(5): 295-339.

Stavrovskaya, I. G. and B. S. Kristal (2005). "The powerhouse takes control of the cell: is the mitochondrial permeability transition a viable therapeutic target against neuronal dysfunction and death?" Free Radic Biol Med **38**(6): 687-97.

Stout, A. K., H. M. Raphael, et al. (1998). "Glutamate-induced neuron death requires mitochondrial calcium uptake." Nat Neurosci **1**(5): 366-73.

Tanke, H. J., P. W. van der Linden, et al. (1982). "Alternative fluorochromes to ethidium bromide for automated read out of cytotoxicity tests." J Immunol Methods **52**(1): 91-6.

Tanveer, A., S. Virji, et al. (1996). "Involvement of cyclophilin D in the activation of a mitochondrial pore by Ca2+ and oxidant stress." Eur J Biochem **238**(1): 166-72.

Terry, R. D., R. DeTeresa, et al. (1987). "Neocortical cell counts in normal human adult aging." Ann Neurol **21**(6): 530-9.

Thangnipon, W., A. Kingsbury, et al. (1983). "Observations on rat cerebellar cells in vitro: influence of substratum, potassium concentration and relationship between neurones and astrocytes." Brain Res **313**(2): 177-89.

Thayer, S. A. and G. J. Wang (1995). "Glutamate-induced calcium loads: effects on energy metabolism and neuronal viability." Clin Exp Pharmacol Physiol **22**(4): 303-4.

Thibault, O. and P. W. Landfield (1996). "Increase in single L-type calcium channels in hippocampal neurons during aging." Science **272**(5264): 1017-20.

Thibault, O., N. M. Porter, et al. (1998). "Calcium dysregulation in neuronal aging and Alzheimer's disease: history and new directions." Cell Calcium **24**(5-6): 417-33.

Tian, L., Q. Cai, et al. (1998). "Alterations of antioxidant enzymes and oxidative damage to macromolecules in different organs of rats during aging." Free Radic Biol Med **24**(9): 1477-84.

Toescu, E. C. (1998). "Apoptosis and cell death in neuronal cells: where does Ca2+ fit in?" Cell Calcium **24**(5-6): 387-403.

Toescu, E. C. (1999). "Activity of voltage-operated calcium channels in rat cerebellar granule neurons and neuronal survival." Neuroscience **94**(2): 561-70.

Toescu, E. C. (2000). "Mitochondria and Ca(2+) signaling." J Cell Mol Med **4**(3): 164-175.
Toescu, E. C. (2005). "Normal brain ageing: models and mechanisms." Philos Trans R Soc Lond B Biol Sci **360**(1464): 2347-54.
Toescu, E. C., N. Myronova, et al. (2000). "Age-related structural and functional changes of brain mitochondria." Cell Calcium **28**(5-6): 329-38.
Toescu, E. C. and A. Verkhratsky (2000). "Neuronal ageing in long-term cultures: alterations of Ca2+ homeostasis." Neuroreport **11**(17): 3725-9.
Toescu, E. C. and A. Verkhratsky (2003). "Neuronal ageing from an intraneuronal perspective: roles of endoplasmic reticulum and mitochondria." Cell Calcium **34**(4-5): 311-23.
Toescu, E. C., A. Verkhratsky, et al. (2004). "Ca2+ regulation and gene expression in normal brain aging." Trends Neurosci **27**(10): 614-20.
Tower, J. (2000). "Transgenic methods for increasing Drosophila life span." Mech Ageing Dev **118**(1-2): 1-14.
Trifunovic, A., A. Wredenberg, et al. (2004). "Premature ageing in mice expressing defective mitochondrial DNA polymerase." Nature **429**(6990): 417-23.
Turrens, J. F. (1997). "Superoxide production by the mitochondrial respiratory chain." Biosci Rep **17**(1): 3-8.
Turrens, J. F., A. Alexandre, et al. (1985). "Ubisemiquinone is the electron donor for superoxide formation by complex III of heart mitochondria." Arch Biochem Biophys **237**(2): 408-14.
Turrens, J. F. and A. Boveris (1980). "Generation of superoxide anion by the NADH dehydrogenase of bovine heart mitochondria." Biochem J **191**(2): 421-7.
Tyler, R. H., H. Brar, et al. (1993). "The effect of superoxide dismutase alleles on aging in Drosophila." Genetica **91**(1-3): 143-9.
Tymianski, M., M. P. Charlton, et al. (1993). "Source specificity of early calcium neurotoxicity in cultured embryonic spinal neurons." J Neurosci **13**(5): 2085-104.
Urushitani, M., T. Nakamizo, et al. (2001). "N-methyl-D-aspartate receptor-mediated mitochondrial Ca(2+) overload in acute excitotoxic motor neuron death: a mechanism distinct from chronic neurotoxicity after Ca(2+) influx." J Neurosci Res **63**(5): 377-87.
Vergun, O., J. Keelan, et al. (1999). "Glutamate-induced mitochondrial depolarisation and perturbation of calcium homeostasis in cultured rat hippocampal neurones." J Physiol **519 Pt 2**: 451-66.
Vergun, O., A. I. Sobolevsky, et al. (2001). "Exploration of the role of reactive oxygen species in glutamate neurotoxicity in rat hippocampal neurones in culture." J Physiol **531**(Pt 1): 147-63.
Verkhratsky, A. and E. C. Toescu (1998). "Calcium and neuronal ageing." Trends Neurosci **21**(1): 2-7.
Wang, G. J. and S. A. Thayer (1996). "Sequestration of glutamate-induced Ca2+ loads by mitochondria in cultured rat hippocampal neurons." J Neurophysiol **76**(3): 1611-21.
Wang, X. M., P. I. Terasaki, et al. (1993). "A new microcellular cytotoxicity test based on calcein AM release." Hum Immunol **37**(4): 264-70.
Wang, Y. and Z. H. Qin (2010). "Molecular and cellular mechanisms of excitotoxic neuronal death." Apoptosis **15**(11): 1382-402.

Ward, M. W., A. C. Rego, et al. (2000). "Mitochondrial membrane potential and glutamate excitotoxicity in cultured cerebellar granule cells." J Neurosci **20**(19): 7208-19.

West, M. J., P. D. Coleman, et al. (1994). "Differences in the pattern of hippocampal neuronal loss in normal ageing and Alzheimer's disease." Lancet **344**(8925): 769-72.

White, R. J. and I. J. Reynolds (1996). "Mitochondrial depolarization in glutamate-stimulated neurons: an early signal specific to excitotoxin exposure." J Neurosci **16**(18): 5688-97.

White, R. J. and I. J. Reynolds (1997). "Mitochondria accumulate Ca2+ following intense glutamate stimulation of cultured rat forebrain neurones." J Physiol **498 (Pt 1)**: 31-47.

Wong, H. K., X. B. Liu, et al. (2002). "Temporal and regional expression of NMDA receptor subunit NR3A in the mammalian brain." J Comp Neurol **450**(4): 303-17.

Xia, Y., R. E. Ragan, et al. (1995). "Developmental expression of N-methyl-D-aspartate (NMDA)-induced neurotoxicity, NMDA receptor function, and the NMDAR1 and glutamate-binding protein subunits in cerebellar granule cells in primary cultures." Neurochem Res **20**(5): 617-29.

Xiong, J., P. J. Camello, et al. (2004). "Mitochondrial polarisation status and [Ca2+]i signalling in rat cerebellar granule neurones aged in vitro." Neurobiol Aging **25**(3): 349-59.

Xiong, J., A. Verkhratsky, et al. (2002). "Changes in mitochondrial status associated with altered Ca2+ homeostasis in aged cerebellar granule neurons in brain slices." J Neurosci **22**(24): 10761-71.

Yonish-Rouach, E., D. Resnitzky, et al. (1991). "Wild-type p53 induces apoptosis of myeloid leukaemic cells that is inhibited by interleukin-6." Nature **352**(6333): 345-7.

Zaidi, A., J. Gao, et al. (1998). "Age-related decrease in brain synaptic membrane Ca2+-ATPase in F344/BNF1 rats." Neurobiol Aging **19**(5): 487-95.

Zhou, M. and M. Baudry (2006). "Developmental changes in NMDA neurotoxicity reflect developmental changes in subunit composition of NMDA receptors." J Neurosci **26**(11): 2956-63.

Zou, H., W. J. Henzel, et al. (1997). "Apaf-1, a human protein homologous to C. elegans CED-4, participates in cytochrome c-dependent activation of caspase-3." Cell **90**(3): 405-13.

Appendix

High-Throughput Method for Dynamic Measurements of Cellular Viability Using a FLUOstar OPTIMA.

(APPLICATION NOTE FOR BMG LABTECH)

High-Throughput Method for Dynamic Measurements of Cellular Viability Using a FLUOstar OPTIMA

Mark S. Chitolie & Emil C. Toescu
Dept. of Physiology, Division of Medical Sciences, University of Birmingham, Edgbaston, Birmingham, B15 2TT UK

Application Note 159 Rev. 04/2008

- Cell viability was measured using the propidium iodide (PI) assay
- Kinetic measurements over 24 h allow for determination of lag times and death rates
- FLUOstar OPTIMA was used to record PI fluorescence over long periods

Introduction

An accurate and reliable method of assessing cellular viability is a vital requirement for any work related to cell culture. This includes drug toxicity studies in addition to basic monitoring of the long-term stability of a culture. Currently there is a wide range of assays that can be used to assess cellular viability based on various different biochemical and molecular principles.

In general, there are two main ways in which a cell can be defined as non-viable. If the cell has: (1) a compromised plasma membrane or, (2) has lost its metabolic functioning. Dyes such as trypan blue and propidium iodide are non-permeable to the plasma membrane. Therefore, only cells with a compromised plasma membrane will take up these types of dye. Another way of identifying a compromised plasma membrane is to detect substances in the extracellular medium which are normally only found within the cytosol of a cell. Therefore they must have leaked through the plasma membrane in order to reach the outside of the cell. An example of this type of method is the lactate dehydrogenase assay, which detects the cytosolic enzyme (lactate dehydrogenase) in the extracellular medium.

The work described in this application note is based on the propidium iodide (PI) assay[1]. This is a very powerful assay, which allows viability to be measured dynamically over long periods of time. This is very useful when studying the effects of various substances, which may not necessarily have an instantly induced effect on the cell. Therefore this method enables the identification of any delayed death, which may be missed when only assessing viability at one specific time-point. Furthermore, since the measurement is dynamic over a long period of time (24 hrs), the rate at which the death is occurring can be fully investigated.

In this experiment we describe a further development of a high throughput method for dynamically assessing neuronal death[2] with the help of a FLUOstar OPTIMA (Figure 1).

Fig. 1: FLUOstar OPTIMA microplate reader

Materials and Methods

- Black 24-well plates (Iwaki, Scientific Laboratory Supplies LTD)
- Propidium iodide (PI, Sigma, UK)
- FLUOstar OPTIMA microplate reader (BMG LABTECH, Offenburg, Germany)

Cerebellar granule cells were obtained from post-natal Wistar rats (P5-8) and cultured directly onto 24-well plates at a plating density of 280-300,000 cells per well[3]. PI was diluted with dH_2O to a concentration of 5 mg/mL and used at a final concentration of 50 µg/mL (diluted in experimental buffer referred to as 'Ctrl') (Protect the PI from light since it is photosensitive)[2].

The FLUOstar OPTIMA microplate reader was set to fluorescent mode with an excitation wavelength of 544 nm and an emission wavelength of 612 nm. The culture medium from each well was removed and replaced with 500 µL of the PI-Ctrl solution. Four measurements were made at 60-second intervals in order to establish a resting level of PI fluorescence (pre-stimulation). This PI-Ctrl solution was removed and stored in a separate 24-well plate. The cultures were incubated for 60 minutes at 27 °C in various concentrations of glutamate all diluted in an experimental buffer containing 50 µg/mL PI, 10 µM Glycine (Sigma, UK) and no Mg^{2+}. Throughout this 60-minute incubation period, measurements were taken at 15-minute intervals. In order to obtain a background level for the PI solution, the PI-Ctrl solution was measured. The glutamate-PI solution was then removed and replaced with the PI-Ctrl solution. Measurements were taken at 30-minute intervals for 23 hours. At the end of the 24 hours, the PI-Ctrl solution was removed and either EtOH (100 %) or Triton X (0.02 %) was added to each well in order to induce maximal death. Then the PI-Ctrl solution was added back and 5 measurements of this level of maximal PI fluorescence were taken.

Results and Discussion

The signal curves in Fig.2 represent the changes in PI fluorescence depending on the glutamate concentration (0-200 µM).

With increasing concentration of glutamate the resulting PI signal is also significantly increased.

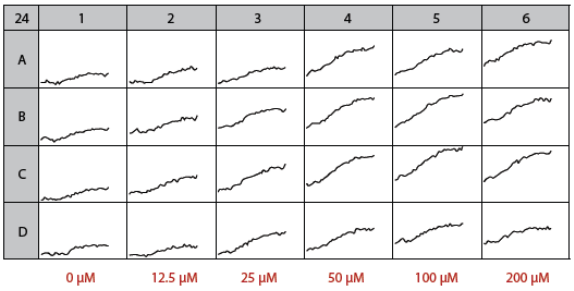

Fig. 2: Current State Picture of PI fluorescence measurement by various concentration of glutamate.

For quantifying the changes in the PI signal two methods can be used: (1) difference of each individual PI signal from its corresponding resting level (Figure 3) and (2) the percentage death normalised against the resting level (0%) and the maximal death (100 %) induced by EtOH (100 %) or Triton X (0.02 %) (Figure 4) referred to as the "Min-Max range".

Both methods show that the death induced by the glutamate is dose dependent. Furthermore, using the temporal dimensions of the measurements, one can estimate the time it takes for a significant amount of death to appear (initiated).

In these experiments, the lag period between the end of the glutamate exposure and the initiation of significant levels of death is dependent on the glutamate concentration hence, cultures exposed to larger doses of glutamate have shorter lag periods.

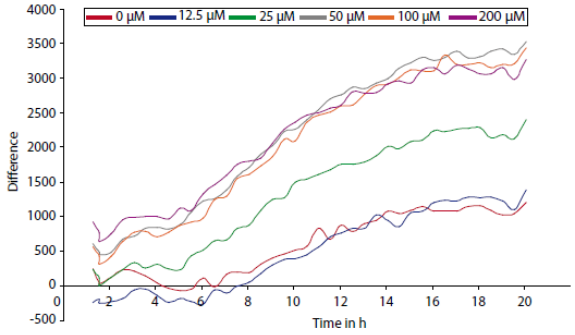

Fig. 3: Dose-response curve for the excitotoxic effects of glutamate. Propidium iodide signals are expressed as a difference between each individual PI measurement and its original resting level. The data was averaged from 4 replicates for each glutamate concentration.

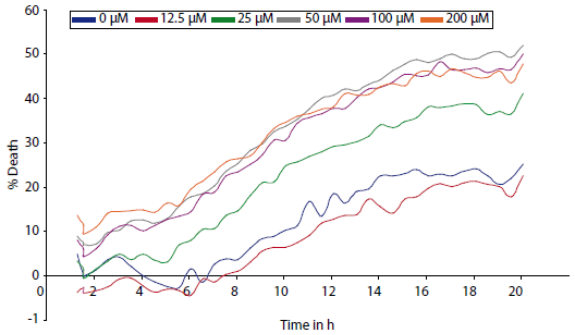

Fig. 4: Dose-response curve for the excitotoxic effects of glutamate. Propidium iodide signals are expressed as a percentage death which is normalized against the resting level (0%) and the maximum death level induced by EtOH/Triton x (100 %). The data was averaged from 4 replicates for each glutamate concentration.

Figure 5 shows the maximum PI signal expressed either as a difference (between each experimental point and the resting point) (Figure 5 A) or as a percentage death (normalised against the Min-Max range) (Figure 5 B). The figure illustrates that this method is well capable of revealing a clear dose-response for the excitotoxic effect of glutamate; such that an increase in the concentration of this neurotransmitter results in an increased level of neuronal death, hence increase in PI fluorescence.

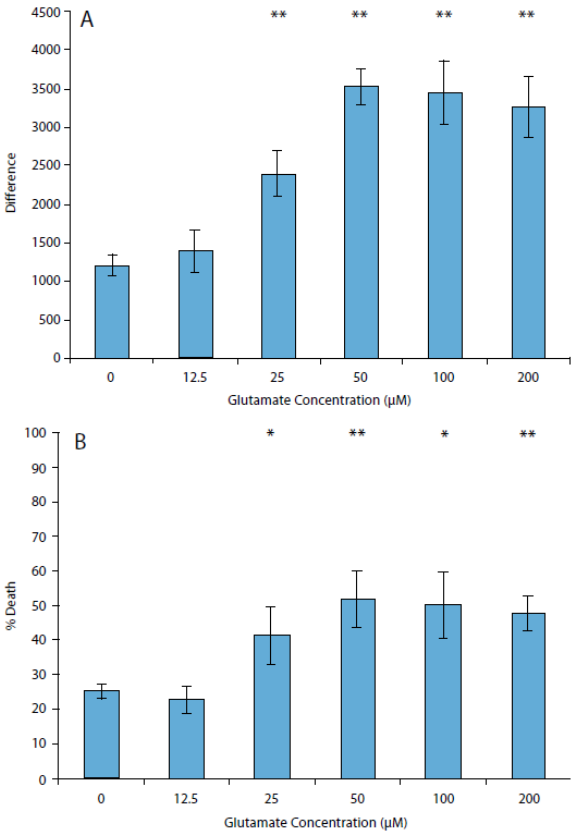

Fig. 5: Dose-response curve for the excitotoxic effects of glutamate. (A) Shows the maximum PI signal (Pre-EtOH/Triton treatment) as a difference ±S.E.M (Unpaired Student 1-tailed T-test, where * p<0.05, **p<0.01), as described in legend to figure 3. (B) Shows the maximum PI signal (Pre-EtOH/Triton treatment) as a percentage death ±S.E.M (Unpaired Student 1-tailed T-test, where * p<0.05, **p<0.01), as described in legend to figure 4.

Conclusion

We show that the PI assay is a very useful tool for monitoring neuronal viability. It allows a complete analysis of the dynamics of the response to a specific substance, which in our case is the neurotransmitter glutamate.

Numerous parameters, including lag times and rates of death can be assessed using this PI method. This is advantageous compared to other methods used for assessing neuronal viability since most of these methods usually involve a single end-point measurement or require termination of the preparation.

References

1. Tanke, H.J. et al. (1982) *J. Immunol. Methods* **52** (1), 91-96.
2. Sattler, R., et al. (1997) *J. Cereb. Blood Flow Metab.* **17** (4), 455-463.
3. Xiong, J., et al. (2004) *Neurobiol. Aging*, **25**(3), 349-359.

Germany:	**BMG LABTECH GmbH**	**Tel: +49 781 96968-0**
Australia:	BMG LABTECH Pty. Ltd.	Tel: +61 3 59734744
France:	BMG LABTECH SARL	Tel: +33 1 48 86 20 20
Japan:	BMG LABTECH JAPAN Ltd.	Tel: +81 48 647 7217
UK:	BMG LABTECH Ltd.	Tel: +44 1296 336650
USA:	BMG LABTECH Inc.	Tel: +1 919 806 1735
Internet:	**www.bmglabtech.com**	**info@bmglabtech.com**